Universidade de Aveiro Departamento de Química
2013/2014

Júlia Catarina Silva de Matos

Alterações metabólicas na insuficiência cardíaca diastólica: uma abordagem proteómica

Metabolic changes in diastolic heart failure: a proteomic approach

Universidade de Aveiro Departamento de Química
2013/2014

Júlia Catarina Silva de Matos

Alterações metabólicas na insuficiência cardíaca diastólica: uma abordagem proteómica

Metabolic changes in diastolic heart failure: a proteomic approach

Dissertação apresentada à Universidade de Aveiro para cumprimento dos requisitos necessários à obtenção do grau de Mestre em Bioquímica Clínica, realizada sob a orientação científica da Doutora Inês Falcão Pires, Professora do Departamento de Fisiologia e Cirurgia Cardiotorácica da Faculdade de Medicina da Universidade do Porto e do Doutor Rui Pinheiro Vitorino, Investigador do Departamento de Química da Universidade de Aveiro.

Thanks are due to Portuguese Foundation for Science and Technology (FCT), European Union, QREN, and COMPETE for funding the QOPNA research unit (project EXCL/BIM-MEC/0055/2012).

Dedicado aos meus pais, irmão e avô,

O júri

Presidente

Prof. Doutora Rita Maria Pinho Ferreira
Professora Auxiliar do Departamento de Química da Universidade de Aveiro

Arguente

Prof. Doutor Daniel Moreira Gonçalves
Investigador de Pós-Doutoramento Centro de Investigação em Atividade Física, Saúde e Lazer da Faculdade de Desporto Universidade do Porto

Prof. Doutora Inês Falcão Pires
Professora Auxiliar do Departamento de Fisiologia e Cirurgia Cardiotorácica da Faculdade de Medicina da Universidade do Porto

agradecimentos

Em especial, ao meu orientador Professor Doutor Rui Vitorino pela incansável orientação, apoio e motivação, pela paciência, acompanhamento no laboratório, disponibilidade e acima de tudo pelo exemplo de dedicação e profissionalismo. À minha orientadora Professora Doutora Inês Pires pela constante orientação científica, disponibilidade, ajuda e apoio ao longo da realização deste trabalho.

À Professora Doutora Rita Ferreira e Doutora Nádia Gonçalves pela colaboração e ânimo.

Aos meus colegas de laboratório, pelo apoio, incentivo e boa disposição.

Aos meus colegas de mestrado, em especial à Maria pela amizade, disponibilidade, apoio, incentivo e todos os momentos de descontração proporcionados. Às minhas melhores amigas pela amizade, apoio e por todos os momentos proporcionados que me permitiram aliviar a ansiedade sentida.

E por último, mas não menos importante, um especial obrigado à minha família e ao meu namorado pelo apoio incondicional, pela enorme paciência em aturar todos os meus dias de intermináveis crises e neuras que toda esta jornada me proporcionou. Em especial, aos meus pais cujo suporte ao longo da minha vida me permitiu chegar aqui, sem vocês não seria possível.

A todos um grande obrigado.

Palavras-chave

Proteínas, tecido adiposo epicárdico, função cardíaca, disfunção diastólica, tecido adiposo visceral, proteoma, obesidade

Resumo

Atualmente é reconhecido que a insuficiência cardíaca (IC) diastólica (ICD) constitui uma importante causa de morbilidade e mortalidade cardiovascular atingindo cerca de 50% dos casos de IC. O aumento da incidência de comorbilidades, tal como a obesidade são fatores de risco que se associam a um pior prognóstico em pacientes com ICD. De facto, atualmente ao tecido adiposo é atribuído um importante papel de modulação da função cardíaca. As adipocinas, citocinas pró-inflamatórias assim como outras substâncias libertadas por este tecido aparentam desempenhar um papel predominante na indução da disfunção cardíaca. Assim, considerando a elevada prevalência de obesidade em pacientes com disfunção diastólica e a falta de informação sobre esta relação, o objetivo deste trabalho é caracterizar o perfil de substâncias libertadas pelo tecido adiposo em condições de ICD, recorrendo a uma abordagem proteómica. Neste sentido utilizou-se o tecido adiposo visceral (TAV) e epicárdico (TAE) de animais obesos com ICD (n=3 , ZSF1 obesos) e os respetivos controlos magros sem ICD (n=3, ZSF1 magros). Primeiro procedeu-se à otimização da metodologia para análise do proteoma dos tecidos onde foram testados 3 protocolos distintos de extração de proteínas. A seleção do protocolo foi feita considerando o número de proteínas extraídas, uma vez que não existiram diferenças significativas nas avaliações realizadas. Após a execução do protocolo de extração elegido, efetuou-se eletroforese de primeira dimensão e cromatografia líquida de alta resolução para a separação de proteínas e péptidos e procedeu-se à identificação dos fragmentos por espectrometria de massa. No TAV, os resultados demonstraram, na obesidade, uma diminuição das proteína catalase e um aumento das proteínas superóxido dismutase, peroxirredoxina-1 e anexina-A1 e A2 levando a crer que existe inflamação, stress oxidativo mas, simultaneamente, uma resposta compensatória do tecido adiposo para prevenir o aumento de produção de espécies reativas de oxigénio e a progressão da inflamação. Observou-se ainda uma diminuição da proteína aldeído desidrogenase mitocondrial, o que sugere maior suscetibilidade ao stress oxidativo. No TAE dos ZSF1 obesos, os resultados demonstraram uma redução da enzima 3-cetoacil-CoA tiolase sugerindo um mecanismo compensatório a fim de inibir a oxidação dos ácidos gordos, e ainda um aumento das proteínas colagénio-alfa1(I) e lumican, sugerindo uma ligação entre a inflamação causada pela obesidade e alterações da matriz extracelular do tecido adiposo. Curiosamente, os dois tecidos demonstraram o aumento de proteínas contrácteis cardíacas nos obesos ZSF1, as quais são consistentes com várias alterações miofilamentares apresentadas na ICD. Por fim, a análise das diferenças entre o TAV e o TAE revela claras diferenças no proteoma de cada um destes tecidos.
Este trabalho apresenta uma abordagem generalista da composição proteica dos tecidos adiposos visceral e epicárdico do modelo animal ZSF1, indicando importantes diferenças no proteoma do tecido adiposo entre animais obesos com ICD e os respetivos controlos e direcionando o desenvolvimento futuro de investigações mais específicas focadas no papel funcional das proteínas mais alteradas na ICD.

Keywords

Proteins, epicardial adipose tissue, cardiac function, diastolic dysfunction, visceral adipose tissue, proteome, obesity

Abstract

Currently, diastolic heart failure (DHF) is recognized an important cause of cardiovascular mortality and morbidity reaching approximately 50% of HF cases. The growing incidence of cardiovascular risk factors, such as obesity and overweight are associated with a worse prognosis in patients with cardiovascular disease, prompting the onset of diastolic dysfunction. In fact, currently the adipose tissue is considered an important modulator of cardiac function. Adipokines, pro-inflammatory cytokines and other important substances are released by this tissue and seem to play an important role in the induction of the cardiac dysfunction. Thus, considering the high prevalence of obesity in patients with diastolic dysfunction and lack of information about this relation, the aim of this work is to characterize the profile of substances released by adipose tissue under conditions of DHF, using a proteomic approach. The visceral (VAT) and epicardial (EAT) adipose tissue from obese animals with diastolic HF (n=3, obese ZSF1) with their respective lean controls without diastolic HF (n=3, lean ZSF1) were analysed. Firstly, the optimization of methodology for analysis of tissues proteome was performed, testing three different extraction protocols. The selection of protocol was made considering the larger number of extracted proteins, since it there were no significant differences in performed evaluations. After execution of the extracted protocol elected, it was performed the separation of proteins and peptides by one-dimension gel electrophoresis and high-performance liquid chromatography and tryptic digestion used to further mass spectrometry identification. In VAT, the results showed in obesity a decrease of catalase protein and increase of superoxide dismutase, peroxiredoxin-1 and A1 and A2-annexin proteins leading to believe that there are inflammation, oxidative stress and, at the same time, a metabolism protection in order to prevent the increase of reactive oxygen species and progression of inflammation. In addition, it was also was evidenced a decrease of the aldehyde dehydrogenase, mitochondrial suggesting greater susceptibility to oxidative stress. In EAT of the obese ZSF1, the results presents a decrease of 3-ketoacyl-CoA thiolase protein enzyme as a compensatory mechanism in order to inhibit fatty acid oxidation and an increase of lumican and collagen-alpha-1(I) proteins suggesting a link between inflammation caused by obesity and increases of adipose tissue extracellular matrix. Curiously, both tissues demonstrated the increase of cardiac contractile proteins in obese adipose tissue, which are consistent with several reported myofilamentary changes in DHF. Finally, it was analysed differences between the VAT and EAT, which suggest that both tissues present a different proteome.

This work is a general approach to the protein composition of the epicardial and visceral adipose tissue of the animal model ZSF1, providing importants differences in adipose tissue proteome between obese animals with DHF and respective controls and helping the future development researches more focused on the functional role of proteins changes in DHF.

Contents

Tables

Figures

Acronyms

1D	1-dimensional
1DE	1-dimensional gel electrophoresis
2D	2-dimensional
2D-DIGE	2-dimensional difference gel electrophoresis
2DE	2-dimensional gel electrophoresis
BAT	Brown adipose tissue
BMI	Body mass index
BNP	Peptideo Natriurético Cerebral
CI	Cardiac index
CO	Cardiac output
CV	Cardiovascular
CVD	Cardiovascular disease
DHF	Diastolic heart failure
EAI	Arterial elastance indexed
EAT	Epicardial adipose tissue
EDP	End-diastolic pressure
EF	Ejection fraction
emPAI	Exponentially modified protein abundance index
ESI	Electrospray ionization
HDL	High-density lipoprotein
HF	Heart failure
HFPEF	Heart failure with preserved ejection fraction
HPLC	High-performance liquid chromatography
IR	Insulin resistance
IVCs	Individually ventilated cages
LC	Liquid chromatography
LDL	Low-density lipoprotein
Ln	Lean
LV	Left ventricle
LVEDV	end-diastolic volume

LVESV	End-systolic volume
LVM	Left ventricular mass
LVPES	End-systolic pressure
MALDI	Matrix-assisted laser desorption/ionization
MeS	Metabolic syndrome
MRI	Magnetic resonance imaging
Ms	Mass spectrometry
MS/MS	Tandem mass spectrometry
MudPIT	Multi-dimensional protein identification technology
MW	Molecular weight
Ob	Obese
OD	Optical density
PCR	Polymerase chain reaction
PFF	Fragment fingerprinting
pI	Isoelectric point
PMF	Peptide mass fingerprint
PT	Protocol-Tris
PTMs	Post-translational modifications
PTU	Protocol-Tris and Urea
PU	Protocol-Urea
PV	Pressure-volume
ROS	Reactive oxygen species
RT	Reverse transcription
RV	Right ventricle
SAP	Systolic arterial pressure
SDS-PAGE	Sodium dodecylsufate polyacrylamide gel electrophoresis
SHF	Systolic heart failure
T2D	Type II diabetes
TG	Triglycerides
TOF	Time-of-flight mass spectrometry
UV	Ultraviolet
VAT	Visceral adipose tissue

WAT	White adipose tissue
WKY	Wistar Kyoto
ZDF, +/fa	Zucker type II diabetic rats
τ	Constant time of isovolumic relaxation

CHAPTER 1

STATE OF THE ART

1.1 - Introduction

Heart failure (HF) is a syndrome that occurs in individuals due to inherited or acquired cardiac abnormalities. These patients develop a set of clinical signs and symptoms consecutive of the hemodynamic failure [1]. Worldwide it is estimated that approximately 26 million people suffer from heart failure and its prevalence tends to increase [2, 3]. A significant proportion of patients with this condition have a normal left ventricular systolic function with preserved ejection fraction. In this subgroup of patients, heart failure is the result of diastolic dysfunction. This condition is, therefore, frequently referred as diastolic heart failure (DHF) [3, 4]. While heart failure with impaired left ventricular systolic function has been extensively studied, patients with preserved systolic function have been grossly under-investigated, and the underlying mechanisms and diagnostic criteria have been controversial [4, 5]. Clinical trials addressing DHF treatment have been quite disappointing [1], possibly because the determinants of this syndrome are still unclear, it is not a homogeneous disease and DHF therapeutic targets remain to clarify. In fact, its treatment remains largely empirical, mostly based on blood pressure control, treatment of symptoms caused by congestion, maintenance of normal atrial contraction and withholding ventricular remodeling or any increase in cardiac dimensions [6]

Diastolic heart failure is associated with delayed left ventricle relaxation and/or increased chamber stiffness (increased diastolic pressure without volume change) [7]. All these myocardial dysfunction can be caused by myocardial abnormalities or by maladaptive cardiac remodelling. Obesity represents an important cause of diastolic dysfunction and its excessive deposition of adipose tissue causes deregulation of the adipokines, which contribute to maladaptive cardiac remodelling. Thus, due to an increase in obesity prevalence together with a shift of the profile of substances released by adipocytes, a substantial amount of research has been devoted to studying the relationship between adipocytes-derived substances and obesity-linked pathologies, such as diabetes mellitus. However, the focus of this relationship relative to diastolic dysfunction has been scarce, once there is no study about changes in adipocytes-derived substances profile in diastolic dysfunction.

In conclusion, unravelling these mechanisms will be of upmost important since they will contribute to a better characterization of diastolic dysfunction pathophysiology,

particularly focusing on the interesting crosstalk between adipose tissue and the myocardium. Furthermore, the comprehension of this "dialogue" may target novel therapies for diastolic heart failure or even specific biomarkers of this disease.

1.2 – Heart failure definition

Heart failure is an abnormality of cardiac structure or function leading to failure of the heart to deliver oxygen at an adequate rate to the requirements of the metabolizing tissues, despite normal filling pressures (or only at the expense of increased filling pressures) [1]. Heart failure is a syndrome associated to typical symptoms (e.g. breathlessness, dyspnoea on exertion, fatigue and peripheral oedema) [8] and signs (e.g. elevated jugular venous pressure, pulmonary crackles, and displaced apex beat) [1].

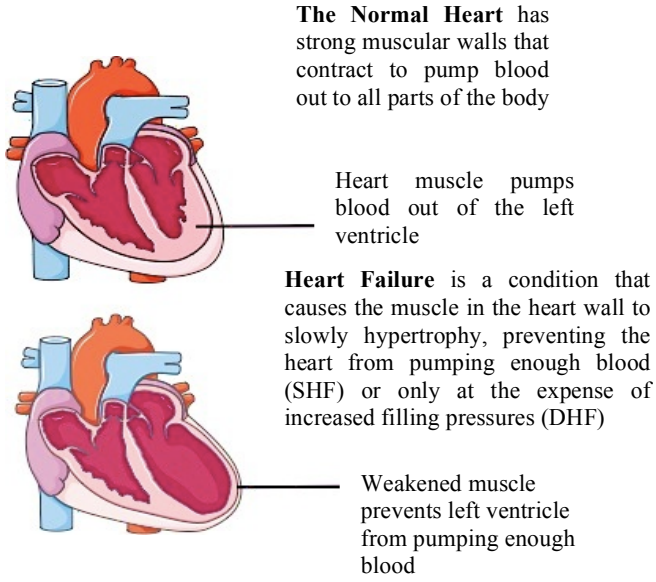

Figure 1 - Differences between healthy and a failing heart. This figure was produced using *Servier Medical Art* and it was adapted from [9]

Heart failure constitutes an important medical, social, and economic problem [2]. The prevalence of heart failure is estimated as 1%-3% of the adult population in developed countries, with the prevalence rising up to more than 10% among patients older than 70 years [1]. Over 26 million people suffer from heart failure around the world and over 3.5 million people are newly diagnosed with HF every year in Europe [2].

Heart failure is categorized as either systolic or diastolic heart failure (SHF and DHF, respectively) [10], with similar prevalence, despite their different pathophysiologic mechanisms and differences of age and gender incidence [11]. SHF is characterized by progressive left ventricular dilation, eccentric hypertrophy, abnormal left ventricular

systolic properties and decreased left ventricular ejection fraction, whereas in DHF, the hearts generally exhibit concentric hypertrophy, normal or reduced LV volume, abnormal diastolic function and normal left ventricular ejection fraction [5, 12]. Differences and similarities between systolic and diastolic heart failure are presented in Table 1.

Table 1 - Differences and similarities between systolic and diastolic heart failure. ↑- Increased; ↓- Decreased; N – Normal. Reprinted with permission from Gaash WH, Zile MR. Left ventricular diastolic dysfunction and diastolic heart failure. Annu Rev Med 2004;

Signs and symptoms	Systolic heart failure	Diastolic heart failure
BNP	↑	↑
Exercise testing		
Duration	↓	↓
Systolic blood pressure	↑	↑↑
Pulse pressure	↑	↑↑
Oxygen consumption	↓↓	↓
Left ventricle remodelling		
End-diastolic volume	↑↑	N
End-systolic volume	↑↑	↓
Myocardial mass	↑ Eccentric LV hypertrophy	↑ Concentric LV hypertrophy
Relative wall thickness	↓	↑↑
Cardiomyocyte	↑ Length	↑ Diameter
Extracellular matrix (collagen)	↓	↑↑
Left ventricle systolic function		
Ejection fraction	↓↓	N - ↑
Stroke volume	N - ↓	N - ↓
Myocardial contractility	↓↓	↓
Left ventricle diastolic function		
Chamber stiffness	N - ↓	↑↑
Myocardial stiffness	N - ↑	↑
Relaxation time – constant	↑	↑
Filling dynamics	Abnormal	Abnormal
End-diastolic pressure	↑↑	↑↑
Preload reserve	Exhausted	Limited

Although SHF and DHF share many clinical features, it is clear the underlying causes and pathophysiological mechanisms are different. In contrast to SHF, for which

knowledge has advanced rapidly over the past decade, little is known about the pathophysiology and mechanism targeted therapy for DHF [5].

1.2.1 - Diastolic dysfunction and diastolic heart failure

Currently, there is an increasing recognition that abnormalities in diastolic function represent a major contributor to congestive heart failure [13]. However, there has been a considerable controversy over the definition of diastolic dysfunction and diastolic heart failure [7].

As already stated, heart failure is a condition in which the heart is no longer able to pump out enough oxygen-rich blood or achieves this at the expense of increased ventricular filling pressures [14]. When heart failure is accompanied by a predominant or isolated abnormality in diastolic function, this clinical syndrome is called diastolic heart failure. Diastolic dysfunction refers to a condition in which abnormalities in mechanical function are present during diastole. That is, diastolic function encompasses ventricular relaxation, distensibility and filling. Therefore, the diastolic dysfunction occurs when these processes are prolonged, retarded, or incomplete [7, 14, 15] leading to slower and/or stiffer ventricles [7]. On the other hand, diastolic heart failure represents an advanced stage of diastolic dysfunction that leads to HF. DHF is defined as a clinical syndrome characterized by the following conditions: 1) symptoms and signs of heart failure, 2) preserved ejection fraction and 3) abnormal diastolic function [7]. So, if diastolic dysfunction refers to an abnormal mechanical property, the diastolic heart failure describes a clinical syndrome.

1.2.2 - Epidemiology and prevalence of diastolic heart failure

In 1998, the European Study Group on Diastolic Heart Failure published a set of criteria for the diagnosis of DHF [16]. At that time, DHF was presumed to account for approximately one-third of all patients with heart failure and its natural history was considered to be more benign than systolic heart failure with a lower mortality and morbidity rate [16, 17]. Over the last two decades, these perspectives have changed substantially. Currently it is accepted that DHF accounts for 40% to 50% of all HF cases and it has a prognosis, which is as ominous as SHF [18].

Although HF is traditionally associated with reduced left ventricular ejection fraction, it has become widely recognized that it can occur even when ejection fraction is

preserved, constituting the syndrome of HF with preserved ejection fraction (HFPEF) or DHF. Notwithstanding the prevalence mentioned before, several clinical studies suggest that the frequency of DHF among patients with HF ranges from 13% to 74%, and there are several reasons for this apparent inconsistency [3]; the prevalence of HF and the frequency of DHF vary dramatically according to age, sex, methods and criteria used to diagnose DHF and the value of ejection fraction that is used as a cut off value. Whereas these factors are largely interdependent, the most important appears to be age (in patients > 70 years old the prevalence of DHF is of 50%) [7]. Thus, because of population demographics continuous changes, the number of persons with HF has and will continue to increase dramatically, contributing to the perception of HF as an epidemic problem (Figure 2) [3].

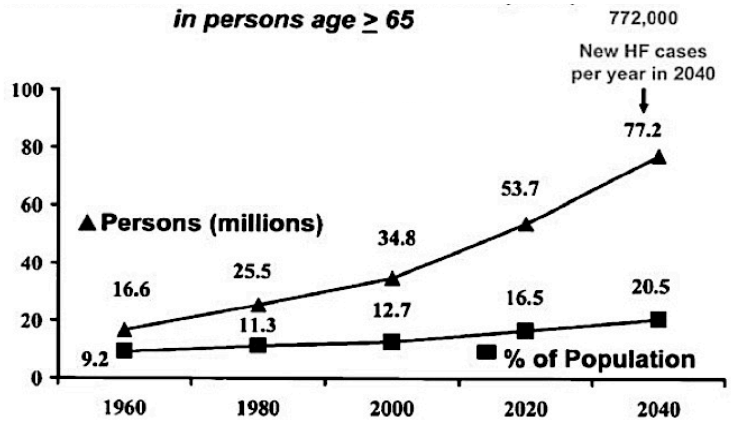

Figure 2 - Demographics of patients with heart failure over time. Rectangles: percentage of the population; Triangles: number of persons (in millions) aged 65 years and older in the United States. The number of persons with HF (grey) will increase dramatically in the next 3 decades [3].

Furthermore, a recent study of Kuznetsova *et al.* [18] showed that in general population, the overall prevalence of LV diastolic dysfunction, estimated from echocardiographic measurements was as high as 27.3% and increased with age. These authors also showed that higher age, body mass index, heart rate, systolic blood pressure, serum insulin and creatinine were significantly associated with a higher risk of LV diastolic dysfunction in the general population. Badelek *et al.* [19] showed that in Europe the prevalence of diastolic heart failure in the total population is over 20%.

1.2.3 - Risk factors

As previously mentioned, the incidence and prevalence of HF and its associated mortality is increasing at alarming rates [3]. Despite the progress made in the development of several new HF therapies, the overall 5-year mortality rate for HF remains extremely

high, nearly 50% [20]. Epidemiologic evidence derived from the Framingham Heart Study [21] indicates that overweight and obesity are potent indicators and predictors of subsequent clinical HF. Moreover, the same study showed that heart failure had developed in 8.4% of the study population, and that the risk of developing HF increases approximately twofold in people with obesity when compared with the non-obese population.

Evidence suggests that age, hypertension and obesity play a central role in the development of diastolic dysfunction [11]. In fact the majority of patients with high blood pressure are overweight. Furthermore, hypertension is about 6 times more frequent in obese than in lean individuals [22]. Thus, obesity becomes one of the most important features of DHF [23].

Obesity typically causes worsening of cardiac relaxation and it is associated with several changes in cardiovascular function related to the increase of cardiac work parameters such as LV filling pressures and left ventricular mass (LVM) [24, 25]. These changes can lead to diastolic heart failure. Moreover, Powell *et al.* [26] examined the relationship among body mass index, LV structure, systolic and diastolic function and showed that a higher body mass index was associated with greater LVM, LV thickness and LV end-diastolic diameter. These findings are consistent with other reports that support obesity as a contributing factor for ventricular remodelling, impaired LV relaxation and higher LV filling pressure, which lead to diastolic dysfunction and consequently DHF [11]. It is important to note, that gender differences in obesity may also influence the development of DHF because overweight and obese postmenopausal women experience DHF at higher numbers compared with overweight and obese men [27].

1.3 - Obesity and metabolic syndrome

In the last decades, the worldwide prevalence of obesity has increased strikingly and will likely lead to a rising incidence of insulin resistance (IR), cardiovascular disease (CVD), type II diabetes (T2D) as well as metabolic syndrome (MeS) [28]. Experts claim that the MeS would never have been formulated if the obesity epidemic had not become the public health concern that it is today [29].

Obesity is a metabolic disease of pandemic proportions. The World Health Organization estimates that 300 million of adults worldwide are obese and more than 1

billion are overweight. Obesity can be defined as an excess of adipose tissue. Generally, the body mass index (BMI) has been used to identify obese individuals, which is determined by weight (kilograms) divided by height squared (square meters) [30]. In clinical terms, a BMI of 25–29 kg/m^2 is called overweight and BMIs over 30 kg/m^2 is called obesity (Table 2).

Table 2 - Classification of obesity according to BMI [30]

Classification	BMI	Risk of comorbidities
Underweight	<18.50	Low (but risk of other clinical problems increased)
Normal range	18.50 – 24.99	Average
Overweight	≥25.00	Increased
Preobese	25.00 – 29-99	Increased
Obese class I	30.00 – 34.99	Moderate
Obese class II	35.00 – 39.99	Severe
Obese class III	≥ 40.00	Very severe

However, the best way to estimate obesity in clinical practice is to measure waist circumference, because an excess of abdominal fat is most tightly associated with the metabolic risk factors than other type of fat [31]. Abdominal fat is located in two major compartments: subcutaneous and intraperitoneal fat, which is also known as visceral adipose tissue (VAT). Although subcutaneous adipose tissue is a much larger compartment than visceral fat, the latter is more strongly related to metabolic risk factors than any other fat compartment [32]. Indeed, the increased prevalence of excessive visceral obesity and obesity-related cardiovascular risk factors is closely associated with the rising incidence of cardiovascular diseases and T2D. This clustering of vascular risk factors in visceral obesity is often referred to as metabolic syndrome [33].

Metabolic syndrome involves a combination of clinically specific risk features including obesity (central adiposity), IR, glucose intolerance or diabetes mellitus, dyslipidaemia (specifically high triglycerides (TG), low levels of high-density lipoprotein (HDL), and low-density lipoprotein (LDL)), hypertension and atherosclerotic disease [34]. However, several conditions have been proposed to define MeS, as depicted in Table 3.

Table 3 - Four definitions more commonly used in metabolic syndrome. W - women; M - men; Rx - pharmacologic treatment. *IGT – impaired glucose tolerance; IFG – Impaired fasting glucose; Urinary albumin excretion of ≥20 µg/min or albumin-to-creatinine ratio of ≥ 30mg/g. * Reliable only patients without T2D. ****Criteria for**

central obesity (waist circumference) are specific for each population; values given are for Europe men and women.

	WHO (1998) [35]	EGIR (1999) [36]	NCEP ATP III (2005 revision) [37]	IDF (2005) [38]
Absolutely required	Insulin resistance* (IGT, IFG, T2D or other evidence of IR)	Hyperinsulinemia *** (plasma insulin > 75th percentile)	none	Central obesity (Waist circumference****): ≥94cm (M) or ≥80cm (W)
Criteria	Insulin resistance or diabetes plus 2 of the 5 criteria below	Hyperinsulinemia, plus 2 of 4 criteria below	Any 3 of the 5 criteria below	Obesity, plus 2 of the 4 criteria below
Obesity	Waist/hip ratio: < 0.90 (M), > 0.85 (W); or BMI > 30Kg/m2	Waist circumference >94 (M) or >80 (W)	Waist circumference >40 in or >35 in (W)	Central obesity already required
Hyperglycaemia	Insulin resistance already required	Insulin resistance already required	Fasting glucose ≥ 100mg/dl or Rx	Fasting glucose ≥ 100mg/dl
Dyslipidaemia	TG ≥150mg/dl; HDL<35(M), HDL<39(W)	TG ≥177mg/dl; HDL<39 mg/dl	TG ≥ 150 mg/dl or Rx	TG≥150mg/dl or Rx
Dyslipidaemia (second separate criteria)			HDL cholesterol: < 40 mg/dl (M), < 50mg/dl (W); or Rx	HDL cholesterol: < 40 mg/dl (M), < 50mg/dl (W); or Rx
Hypertension	≥140/90mmHg	≥140/90mmHg or Rx	> 130 mmHg systolic or >85 mmHg diastolic or Rx	> 130 mmHg systolic or >85 mmHg diastolic or Rx

1.3.1 – Adipose tissue

There has been a revolution on the perception of the adipose tissue, which has evolved from being recognized as a mere deposit of fat to a highly metabolically active organ [39].

Based on morphology, the expression of specific genes and on the predominant type of adipocytes, the adipose tissue is classified into two main forms, brown and white adipose tissue [40]. Brown adipose tissue (BAT) is especially abundant in hibernating mammals. It has a large number of mitochondria and is specialized in heat production and, therefore, energy expenditure. Nevertheless, in humans, BAT is present only in newborns for regulating thermogenic processes [40, 41]. White adipose tissue (WAT) is the major cellular component of the visceral and subcutaneous depots in humans (25% in adults) and stores excess energy in the form of TG [40].

The adipose tissue is an endocrine organ with many functions: heat insulation, mechanical cushioning and storage site for fat in the form of TG [39]. Furthermore,

adipocytes secrete a multiplicity of protein signals and factors, termed adipokines or adipocytokines as well as other adipocytes-derived substances that can affect the function of the organs [42]. The diversity of these adipocytes-derived substances is considerable, in terms of both protein structure and function [43]. The adipokines encompass classical cytokines (e.g., TNF-a, IL-6), chemokines (e.g., MCP-1), proteins of the alternative complement system (e.g., adipsin), and proteins involved in vascular hemostasis (e.g., PAI-1), the regulation of blood pressure (angiotensinogen), lipid metabolism (e.g., retinol binding protein), glucose homeostasis (e.g., adiponectin), and angiogenesis (e.g., VEGF) [44]. Disturbed production of these bioactive molecules contributes to the development of obesity-linked metabolic disorders and cardiovascular disease. A dysregulation of these adipokines can be observed under conditions of excessive adipose tissue, such as obesity (Figure 3) [45, 46].

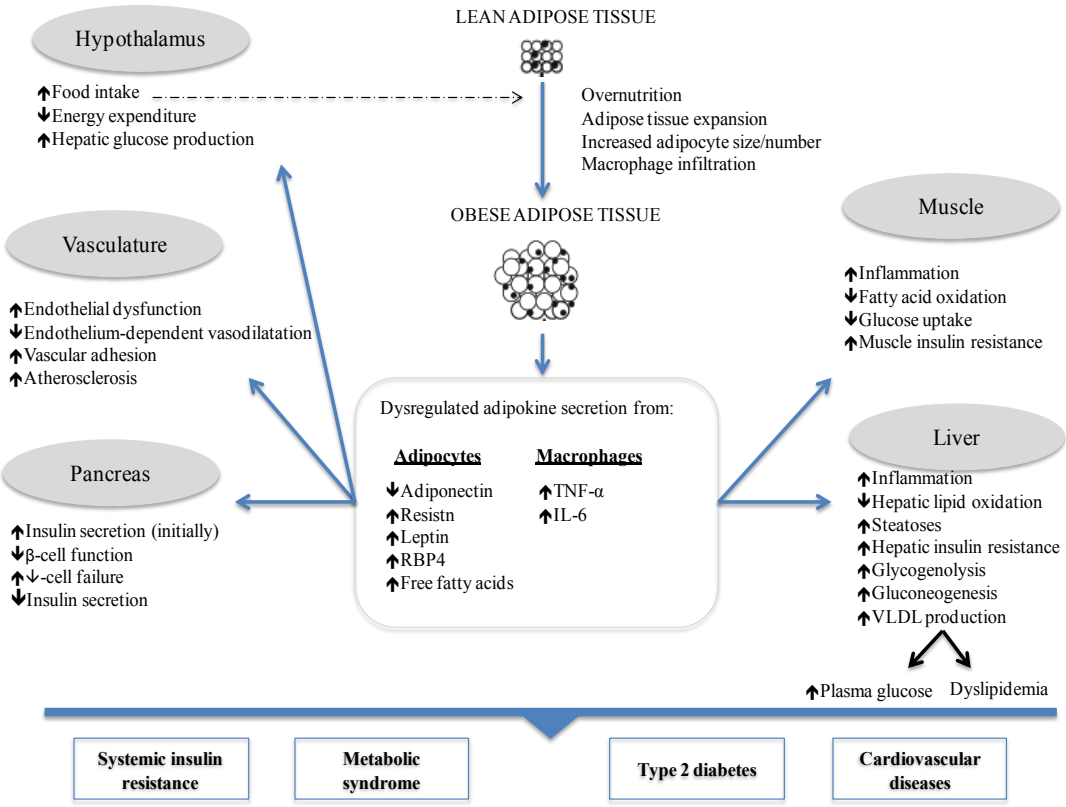

Figure 3 - Effects of obesity-induced changes in adipokine secretion that lead to the development of systemic insulin resistance, metabolic syndrome, type II diabetes, and cardiovascular disorders. Over-nutrition that results from a combination of increased food intake and reduced energy expenditure leads to adipose tissue expansion, increased adipocyte size and number, and increased macrophage infiltration that, together, lead to increased free fatty acid release, deregulated secretion from adipocytes of a variety of adipokines, including adiponectin, leptin, resistin, and retinol binding protein 4 (RBP4), and increased release from resident macrophages of the inflammatory cytokines, tumor necrosis factor α (TNF-α) and interleukin 6 (IL6). Deregulated secretion of these adipokines elicits a variety of adverse effects on numerous tissues including the hypothalamus, liver, skeletal muscle, pancreas, and vasculature that further increase food intake and reduce energy expenditure and lead to the development of systemic insulin resistance that increases the risk for development of the metabolic syndrome, type II diabetes, and a variety of cardiovascular disorders. Adapted from [46].

The normalization of the adipokines secretion profile associated with weight loss due to long-term caloric restriction correlates well with the normalization of metabolic parameters. This is consistent with the idea that adipokines play an important role as molecular messengers and regulators of whole body energy balance [47]. Therefore, the proteins secreted by a particular type of cell, in this case adipocytes, play an important role in the regulation of many physiological processes via paracrine/autocrine mechanisms, and they are of increasing interest as potential biomarkers and therapeutic targets in CVD [48].

The VAT is recognized as a predictor of metabolic syndrome and may contribute to the risk of CVD via adipokines production. However, the risk of this depends on adipose tissue distribution in the body, and mainly on the increase and ectopic accumulation of visceral fat [49]. Increased VAT not only involves greater adipocyte size, but also an

increased expression of pro-inflammatory adipokines with harmful effects at both local and systemic levels. The expression of adipokines varies depending on the site of an adipose tissue depots (Figure 4) [50].

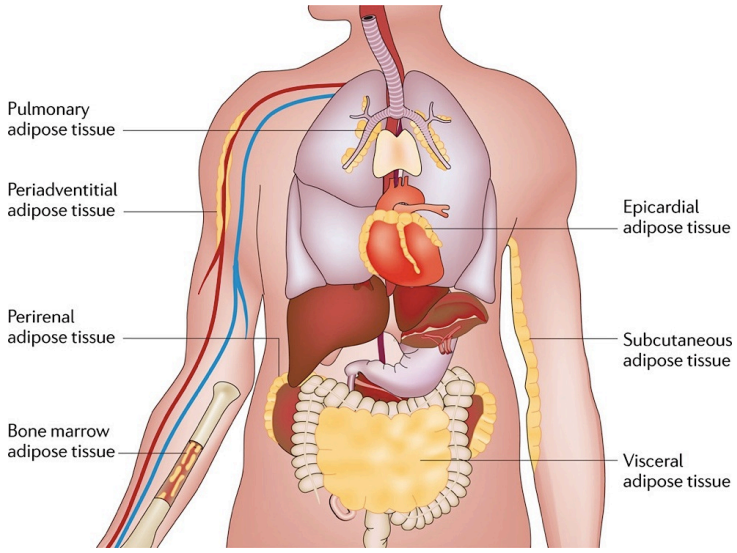

Figure 4 - Different sites of adipose tissue depots [50].

However, scientific interest has been focused on the study of certain extra-abdominal visceral fat deposits, namely epicardial adipose tissue (EAT). Indeed, its close relation to the myocardium and coronary arteries has provided a new understanding of the association between obesity and cardiovascular disease [51].

1.3.1.1 - Epicardial and visceral adipose tissue

Currently, as already known increased VAT is a better predictor of incidence of cardiovascular disease when compared to subcutaneous adipose tissue [52]. Anatomically, VAT is present mainly in the mesentery and omentum, and drains directly through the portal circulation to the liver. Nevertheless, visceral adipose tissue is vascular, innervated and contains a large number of inflammatory and immune cells, a great percentage of large adipocytes and it has a great capacity to generate free fatty acids and to uptake glucose. VAT adipocytes are metabolically active and sensitive to lipolysis [33].

The detection of VAT might be important for CVD risk stratification. However, it is difficult to obtain an accurate measurement and characterization of VAT. Several methods are applied as surrogates for estimation of VAT. Anthropometric measurements are the most used, but are frequently imprecise. Imaging techniques are certainly more precise and reliable than anthropometric measurements. Nonetheless, although the magnetic resonance

imaging (MRI) is the gold standard technique to estimate VAT accurately, it is quite expensive [53]. Thus, Iacobellis *et al.* [54, 55] have proposed epicardial fat as a true visceral fat tissue deposited around the heart. They suggested that it might serve as a new indicator of visceral adiposity and its echocardiographic assessment allows identifying patients with high cardiovascular risk. Its metabolic and secretory functions are thought to be similar to VAT, with which it shares common embryonic origin [56]. Interestingly, although EAT and VAT share the same embryological origin, there are no studies that compare the adipocytes-derived substances secreted and the differences of expression of them among these tissues.

Cardiac fat tissue resides in four locations: intracellular, perivascular, pericardial, and epicardial fat [57]. Epicardial fat is present on the surface of the heart between the myocardium and visceral pericardium and covers more than three quarters of the heart surface (approximately 20% of the heart mass) [57, 58]. In the adult human heart, epicardial fat is commonly found in the atrioventricular and interventricular grooves, along the major branches of the coronary arteries, around the atria, over the free wall of the right ventricle (RV) and over the apex of the left ventricle (LV) (Figure 5) [57]. In rodents however, epicardial fat is absent. Only overweight or obese animals present a scarce fat depot such as pericardium adipose tissue [59].

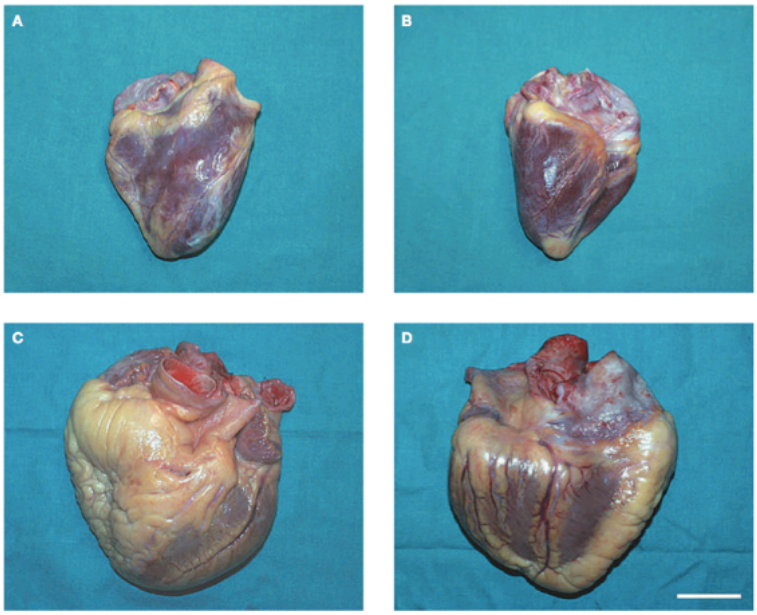

Figure 5 - Macroscopic appearance of epicardial adipose tissue in adult human heart. (A) Anterior view of a normal heart. (B) Posterior view of a normal heart. (C) Anterior view of a hypertrophic heart. (D) Posterior view of a hypertrophic heart; In the normal heart, the fat distribution is limited to the atrioventricular and interventricular grooves, and along the major coronary branches (A, B); In the hypertrophic heart—the hypertrophy is mainly on the right-hand side—the adipose tissue also fills the epicardial spaces between these sites. Scale bar = 4 cm [56].

EAT increases in obese people [60] and may therefore cover the spaces between the ventricles and eventually all the epicardial surface. As epicardial fat volume increases, the coronary arteries become compressed between the fat and the myocardium. It's important to note that when epicardial fat increases, it extends over the anterior surface of the heart (more on the RV than on the LV) and over the LV midway between the apex and base [61]. Furthermore a small amount of adipose tissue extends from the epicardial surface to the myocardium, often following the adventitia of coronary artery branches [56]. It also should be noted that there is no fascia or similar tissue separating epicardial fat from the myocardium or even from coronary vessels, which means that there is a strong interaction between these structures [51]. Therefore, EAT can locally modulate both myocardium and coronary arteries [57]. Because of its anatomical proximity and the absence of fascial boundaries, epicardial adipose tissue can interact locally with the myocardium through secretion of adipokines and cytokines via two mechanisms, paracrine and vasocrine (Figure 6) [58].Paracrine signalling can be defined as when adipokines secreted from epicardial adipocytes overlying the lipid core of atherosclerotic plaques diffuse in interstitial fluid across the adventitia, media, and intima and interact respectively with vasa vasora, vascular smooth muscle cells and endothelium. On the other hand, vasocrine signalling can be defined as when adipokines secreted by epicardial adipocytes are released from epicardial tissue directly into vasa vasorum and then they are transported downstream to react with cells in the media and the intima around plaques [62].

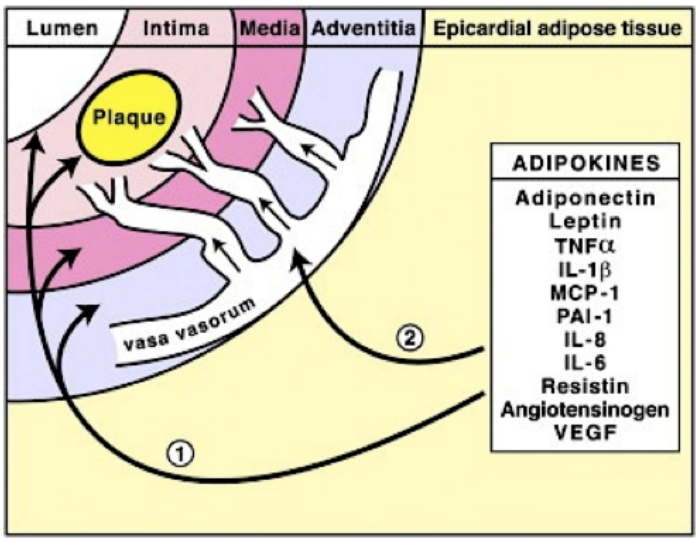

Figure 6 - Representative scheme of the paracrine (pathway 1) and vasocrine (pathway 2) mechanisms [62].

1.3.1.2 – Adipokines

Adipokines are proteins synthesized by adipose tissue and over 50 have already been identified [63]. The increased visceral adiposity is associated with a chronic low inflammatory state due to changes in function of adipocytes and macrophages. This indicates that there is not only an increase in the secretion of proteins but also a pathological state, i.e. inflammation, which results from changes in the secretory function disturbing the adipokines secretion [33, 61] (Figure 7). The term adipose tissue dysfunction is used for inflammatory-related hypersecretion of pro-atherogenic, pro-inflammatory and pro-diabetic adipokines [33].

In 1987, it was discovered adipsin and it was identified as an adipokine [64]. In 1993, tumour necrosis factor-alfa (TNF-α) was identified as a pro-inflammatory product of adipose tissue and it showed the existence of a link between obesity and inflammation [65]. In 1994, the discovery of leptin established beyond doubt the adipose tissue as an endocrine organ [66]. Likewise, the recognition of plasminogen activator inhibitor 1, an inhibitor of fibrinolysis, as an adipokine strongly up regulated in visceral adipose depots in obesity, established a linkage between obesity and thrombotic disorders [67]. Other adipokines produced by adipose tissue have also been identified, including interleukin 6 (IL-6), monocyte chemotactic protein 1 (MCP-1), resistin, visfatin and adiponectin [68]. Contrarily to these pro-inflammatory adipokines, adiponectin is the most abundant adipose-derived protein in the circulation (5–30 μg/ml) and its decline has been observed in obesity [50, 68]. Adiponectin has cardioprotective effects that were confirmed by the reduced apoptosis and inflammation levels observed in cultured cardiomyocytes and animals exposed to hypoxia-reoxygenation cycle after its administration [69]. Studies in experimental organisms showed that adiponectin protects against several metabolic and cardiovascular disorders that are associated with obesity [70]. Adiponectin decreased the size of cardiac lesion through modulation of pro-survival reactions, cardiac energy metabolism and inhibition of hypertrophic remodelling [71]. In fact, experimental studies on rodents have demonstrated that adiponectin inhibits hypertrophic signalling in the myocardium, suggesting that a decrease in the blood adiponectin levels could cause cardiac muscle hypertrophy and so that hypoadiponectinemia contributes to the worsening of diastolic dysfunction in hypertension-induced diastolic HF patients [72]. In addition to these adipokines, there is another that has had a great interest in research, fatty acid-

binding protein 4 (FABP4). Adipocyte fatty acid-binding is a member of the cytosolic fatty acid-binding protein family and is highly expressed in adipose tissue by means of adipocytes and macrophages [73]. Several animal-based and clinical studies have demonstrated that FABP4 has an important role in obesity-related insulin resistance, inflammation and atherosclerosis, suggesting FABP4 as a potential link between obesity and cardiometabolic diseases [74-76]. Moreover, the FABP4 has also been shown to directly suppress cardiomyocyte contraction in vitro suggesting a pathogenetic role of FABP4 in heart dysfunction [77]. According with these in vitro data, serum concentrations of FABP4 are elevated in HF patients and are associated with the incidence and severity of HF [78]. A recent study showed that increase of circulating FABP4 may contribute to LV diastolic dysfunction in obesity and affirm that FABP4 is a novel target for prevention of heart failure [79]. These data suggest that FABP4 may have a causal role in the pathogenesis of HF, particularly in obese subjects with metabolic alterations.

Low grade inflammation that accompanies obesity and its relation to plasma adipokines concentration have been shown to be associated with increased LVM and abnormalities of diastolic function [80]. A brief overview of the most important actions of adipokines is illustrated in Figure 7.

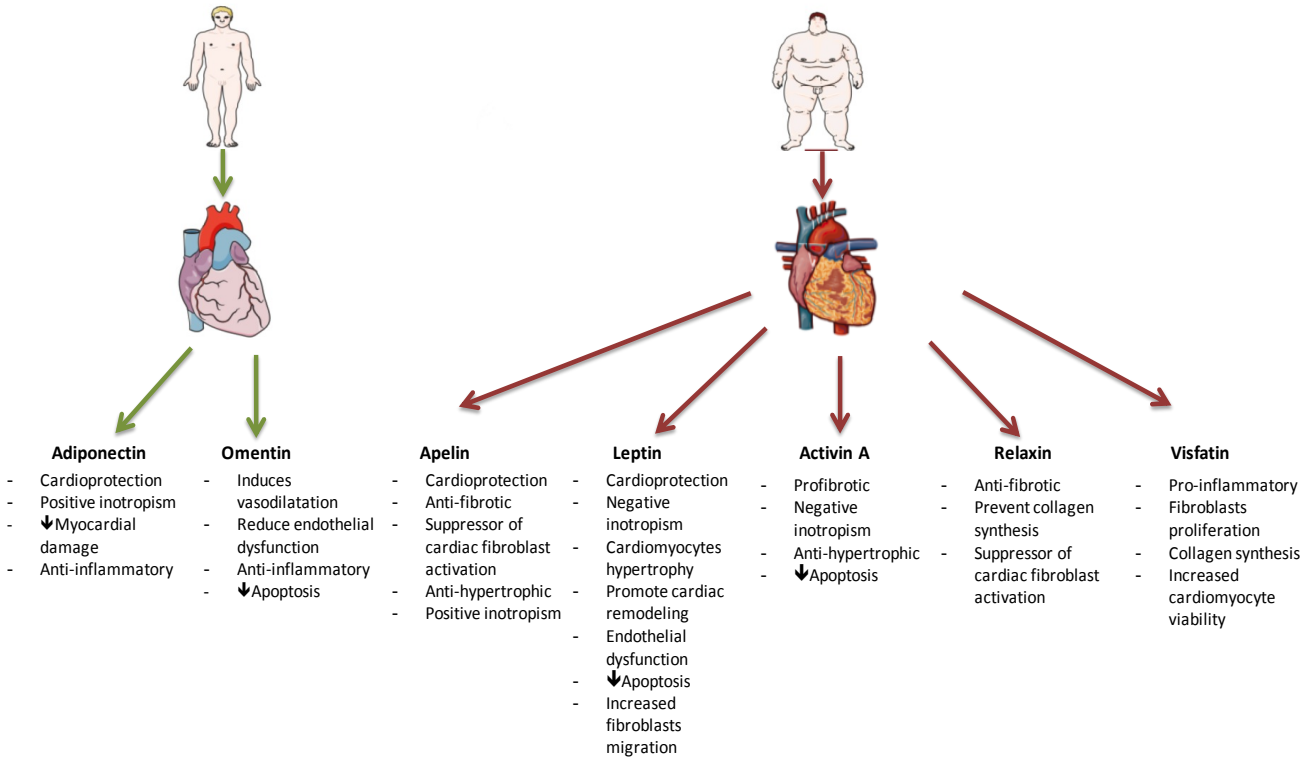

Figure 7 - Contribution of adipokines to obesity and metabolic syndrome abnormalities. The schematic overview illustrates some adipokines' actions with peripheral and central metabolic processes. IL-6 - interleukin-6; ROS - reactive oxygen species; RAS - Renin-angiotensin System; TNF-α - tumor necrosis factor-α. Adapted from [69].

1.3.1.3 - Impact of epicardial adipose tissue and diastolic function

In cases of extreme obesity, the epicardial fat can completely cover the heart and may extend up to 2 cm or more in thickness [62]. In addition, increased LVM, a hallmark of left ventricular diastolic dysfunction, is associated with increased epicardial fat thickness [81, 82]. Indeed, a strong correlation between increase epicardial fat thickness, enlarged atria and impaired RV and LV diastolic filling in morbidly obese subjects has been reported [83]. Additionally, in high-risk cardiac patients, EAT is described as a source of pro-inflammatory mediators, such as IL-6, TNF-α, MCP-1 and resistin as well as a source of protective anti-inflammatory and anti-atherogenic proteins, such as adiponectin [84, 85]. These facts show the potential role of epicardial adipose tissue as a reliable indicator of CV risk.

The epicardial adipose tissue can mechanically and functionally modulate the myocardium and vasculature thereby possibly playing a role not only in obesity-related atherosclerosis [57] but also in cardiac dysfunction. Adiponectin, resistin and leptin are molecules involved in the induction of endothelial dysfunction, mostly by modulation the inflammatory reaction [86, 87]. Piestrzeniewicz *et al.* [88] established a relation between

adiponectin, resistin and leptin with LV hypertrophy and abnormal LV relaxation. They highlighted the impact of leptin on the risk of abnormal LV relaxation, which was stronger after adjustment for obesity, suggesting that its deleterious effect is more significant in obese subjects. Barouch *et al.* [89] stated that leptin deficiency in obese mice leads to left ventricular hypertrophy. Moreover, Hong *et al.* [90] showed a negative correlation between the protective adipokine adiponectin and LVM, that is, the results presented a decrease in plasma adiponectin concentration associated with the progression of left ventricular hypertrophy with diastolic dysfunction. Therefore, leptin and adiponectin can be biochemical markers of obesity related to left ventricular hypertrophy and abnormal left ventricular relaxation.

Overall, the metabolic dysfunction that is due to excessive adipose tissue may partly result from an unbalance between the expression of pro- and anti-inflammatory adipocytes-derived substances thereby contributing to the development of obesity-linked complications [50] such as diastolic heart failure.

1.4 - Animal model of diastolic heart failure

The incidence of DHF continues to rise and its prognosis fails to improve partly because of lack of specific therapeutic approaches [91]. A comprehensive examination of cardiac structure and function and its association with morbidity and mortality is an important and necessary step toward meeting the drawbacks of diagnosis, prognosis, and treatment of patients with DHF [92]. Moreover, the absence of an appropriate animal model of DHF was restraining the progression on diastolic dysfunction comprehension. Recently, a full description of a rat model that meets the criteria of DHF was described, the obese ZSF1 [91]. ZSF1 rats were generated by crossing non-hypertensive lean female Zucker Diabetic Fatty rats (ZDF, +/fa) with lean spontaneously hypertensive HF prone male rats (SHHF/Mcc, +/facp) that share a common genetic background with Wistar Kyoto (WKY) rats and derive from spontaneously multifactorial hypertensive rats [93-98]. Both lean and obese ZSF1 animals inherit a hypertensive gene from the spontaneously hypertensive rat strain and show elevated blood pressure [94].

ZSF1 rats have myocardial hypertrophy induced by hypertension, more notorious in obese than in lean ZSF1 rats. The obese ZSF1 rats present considerable diastolic abnormalities such as increased left atrial area, prolonged time constant of isovolumetric

relaxation, elevated arterial elastance and end-diastolic pressure as well as an upwards shift of end-diastolic pressure-volume relation, thus highlighting a worse ventricular-vascular coupling. Systolic function remained preserved in lean and obese ZSF1 rats [91].

In terms of metabolic disturbances, obese ZSF1 animals developed obesity, abdominal adiposity, oral glucose intolerance, hyperglycemia and glycosuria, consistent with type II diabetes mellitus phenotype [99] and thus represent a good animal model of metabolic syndrome.

1.5 – Proteomic advances in cardiovascular diseases

The prevalence of DHF continues to rise more and more and its prognosis fails because of lack of knowledge about its underlying mechanisms [100]. Alterations of the CV system (or heart) in response to any pathology or acute injury have a major impact on the cellular environment, changing the proteins profiles. Proteins are involved in many cardiac cellular functions as well as its regulatory mechanisms. Additionally, they are modified in diseases as the cause or effect [101]. Proteomic technology enables detection of these changes, in either tissues, cells or associated biologic fluids [102]. “Proteomic” derived from “proteome” which was used at first time by Mark Wilkins in 1995 [103]. He used the term proteome to describe the entire complement of proteins expressed in a cell, tissue or organism. Specifically, the proteomic is the large-scale characterization of proteins and it provides detailed information about the changes in gene regulation, protein transcription, protein quantity, and protein post-translational modifications [104]. Thus, proteomic can be a tool of great value for studying changes in cardiac proteome.

As outlined in Figure 8, numerous steps are involved in proteomic: sample preparation, protein separation, quantification and identification.

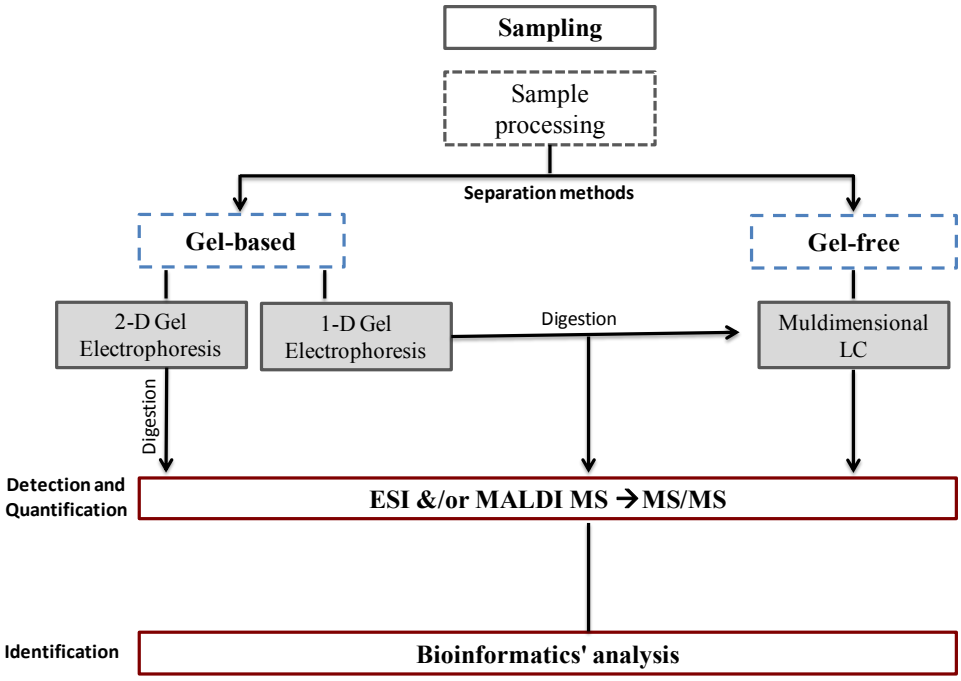

Figure 8 - Overview of the main differential proteomic strategies. LC – Liquid chromatography; MS – mass spectrometry; MS/MS – Tandem MS; MALDI - Matrix-Assisted Laser Desorption/Ionization; ESI - Electrospray Ionisation

1.5.1 - Methodological approaches

Current proteomic techniques can be categorized into two classes: (1) gel-based proteomic approaches, which include separation of proteins by gel electrophoresis (e.g. 2-dimensional gel electrophoresis (2DE)) followed by mass spectrometry (MS) analysis for identification of proteins, (2) and gel-free proteomics, which relies in the utilization of protein and peptide separation using liquid chromatography (Figure 8). These techniques have provided orientation for the study of changes in adipose tissue proteome involved in disorders related to cardiovascular diseases (Table 4).

Gel-based proteomics includes classical 1-dimensional (1D), native PAGE, and 2-dimensional (2D) electrophoresis (1DE and 2DE) [105]. A 1DE is especially more straightforward and simpler than any previous method of protein analysis, mainly, because it can be used to separate any proteins regardless of their inherent solubility in aqueous solution [106]. This approach was used by Salgado-Somoza *et al.* [107] and allowed to detect 41 proteins related with coronary artery disease (Table 4). However, due to its high resolution and sensitivity, the 2DE technique is a powerful tool for the analysis and detection of proteins from complex biological sources [108]. It is a protein profiling technique that carries out separation using the combination of two different separation

strategies. In the first dimension, proteins are separated based on their charge properties by isoelectric focusing (pI). Then, in the second dimension, proteins are resolved based on their molecular weight (MW) by sodium dodecylsulphate polyacrylamide gel electrophoresis (SDS-PAGE) [105]. The result is a set of spots to which can be assigned specific *X* and *Y* coordinates, unlike protein bands obtained in one-dimensional techniques. Each spot of the gel contains one or a very small number of proteins, depending on the complexity of the sample [109]. Thus, thousands of proteins can be separated in a single gel, allowing the determination of the *pI* values, MW and relative abundance [110]. Another aspect of 2DE is the ability to separate proteins based on the presence of post-translational modifications (PTMs) [105]. This technique has been applied in to adipose tissue, being generally employed on comprehension of mechanisms related with CVD [111] and obesity [112, 113] (Table 4).

Accordingly to Bland *et al.* [114] to obtain reliable and confident data with 2DE several replicates per sample are required to achieve a low variability. However, an improvement in 2DE, applying fluorescent labels to samples, named two-dimensional difference gel electrophoresis (2D-DIGE), has allowed the analysis of two or three marked protein samples in the same gel, reducing gel-to-gel variation and increasing reproducibility [115, 116]. This strategy enabled to identify and evaluate eleven proteins involved in the progression of type II diabetes in pre-obese subjects [117] (Table 4). Although 2DE can provide valuable information, it suffers from many limitations, such as difficulty to detect low abundance proteins and analyse hydrophobic proteins or proteins with extreme *pI* or MWs (e.g. cannot detect proteins below the 10kDa) [118].

Face to the constrains and limitations presented in gel-based approaches, gel-free has been developed to improve protein characterization with respect to biological function or biochemical structure, allowing specific protein classes and protein modifications to be isolated [119]. This technique solves some limitations of 2DE, i.e., it has greatest depth of protein coverage and widest dynamic range of size of proteins identified [120]. This technique can be used to separate proteins according to their molecular mass, isoelectric point or hydrophobicity [105]. There are two strategies using gel-free, 1D-LC and 2D-LC. 1D-LC can be used to separate proteins according to their molecular mass, isoelectric point or hydrophobicity. On the other hand, in 2D-LC the proteins are separated in first dimension by an isoelectric point and in second dimension by hydrophobicity [121].

Adopting this strategy, Kim *et al* [122] identified 2338 proteins in visceral adipose tissue in type II diabetes (Table 4). In addition to these approaches, the gel-free can be combined with gel-based to improve the protein separation. Alvarez-Llamas *et al.* [123] used this method identifying 295 proteins (Table 4). First the sample was submitted to 1DE and next it was applied 1D-LC to separate proteins from each gel band with more specificity.

Liquid chromatography technologies help to reduce sample complexity, being a common strategy the use of a preparative chromatography previous to LC-MS/MS analysis. Moreover, it enables the sample fractionation and increase substantially proteome coverage [124]. The combination of successive chromatography steps for peptides separation, according to various physicochemical properties and/or affinity interactions, is named multi-dimensional protein identification technology (MudPIT) and from this principle results the increase of dynamic range of protein identification and several samples with less complexity [105].

After proteins separation, it follows the respective detection and identification. The traditional approach to identify proteins is its enzymatic digestion (e.g. trypsin) and analysis of peptides by mass spectrometry. Three approaches are generally used for identifying of proteins: peptide mass fingerprint (PMF), peptide fragment fingerprinting (PFF) and *de novo* sequencing [125]. The most common protein identification technique is PMF. In this case, the *m/z* ratio obtained for each peptide after enzymatic or chemical digestion is accurately measured and compared with all theoretical masses present in databases obtained by *in silico* proteolytic digestion [126].

Mass spectrometry techniques are the most widely used tools for protein analysis and identification. Different mass spectrometry methods are classified in distinct ionization processes, and two of them are widely applied in the study of proteomics [125]. In matrix-assisted laser desorption/ionization (MALDI), the sample that will be analysed is incorporated into a matrix that promotes ionization containing acid components such as α-cyano-4-hydroxycinnamic acid, which is activated by laser and results in the formation of sample ions. These enter into the gas phase and are analysed [127]. The peptide mass-to-charge ratios are matched to theoretical fingerprints, derived from sequence databases, in order to identify the protein of interest. These theoretical fingerprints are based on the peptides that are expected to produce when digesting proteins with a specific protease. For example, digestion with trypsin will always cleave a protein in the carboxylic side of lysine

and arginine residues, resulting in a predictable peptide mass fingerprint [128]. Another technique is electrospray ionisation (ESI) and is achieved by spraying a solution through a charged needle at atmospheric pressure towards the inlet to the mass spectrometry; the voltage applied to the needle tip and a pressure differential result in the formation of ions for mass analysis and their transfer into the mass spectrometer [129]. This approach is good to analyse compound multi-loaded [125].

The analysis of proteins/peptides by MS produces a considerable amount of data, being necessary the use of bioinformatics [130]. There are several programs able to perform the analysis, of which are examples SEQUEST and MASCOT [125]. These programs are powerful search engines that correlate un-interpreted MS spectra of peptides with amino acid sequences from protein and nucleotide databases to identify proteins. [130, 131].

Table 4 - Summary of proteomic analysis methodologies used for epicardial and visceral adipose tissue

Methodologies	Goal	Sample	Pathology	Results	Main findings	Ref.
2DE-MALDI-TOF/TOF-MS	Identification of the protein expression profiles of EAT and SAT and analysis of molecules that characterize EAT in patients with cardiovascular disease.	EAT of the right ventricle and SAT of the thorax human	Patients undergoing heart surgery (valve replacement or coronary artery bypass graft)	8 proteins identified	In cardiac patients the expression of proteins in EAT were: Up-regulated: GSTP1; PDIA1; PGAM1and Down-regulated: CATA	[111]
2DE-MALDI-TOF/TOF-MS/MS	Characterization of the secretome of rat adipose tissue explants from different anatomical localizations and its differential analysis.	Visceral, subcutaneous and gonadal adipose tissue of the Sprague Dawley rat	Obesity	106 proteins of the visceral fat identified; 49 proteins of the subcutaneous fat; 53 proteins of the gonadal fat	Proteins more abundant in visceral fat: Transgelin, Heat shock protein 60KDa, Peptidyl-prolul cis-trans isomerase A, Actin, Omega-amidase NIT2, Enoyl-CoA hydratase, Gelsolin, Thrombospondin-1.	[112]
SDS-PAGE-LC-MS/MS	Characterization of the adipose tissue secretome	Human visceral adipose tissue secretome	Non-carcinogenic gynaecologic disorders	259 proteins identified	This study revealed that 108 of 259 proteins were secreted following a classical pathway (endoplasmic reticulum/Golgi-dependent pathway). Of 108 secreted proteins, 70 proteins (such as adiponectin, adipsin, gelsolin, macrophage colony-stimulating factor-1 (MCSF), pigment epithelium-derived factor, plasma retinol-binding protein, and PAI-1 among others) were considered genuine adipose tissue-secreted proteins.	[123]
2DE-MALDI-TOF	Assessment of differences in the proteome and the secretome between epicardial and subcutaneous adipose tissue (SAT) from patients with and without CAD.	Human epicardial adipose tissue	Coronary artery disease	41 proteins identified	This study showed that in CAD patients, the expression of proteins in EAT were: Up-regulated: ALB; FABP4; GPI and SERPINA1 and Down-regulated: APOA1	[107]

Table 4 - (Continue…)

Methodologies	Goal	Sample	Pathology	Results	Main findings	Ref.
2DE-LC-MS/MS - Western Blot	Comprehension about proteomic analysis of VATs in drug naive, early T2DM patients and subjects with normal glucose tolerance	Human visceral adipose tissue	Type II diabetes mellitus	2338 proteins identified	This analysis revealed that 444 up-regulated proteins were mainly involved in inflammatory/immune responses, cytoskeleton, organization-related processes, responses to ROS and oxidative stress while 328 down-regulated proteins were mainly involved in glucose and fatty acid metabolic processes that highly contribute to T2DM pathogenesis	[122]
2D-DIGE-MALDI-TOF/TOF	Comprehension the mechanisms involved in the progression to overt diabetes in pre-obese subjects	Human visceral adipose tissue	Type II diabetes	11 proteins identified	Diabetic patients showed increased VAT abundance of glutathione S-transferase Mu 2, peroxiredoxin-2, antithrombin-III, apolipoprotein A-IV, Ig κ chain C region, mitochondrial aldehyde dehydrogenase and actin, and decreased abundance of annexin-A1, retinaldehyde dehydrogenase-1, and vinculin, compared with their non-diabetic counterparts.	[117]
2DE-MALDI-TOF/TOF	Investigate differentially expressed proteins of visceral adipose tissues between low-fat diet-fed obesity-resistant and obesity-prone c57Bl/6 mice	Visceral adipose tissue of c57Bl/6 mice	Obesity	14 proteins identified	Proteomic analysis showed that ubiquinol-cytochrome c reductase core protein 1 (Uqcrc1) and enolase 3, β muscle were decreased in the visceral adipose tissues of the obesity- prone mice, while monoglyceride lipase (MGll) and glucose-6-phosphate dehydrogenase (G6PdH) X-linked were increased.	[113]

The studies of Table 4 present several proteins matched between them (Appendix A - Supplemental Table A1). The main proteins shared between the studies of Table 4 are actin cytoplasmic-1 (ACTB), glutatione-S-transferase-P (GSTP1), fatty acid-binding protein 4 (FABP4), protein DJ-1 (PARK7), peroxiredoxin-2 (PRDX2), peroxiredoxin-3 (PRDX3), Ig kappa chain C region (IGKC), retinal dehydrogenase (ALDH1A1), L-lactase dehydrohenase B chain (LDHB) and alpha-2-macroglobulin (A2M) (Table 5). Table 5 presents the genes of the respective proteins and its expression in each study.

Table 5 - Genes of the main proteins shared between studies of the Table 4 and their expressions.↑- Proteins up-regulated; ↓- Proteins down-regulated; − - Proteins not identified; NPEA – no protein expression was analysed.

	Reference of the study						
Gene name	[111]	[112]	[123]	[107]	[122]	[117]	[113]
ACTB	−	−	NPEA	−	↑	↑	−
GSTP1	↑	−	NPEA	↑	NPEA	−	−
FABP4	−	↑	NPEA	↑	↑	−	−
PARK7	−	NPEA	NPEA	NPEA	−	−	−
PRDX2	−	NPEA	NPEA	NPEA	NPEA	↑	−
PRDX3	−	NPEA	NPEA	−	NPEA	−	−
IGKC	−	NPEA	NPEA	NPEA	↑	↑	−
ALDH1A1	−	NPEA	NPEA	−	NPEA	↓	−
LDHB	−	NPEA	NPEA	−	NPEA	−	−
A2M	−	−	NPEA	NPEA	NPEA	−	−

In Table 5 it is possible to observe that independently of the pathophysiology, the majority of proteins are up-regulated in relation to their controls. This fact is consistent with the notion that metabolic dysfunction may partly result from an imbalance in the expression of pro- and anti-inflammatory adipokines thereby contributing to the development of obesity-linked complications [50], such as diastolic heart failure. It is also important to note in Table 5, that although these (and many others) proteins have been identified, its relative abundance analysis is missing. This can be a problem regarding the comprehension of many mechanisms involved in metabolic disorders. In this way, its research is important.

Studies using proteomic technologies have yielded examples of novel insights into the mechanisms of obesity-related diseases, particularly in type II diabetes mellitus and coronary disease (Table 4). However, as observed in Table 4, there are no studies focusing on the impact of epicardial or visceral adipose tissue on diastolic heart failure. Thus, the integration of proteomics is needed to clarify complex protein changes associated not only

with diastolic dysfunction but also with pharmacological interventions taken in response to this dysfunction.

1.6-Objective

Diastolic heart failure is more and more an important cause of cardiovascular mortality and morbidity. Although the knowledge of metabolic changes may help in comprehension of the mechanisms involved in this pathophysiology, its proteome and respective expression remain unknown. Therefore the aim of the present work is to understand the changes in proteins that occur in the diastolic dysfunction during obesity. In order to achieve this goal we intend to:

- Characterize epicardial and visceral adipose tissue proteome of the obese animals presenting DHF and to compare them with lean control rats
- Assess and quantify proteome profile and association of their expression changes with diastolic dysfunction.

CHAPTER 2

MATERIALS AND METHODOLOGY

2.1. - Experimental Design

In order to achieve the proposed aims for this study, the experimental approach shown in Figure 9 was performed. Briefly, first the optimization of a protocol for protein extraction from different tissues (epicardial and visceral fat) was performed. After that, it was done the study of the visceral adipose tissue proteome in obese and lean ZSF1 rats in order to compare them. Six ZSF1 rats were divided into two groups: obese animals with diastolic dysfunction (n=3) and the correspondent lean animals (n=3). After 20 weeks of age, animals were sacrificed and epicardial and visceral fat was collected. The tissue samples were immediately frozen and stored at -196 °C. The experimental groups and methodological approaches used are described in the following sections.

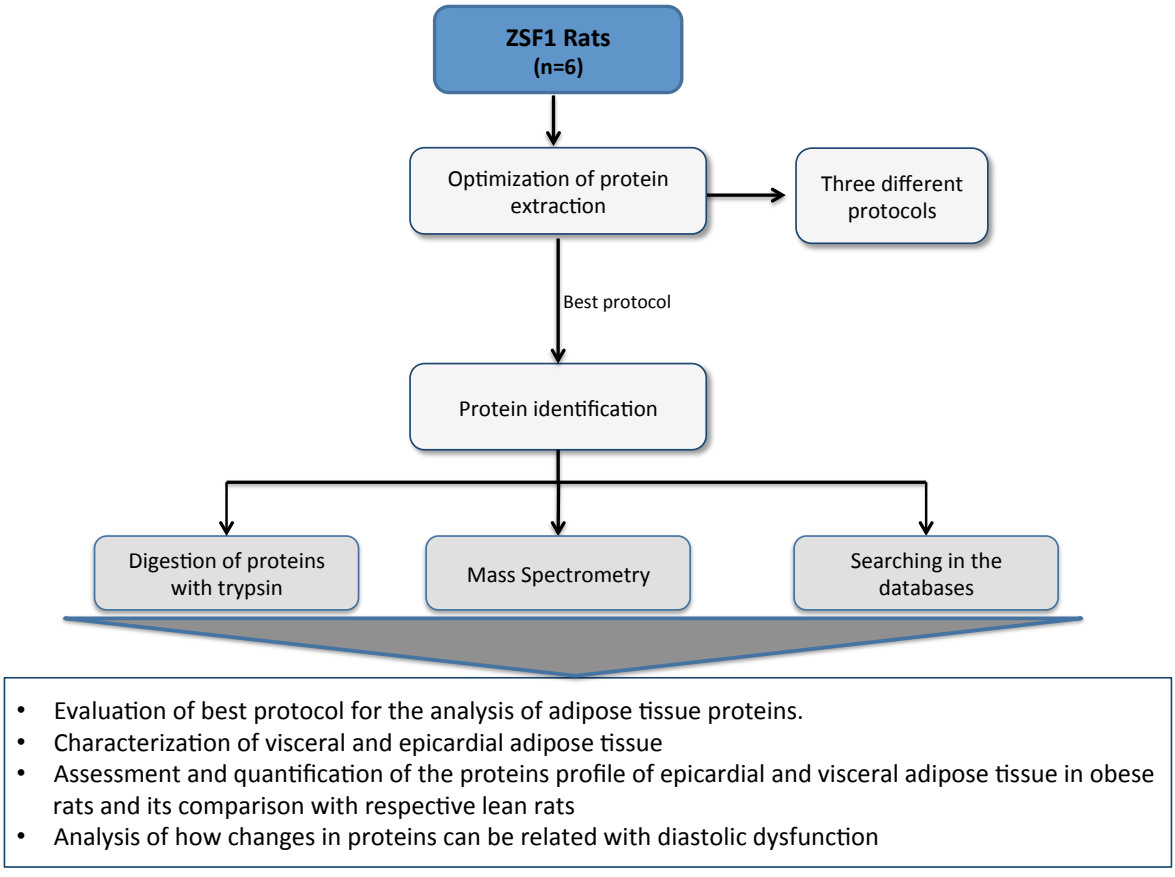

Figure 9 - Scheme of the methodological procedures used in the analysis of different tissues of ZSF1 rats

2.2 – Methods

2.2.1 – Animal Protocol

All animal experiments were performed according to the Portuguese law for animal welfare and accordingly to the Guide for the Care and Use of Laboratory Animals published by the National Institutes of Health (NIH Publication 85-23, Revised 2011). The Faculty of Medicine of Porto is a governmental institution, granted approval by the Portuguese government to perform animal experiments.

The animal protocol was accomplished using six ZSF1 rats (Lean ZSF1, n= 3; obese ZSF1, n= 3). The animals were obtained at the age of 9 weeks from Charles River (Barcelona, Spain). During the experimental protocol, animals were housed in groups of two rats/cage in individually ventilated cages (IVCs), maintained on a 12-hour light-dark cycle, with full access to the recommended diet (LabDiet® 5008, International Product Supplies Ltd.) and water *ad libitum*. The IVCs were maintained under controlled environment temperature (22°C), relative humidity (30–70%), and air exchange rate (40–50 air changes per hour). For metabolic characterization, animals were periodically subjected to metabolic cage studies, oral glucose-tolerance and insulin-resistance tests. For cardiac function assessment, terminal hemodynamic evaluations were performed by rats' 20th weeks of age. The Physiology and Cardiothoracic Surgery Department of Faculty of Medicine of Porto provided all this information about the animal characterization.

2.2.1.1 - Metabolic studies and renal-function assessment

After 24-hours of metabolic cages adaptation (Techniplast, Buguggiate), the hydric and energetic ingestion as well weight gain and urinary output was registered and 24-hour urine specimen collected. Twenty-four hours later and 12 hours of fast, the animals were successively submitted to oral glucose-tolerance and insulin-resistance tests. Glycaemia was assessed after 15, 30, 60, 90 and 120 minutes following the administration of glucose (1g.Kg^{-1}) and insulin (0.5 U.Kg^{-1}) by gavage and intraperitoneal injection, respectively.

2.2.1.2 - Echocardiography evaluation

An echocardiography evaluation was performed at the beginning of the study, at the 10th week, and repeated at the 14th and 18th week. The animals were sedated (mixture of 8% of and 1-2.5% of sevoflurane with oxygen, for induction and maintenance,

respectively), endotracheally intubated and mechanically ventilated (150 min^{-1}, 100% O_2, 14–16 cmH_2O inspiratory pressure, with tidal volume adjusted to animal weight, and 4 cmH_2O end-expiratory pressure (TOPO Small Animal Ventilator, Kent Scientific Inc.). Two-dimensionally (2D)-guided M-mode echocardiography and pulse-wave Doppler echocardiography were performed using an echocardiographic system equipped with a 15-MHz linear-transducer (Sequoia 15L8W), and the exams were performed with the animals placed over a heating pad, in the prone left lateral decubitus position with a full chest shaving.

Parasternal long-axis images of the aorta, left atrium and LV were first obtained; 90° rotation from the long-axis view produced a short axis view of the heart. M-Mode short-axis view at the level of the papillary muscle was used to assess wall thickness as well as systolic and diastolic left ventricular cavity dimensions. From these measurements end diastolic and end systolic volumes, (EDV and ESV, respectively), fractional shortening (FS), ejection fraction (EF) of the LV, stroke volume (SV) and cardiac output (CO) were derived. The following Doppler and tissue Doppler measurements were taken using the apical four-chamber early diastolic filling peak velocity (E wave), late diastolic peak velocity (A wave), E/A ratio, deceleration time (DT), isovolumic relaxation time (IVRT) , isovolumic contraction time (IVCT) , early peak diastolic filling velocity (E'), late peak diastolic filling velocity (A') and mitral annular systolic velocity (S'). Three representative cycles were measured per rat and their average was calculated.

2.2.1.3 - Hemodynamic instrumentation

At their 20^{th} weeks of age, after intraperitoneal sedation by a mixture of fentanyl and midazolam (100µg.kg^{-1} e 5mg.kg^{-1}, respectively), rats were anaesthetized (with a mixture of 8% and 1-2.5% sevoflurane with oxygen for induction and maintenance, respectively), endotracheally intubated, (mechanically ventilated (150 min^{-1}, 100% O_2, 14–16 cmH_2O inspiratory pressure, with tidal volume adjusted to animal weight, and 4 cmH_2O end-expiratory pressure; TOPO Small Animal Ventilator, Kent Scientific Inc.) and placed over a heating pad (38°C).

To compensate for perioperative fluid losses, the femoral vein was cannulated and warm Ringer lactate's solution fluid was administered with a perfusion pump (Multi-Phaser™, NE-1000, New Era Pump Systems). Under surgical microdissection (Wilde M651, Leica microsystems), left thoracotomy was performed, pericardium was widely

opened and pressure–volume (PV) catheters were implanted through the apex along the LV and the RV (SPR-838 and PVR-1045, Millar Instruments, Houston, TX, respectively). After 15 min of stabilization, recordings were done at the end-expiration under basal conditions and transient IVC and aortic occlusions in order to assess PV relationships. The systemic blood pressure was recorded by advancing the LV catheter to the aorta. Parallel conductance and field inhomogeneity were estimated by 50μL 10% saline injections and cardiac output (CO) measurement (Perivascular Flowmeter Module, AD Instruments Technology), respectively. Data were continuously acquired (MPVS 300, Millar Instruments), digitally recorded at 1000 Hz (ML880 PowerLab 16/30, Millar Instruments), and analyzed (PVAN 3.5™, Millar Instruments). Heart rate, stroke volume, end-diastolic volume (LVEDV), end-systolic volume (LVESV), EF, end-diastolic pressure (LVPED) and end-systolic pressure (LVPES) were determined from the pressure–volume tracings. Effective systemic arterial elastance, as a measure of LV afterload, was calculated dividing LVPES by stroke volume. Maximal LV wall-stress [LVW_{STRESS}] was calculated from LV pressure [P(t)] and volume [V(t)] and LV wall volume (Vwall) according to the following formula: LVW_{STRESS}=P(t)1+3[V(t)/Vwall. LV wall volume (Vwall) was approximated as the sum of the LV free wall mass and half of the interventricular septum mass. Relaxation rate was estimated with the time constant τ using the Glantz method.

At the end the animals were euthanized under anaesthesia (100 $mg.kg^{-1}$ pentobarbital sodium endovenous). Heparinised blood was used for volume calibration using a cuvette with standard wells (910-1048, Millar instruments). The heart, the RV, the LV, the interventricular septum, and the lungs were weighed, snap frozen in liquid nitrogen and stored at −196°C. The weights were normalized to tibial length given the body weight differences observed between groups. Moreover, visceral adipose tissue (from intestinal region) and epicardial adipose tissue were collected and were immediately frozen and stored at -196 °C.

2.2.1.4 - Statistical analysis.

Statistical analysis was performed using Prim (version 5.0) and SigmaStat (version 3.5). Analysis by two-way repeated-measures ANOVA was performed when repeated measures were performed to the same animal and one-way ANOVA for comparison among groups. When treatments were significantly different, the Holm-Sidak test and Bonferroni test was selected to perform pairwise comparisons. After a logarithmic

transformation, a four-parameters logistic curve was used to determine adipokines levels accordingly to ELISA manufacturer instructions. Correlations between two continuous variables were assessed with Pearson correlation analysis. Group data are presented as means ± SEM. Statistical significance was set at $P < 0.05$.

2.2.2 – Optimization of Protein Extraction

2.3.2.1 - Protein extraction solution

Before protein extraction protocol, the samples were divided in similar weights. Frozen samples (EAT and VAT) were slowly thawed in the ice and then were washed three times by cold phosphate buffer saline (PBS) to remove excessive blood contamination. Then these fat tissues (with ~0.100 – 0.200g wet weight) were submitted to three protein extraction protocols (Figure 10). In **protein extraction protocol – TRIS (PT),** the fat samples were homogenized in 125mM Tris-HCL, 2% sodium dodecyl sulfate (SDS), 50mM dithiothreitol (DTT) and 10µL of phenyl methyl sulfonyl fluoride (PMSF) by Potter-Elvehjem with Teflon pestle. Then, samples were sonicated (Sonics vibra cell sonicator - Time-30s, Pulse-10 01 and Amplitude-70%) to better disrupt the cells. The lysate was centrifuged (Centrifuge 2-16 KC, Sigma, Germany) at 14000*g* for 30 min at 4ºC and the supernatant was carefully recovered to a new microtube. The removal of the lipidic pellet is crucial since it interferes with proteins solubilisation and subsequent separation of proteins from lipids [122]. In p**rotein extraction protocol – UREA (PU),** fat tissues were homogenized in 8M urea, 2M thiourea, 2% 3-[(3-cholamidopropyl) dimethylammonio] propane sulfonate (CHAPS), 2% ampholytes (pH 3-10), 1% NP-40, 50mM DTT and 10µL PMSF. Afterwards samples were sonicated and the lysate was treated similarly to protocol-Tris. Finally, in **protein extraction protocol – TRIS and UREA (PTU),** the samples were submitted first to the extract solution of PT and then its pellet was submitted to PU.

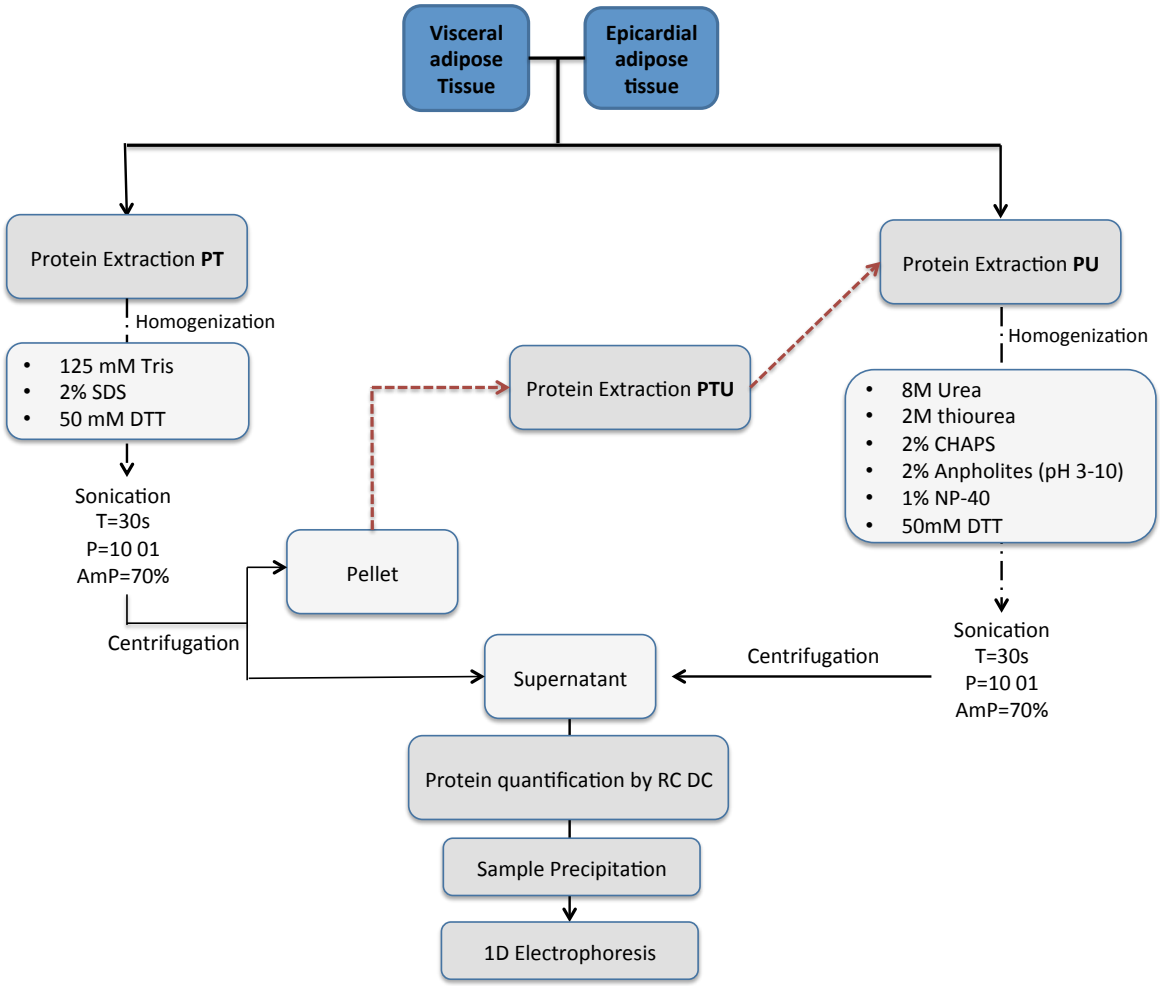

Figure 10 - Scheme of three proteins extraction protocols. Protein extraction PT – protein extraction protocol-Tris; Protein extraction PU – protein extraction protocol-Urea; Protein extraction PTU – protein extraction protocol-Tris and Urea.

2.2.2.2 – Protein quantification by RC DC assay

The amount of total protein was determined in adipose tissue samples by the RC DC assay (Bio-Rad, Hercules, CA, USA). This assay is based in Lowry *et al.* [132] and allows quantifying proteins in the presence of reducing agents and detergents.

A calibration curve was prepared using eight bovine serum albumin (BSA) dilutions ranging from 0.05mg/mL to 1mg/mL. Ten µL of each samples and standard solutions were pipetted to separate microtubes 125µL of reagent I and IIwere added and this solution was stirred in a vortex, followed by a centrifugation (Microcentrifuge, Centurion scientific) at 16000g for 5 minutes. The supernatant was carefully removed and the microtubes were placed in SpeedVac (Speed Vac Plus SC 210 A, Thermo Savant, USA) removing liquid in totality. Posteriorly, 20µL of S reagent from the Bio-Rad kit were added to 1mL of A reagent (to make A´ reagent). Then, 50µL of A´ reagent and 400µL of

B reagent were added to samples and standard solutions and incubated at room temperature for 15 minutes. Finally, the absorbance of samples and standard solutions was measured at 750nm in a microplate reader (Multiskan GO, ThermoScientific).

2.2.2.3 – One dimensional electrophoresis (1DE)

In order to evaluate the expression of proteins, these were separated according to their molecular weight on polyacrylamide gels in denaturing and reducing conditions. The 1DE was performed simultaneously for all samples (under study) in order to reduce inter-assay variability. Firstly, a given sample volume corresponding to 50μg of protein of the each sample were precipitated with frozen acetone (with an amount of 6 times the amount of proteins sample) during 2 hours. The precipitated sample was centrifuged at 14000*g* for 30 minutes at 4ºC and the supernatant was carefully removed with micropipette. Posteriorly, the pellet was dissolved in a 15μL of loading buffer and was placed in the Thermocell mixing block MB-102 at 100ºC during 5 minutes at 600rpm. After solubilizing the pellet in loading buffer, each sample was loaded on a 15% SDS-PAGE. A 200V electrophoresis was performed up to the point where the dye reached the bottom of the gel. For bands visualization, the gel was revealed with Blue safe for 1 hour and then the gel was placed in distilled water.

2.2.3 - Analysis of the 1DE data

The gels were scanned using a Gel Doc XR+System (Bio- Rad) and bands intensity quantified by Image Lab software. The quantification of each protein band was performed on images of 1DE gels based on optical densities. All data were exported to Graphpad Prism 6 for statistical analysis.

2.2.4 – Protein identification

2.2.4.1 – Protein digestion with trypsin

The protocol of the digestion with trypsin was carried out using modified bovine trypsin - N-tosyl-L-phenylalanine chloromethyl ketone (TPCK, AB Sciex, USA). Protein bands were excised from the gel, cut into small pieces, and transferred into a 96-well microliter plate. Each gel piece was subjected to tryptic digestion. Briefly, each gel piece was washed and aspired by vacuum twice with 50μL of 28.3mM ammonium bicarbonate and 100% acetonitrile, dried in the Speedvac and rehydrated with 20μL of trypsin (25

μg/2mL H_2O) and 30μL of 50mM of ammonium bicarbonate and, lastly, incubated at 37°C overnight. After digestion, the gel pieces were washed and aspired by vacuum with 10% formic acid. Then, they were washed and aspired by vacuum twice with a solution containing 100% acetonitrile (ACN) and 10% formic acid in a proportion 1:1. Finally, the peptides were extracted to new 96-well microliter plate and were completely dehydrated in the SpeedVac and stored at -80ºC.

2.2.4.2 –Liquid chromatography separation of peptides

Samples were rehydrated with 5μL of a solution of 50% ACN and 0.3% trifluoroacetic acid (TFA). The samples were sonicated for 3 minutes and then spined down. Twenty-five μL of 0.1% TFA and was executed the sonication and spin again. Finally, 11μL of each sample was transferred for a new 96-well microliter plate and was analysed.

The nano-HPLC separation was performer on the Ultimate 3000 module (LC Packings) using a capillary column (Zorbax SB C18 300; 0.75μm an internal diameter, 15cm length). It was used the solvent A, water/ACN/TFA (95:5:0.05 v/v/v) and solvent B, water/ACN/TFA (10:90:0.05, v/v/v). 8μL of the sample was injected. The separation was performed using a linear gradient (5-55% A for 30 min, 55-80% over 10 minutes, 80-5% during 5 minutes) with a flow rate of 0.3uL/min. The various fractions separated were applied on a plate for MALDI analysis.

2.2.4.3 – Mass spectrometry analysis and database searching

The MALDI-TOF/TOF MS analysis was performed using a 4800 MALDI-TOF/TOF Analyser (Applied biosystems, Foster City, CA, USA) with reflectron in positive mode and spectra obtained in the mass range from 700 to 4000Da, with 1500 laser shots. The spectra were processed using T2S software (v.1.0; Matrixscience) and analysed by internal Mascot software (Version 2.1.0.1, Matrix Science Ltd, UK) for protein/peptide identification based on peptide mass fingerprints and MS/MS data. Searches were performed based on the SwissProt protein database for Rattus. The parameters defined were a peptide tolerance of 40ppm, two missed cleavages and propionamide (C) as variable modification.

CHAPTER 3

RESULTS

3.1 Characterization of the animal model

3.1.1. Weight gain, energy intake, body composition and metabolic function

As presented in Table 6, animals showed considerable body weight differences, therefore, most of the morphometric parameters measured were normalized to tibial length. The obsese ZSF1 present higher body weight than ZSF1 lean, and shows hypertrophic heart, with a significant increase in heart and LV+septum weight normalized to tibial length. As for body composition, differences were observed in obese group showing a substantial increase in kidney, liver, lungs, perigonadal and perirenal fat pad weights normalized to tibial length compared to the non-obese group (Table 6).

Table 6 - Morphological data. Left ventricle (LV); inter-ventricular septum (IVS); right ventricle (RV) tibial length (TL). The values are represented as means ± S.E.M. P<0.05: * vs ZSF1 Ln.

	ZSF1 Ln	ZSF1 Ob
Weight/TL(mg.mm^{-1})	416 ± 8	601 ± 10*
TL (mm)	42.1 ± 0.4	40.9 ± 0.4*
Heart weight/TL (mg.mm^{-1})	34.4 ± 1.2	40.0 ± 1.3*
LV+IVS weight/ TL (mg.mm^{-1})	16.6 ± 0.8	19.7 ± 1.1
Cardiomyocyte area (μm^2)	536±15	628±14*
RV weight/ TL (mg.mm^{-1})	4.5 ± 0.3	5.5 ± 0.3
Lung weight/ TL (mg.mm^{-1})	53 ± 2	75 ± 3*
Liver weight/ TL (mg.mm^{-1})	314 ± 12	906 ± 55*
Kidney weight/ TL (mg.mm^{-1})	26.0 ± 0.8	37.1 ± 0.9*
Perirenal fat weight/ TL (mg.mm^{-1})	58 ± 6	362 ± 12*
Perigonadal fat weight/ TL (mg.mm^{-1})	56 ± 5	161 ± 6*
Gastrocnemius weight/ TL (mg.mm^{-1})	63 ± 2	53 ± 1*

Regarding to metabolic function, ZSF1 Ob shows hyperlipidemia, proteinuria, impaired glucose tolerance, insulin resistance, hyperglycemia, consistent with the diagnosis of metabolic syndrome (Table 7).

Table 7 - Metabolic function data. Oral glucose tolerance test (OGT); Insulin resistance (IR); AUC: area under curve. The values are represented as means ± S.E.M. P<0.05: * vs ZSF1 Ln.

	ZSF1 Ln	ZSF1 Ob
Proteinuria level ($mg.dL^{-1}$)	29±1	174±9*
Glycaemia level ($mg.dL^{-1)}$	73±5	134±10*
OGT AUC ($mg.dL^{-1}.h^{-1}$)	105±5	224±10*
IR AUC ($mg.dL^{-1}.h^{-1}$)	105±5	152±9*
Cholesterol level ($mg.dL^{-1}$)	68±3	240±21*

3.1.2. Cardiac functional and structural changes

In both echocardiographic (Table 8) and terminal hemodynamic evaluation (Table 9) ZSF1 Ln, ZSF1 Ob showed preserved cardiac index, ejection fraction and indexed end-diastolic volume (Table 9). In the ZSF1 groups the maximum rate of pressure rise and the slope of the end-systolic pressure-volume relationship were increased, denoting hypercontractility (Table 9). However, when left ventricular mass was accounted, as in preload-recruitable stroke work, this increase was no longer significant (Table 9). Overall cardiac performance as assessed by the Tei myocardial performance index was also not altered (table 8). The raise in arterial elastance with preserved systolic function indexes indicates worse in ventriculo-vascular coupling ZSF1 Ln, ZSF1 Ob due to the hypertension displays by both groups (Table 9).

Contrarily, significant disturbances of diastolic function were observed in ZSF1 Ob compared with ZSF1 Ln (Tables 8 and 9). Namely, an increase in the maximum velocity of early diastolic transmitral flow to maximum velocity of myocardial displacement ratio at the lateral mitral annulus also in early diastole (E/E') during echocardiographic evaluation (Table 8) and prolonged time constant of isovolumetric relaxation τ, elevation of end-diastolic pressures and an upward shift in the end-diastolic pressure-volume relationship in terminal haemodynamic evaluation (Table 9). Additionally, and also only in ZSF1 Ob it was observed increased left atrial area on echocardiography (Table 8) and an increased lung weight on terminal morphometric evaluation (Table 6).

Table 8 - Echocardiographic assessment of diastolic parameters. Ejection fraction (EF); Ratio of mitral velocity to early diastolic velocity of the mitral annulus (E/E'); Early and late LV filling velocities ratio (E and A, respectively); Heart rate (HR); left ventricle (LV). The values are represented as means ± S.E.M. P<0.05: * vs ZSF1 Ln.

	ZSF1 Ln	ZSF1 Ob
EF (%)	74 ± 2	75 ± 2
Cardiac index (ml.min^{-1}.cm^{-2})	212 ±16	255 ± 22
HR (bpm)	336 ± 9	328 ± 16
LV mass (mg)	517 ± 29	714 ± 33*
E/E'	12 ± 0.60	17.20 ± 0.80*
E/A	1.61 ± 0.12	1.32 ± 0.08
Left atrium area (mm)	2.60 ± 0.20	3.60 ±0.20*
MPI (Tei)	0.76 ± 0.05	0.78 ± 0.02

Table 9 - Hemodynamic data. Arterial elastance indexed (EAI); Body surface area (BSA); Cardiac Index (CI); Constant time of isovolumic relaxation (τ); Diastolic arterial pressure (DAP); End-diastolic pressure (EDP); End-diastolic pressure-volume relations (EDPVR); End-diastolic volume indexed (EDVI); End-systolic volume indexed (ESVI); Ejection fraction (EF); Heart rate (HR); Maximal velocity of pressure rise and decrease (dP/dtmax, dP/dtmin, respectively); Mean arterial pressure (MAP); Preload recruitable stroke work (PRSW); Systolic arterial pressure (SAP); Stroke volume indexed (SVI); Stroke work indexed (SWI); The values are represented as means ± S.E.M. P<0.05: * vs ZSF1 Ln.

	ZSF1 Ln	ZSF1 Ob
BSA (cm^2)	508 ± 7	651 ± 5*
SAP (mmHg)	146 ±6	181 ± 6*
MAP (mmHg)	127 ± 6	149 ± 5*
DAP (mmHg)	106 ± 7	125 ± 6
HR (bpm)	391 ± 9	354 ± 12*
EDP (mmHg)	4 ± 1	9 ± 1*
dP/dtmax (mmHg.s-1)	11700 ± 964	13000 ± 680
dP/dtmin (mmHg.s-1)	-12600 ± 686	-11700 ± 541
τ (ms)	7.6 ± 0.4	10.5 ± 0.6*
SVI (mL.cm^{-2})	0.33 ± 0.03	0.34 ± 0.01
CI (mL.min^{-1}.cm^{-2})	128 ± 11	120 ± 8
EF (%)	55 ± 3	59 ± 4
EDVI (mL.cm^{-2})	0.65 ± 0.07	0.63 ± 0.05
ESVI (mL.cm^{-2})	0.37 ± 0.05	0.33 ± 0.04
SWI (mmHg.mL.cm^{-2})	35.4 ± 4.2	45.0 ± 2.6
EAI (mmHg.mL^{-1}.cm^{-2})	466 ± 65	526 ± 31
ESPVR (mmHg. mL^{-1}.cm^{-2})	2.49 ± 0.71	2.00 ± 0.39
PRSW (mmHg)	79 ± 14	86 ± 8
EDPVR (mL^{-1}.cm^{-2})	0.023 ± 0.002	0.028 ± 0.002

3.2 - Optimization of methodology for analysis of the epicardial and visceral adipose tissue proteome

The current proteomic state of the art shows only a few studies comparing epicardial to visceral adipose tissue protein expression profile with a huge variability regarding protein extraction protocols. Therefore a selection and optimization of the extraction protocol were performed. This optimization was based in three different protocols (PT, PU and PTU (Figure 10)) whose analysis allowed defining the best protocol to study proteome changes. Analysis of different protocols is performed in the present chapter.

The tryptic peptide digests of epicardial and visceral fat of the obese animals, separated by nano-HPLC, were analysed in the mass spectrometer MALDI-TOF/TOF have been identified 291 proteins in the VAT (Appendix B – Supplemental Table B1-3) and 216 proteins in the EAT (Appendix B – Supplemental Table B4 - 6). In order to assess the best protocol in each tissue, the proteins were distributed according to the protocol in a Venn diagram.

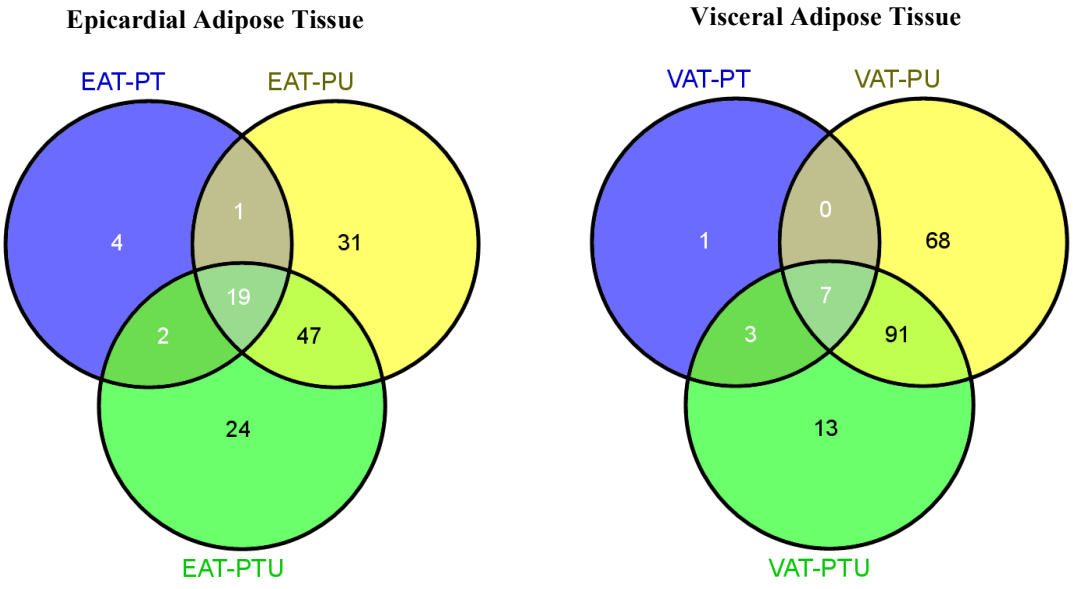

Figure 11 - Venn diagram representing the distribution of identified proteins *per* protocol evidencing the overlapped and unique proteins. VAT – Visceral adipose tissue; EAT – Epicardial adipose tissue; PT – Protocol-Tris; PU – Protocol-Urea; PTU – Protocol-Tris and Urea.

The Venn diagram allows the recognition of the unique proteins extracted in each protocol. As it is possible to observe in Figure 11, the protocol-TRIS (PT) only extracted 1 and 4 unique proteins in visceral and epicardial fat, respectively. On the other hand, the

protocol –Urea (PU) and protocol – Tris and Urea (PTU) were more successful in term of the amount of proteins extracted. In visceral adipose tissue, it was obtained 68 and 13 unique proteins, respectively, while in EAT was extracted 31 and 24 unique proteins. Evaluating the number of unique proteins extracted, the PT, in both cases, was excluded. In contrast, the proteins extracted by PU and PTU were assessed according to its biological process, molecular function and cellular component, as indicated in Figure 12 with the PANTHER classification system (http://www.pantherdb.org).

In figure 12A-left and right panel, in general and independently of the tissue and protocol, it is possible to observe that the proteins constitute almost the same biological processes. According to PANTHER bioinformatics tool the larger groups of biological processes of VAT proteins in PU are "cellular process" (21%), "localization" (10%) and "metabolic process" (28%), while in PTU are "cellular component organization or biogenesis" and "metabolic process" (13%), "cellular process" (23%) and "developmental process" (20%) (Figure 12A – left panel, blue and red bar respectively). However, there are minor differences between biological processes groups. Observing figure 12A-left panel is possible to see that the main difference between them is the presence the group "localization" in the PU. "Localization" refers to any process in which a cell, a substance, or a cellular entity, such as a protein complex or organelle, is transported to, and/or maintained in a specific location [133]. Similarly, the larger groups of EAT proteins in PU are "cellular component organization or biogenesis" and "cellular process" (13%), "developmental process" (14%) and "metabolic process" (25%), whereas in PTU are "cellular component organization or biogenesis", "developmental process", "localization and multicellular organismal process" (10%), "metabolic process" (17%) and "cellular process" (19%) (Figure 12A – right panel, blue and red bar, respectively). The main differences in biological processes of the PU and PTU relates to "biological regulation" (in PU) and "reproduction" (in PTU) groups (Figure 12A – right panel).

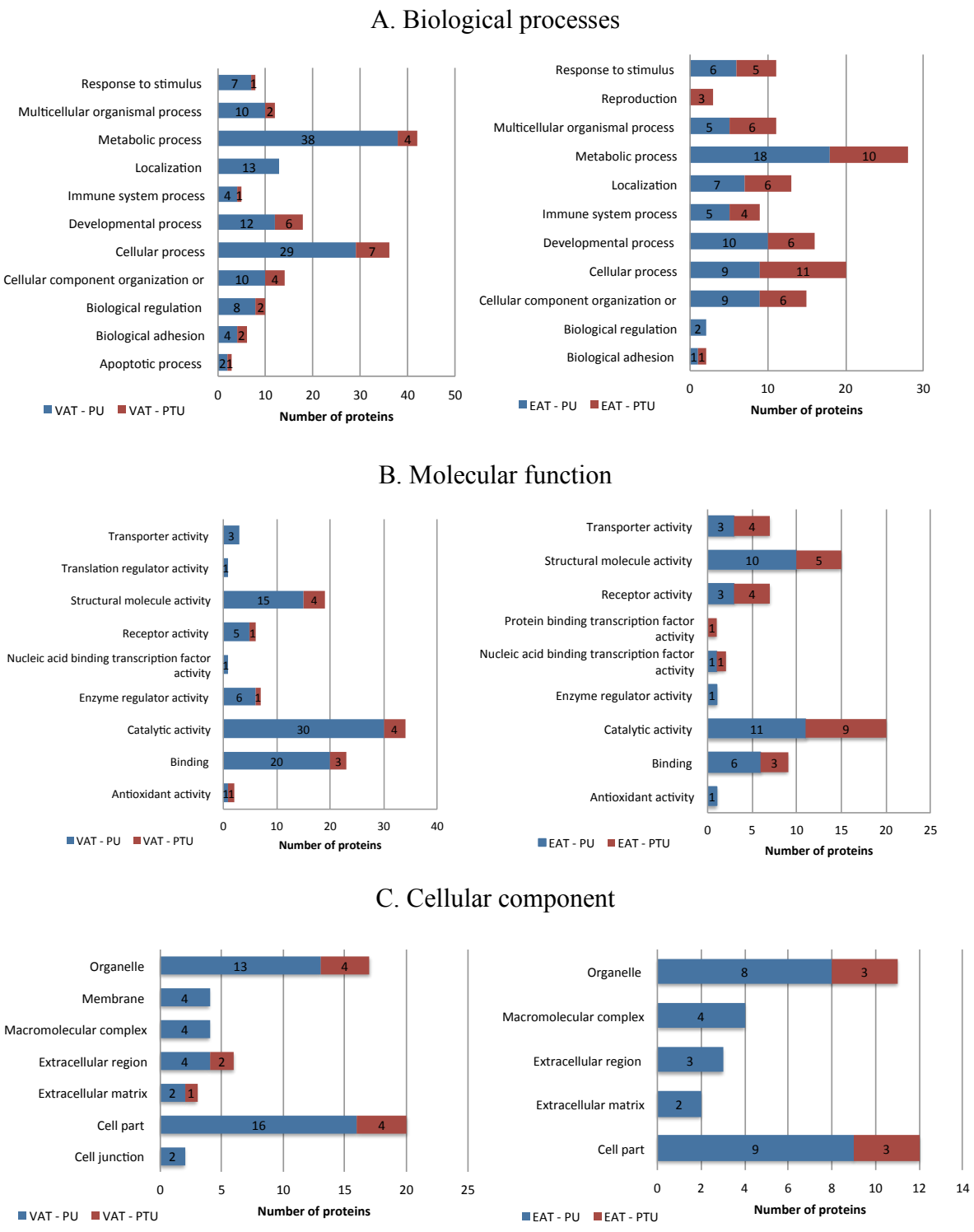

Figure 12 - Distribution of visceral and epicardial unique proteins identified in protocol-Urea and protocol-Tris and Urea in obese ZSF1 according to its biological processes (A), molecular function (B) and cellular component (C). VAT-PU – Proteins extracted from Protocol-Urea of the visceral adipose tissue; VAT-PTU – Proteins extracted from Protocol-Tris and Urea of the visceral adipose tissue; EAT-PU – proteins extracted from Protocol-Urea of the epicardial adipose tissue; EAT-PTU – proteins extracted from protocol-Tris and Urea of the epicardial adipose tissue. Blue – protocol-Urea; Red – protocol – Tris and Urea.

Figure 12B describes the distribution of the proteins extracted by PU and PTU from visceral and epicardial tissues according to its molecular function. The left panel of figure 12B shows that protocol VAT-PU was able to extract a large number of proteins, thus covering the same molecular function groups that VAT-PTU. The same happens in the right panel of figure 12B, in which the proteins extracted by PU cover almost the same groups that PTU. Nonetheless, there is an exception for "protein binding transcription factor activity" group, which is insignificant considering that this group has just one protein.

Lastly figure 12C shows, by PANTHER analysis of VAT and EAT, that the expressed proteins were classified into 7 and 5 groups, respectively. As observed in both panels, the predominant groups are organelle and cell part. The cell part involves the intracellular and plasma membrane proteins. On the other hand, the organelle group encompasses the cytoskeleton proteins, in which can be actin cytoskeleton or intermediate filament cytoskeleton proteins. Although these groups are typical of cardiac tissue, as demonstrated in analysis of the proteins obtained in studies of the Table 4 of the Subchapter 1.5.1 (Appendix A – Supplemental Figure A1), these results are also commonly obtained from epicardial and visceral fat. Moreover, and once again, both panels of Figure 12C shows that PU protocol extracts proteins from more "cellular component" groups.

After the classification of proteins according to their biological processes, molecular function and cellular components, the hydrophobicity level and molecular weight of the epicardial and visceral adipose tissue proteins extracted by both protocols was evaluated. Figure 13 presents, the level of hydrophobicity and hydrophilicity of the proteins extracted by PU and PTU in VAT and EAT according to GRAVY Score (http://www.gravy-calculator.de/).

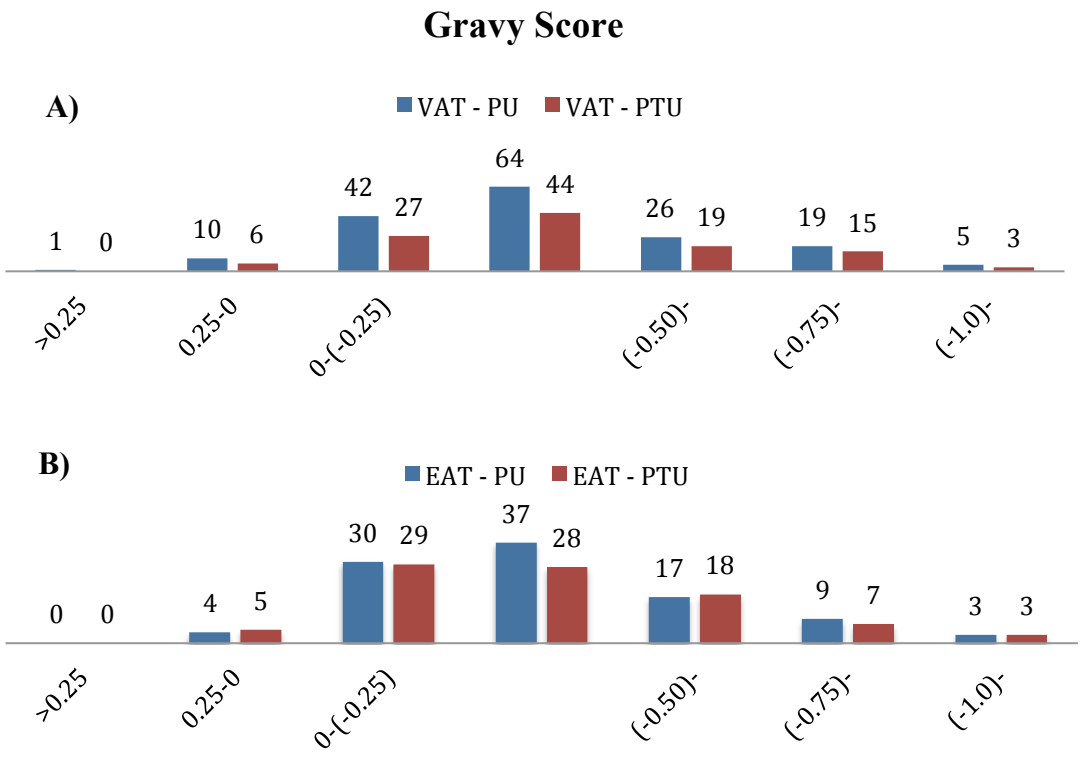

Figure 13 –Gravy index score (average hydrophobicity and hydrophilicity) of visceral and epicardial adipose tissue proteins extracted by protocol-Urea and Tris and Urea in obese ZSF1. Hydrophobicity score below 0 are more likely cytoplasmic (hydrophilic protein), while scores above 0 are more likely membranous (hydrophobic). The bar panel represents number of proteins that exist in the respective range of gravy score. A – Visceral adipose tissue; B- Epicardial adipose tissue. VAT-PTU – Proteins extracted from Protocol-Tris and Urea of the visceral adipose tissue; EAT-PU – proteins extracted from Protocol-Urea of the epicardial adipose tissue; EAT-PTU – proteins extracted from protocol-Tris and Urea of the epicardial adipose tissue. Blue – protocol-urea; Red – protocol – Tris and Urea.

As presented in Figure 13, there is no significant difference between proteins extracted by PU and PTU in both tissues, that is, the large majority of proteins, in both tissues and protocols, present a gravy score between -0.25 and -0.50, followed by 0 and -0.25. This means that both visceral and epicardial adipose tissue have mainly cytoplasmic hydrophilic proteins.

Lastly, Figure 14 represents the distribution of proteins in each tissue and protocol according to their molecular weight.

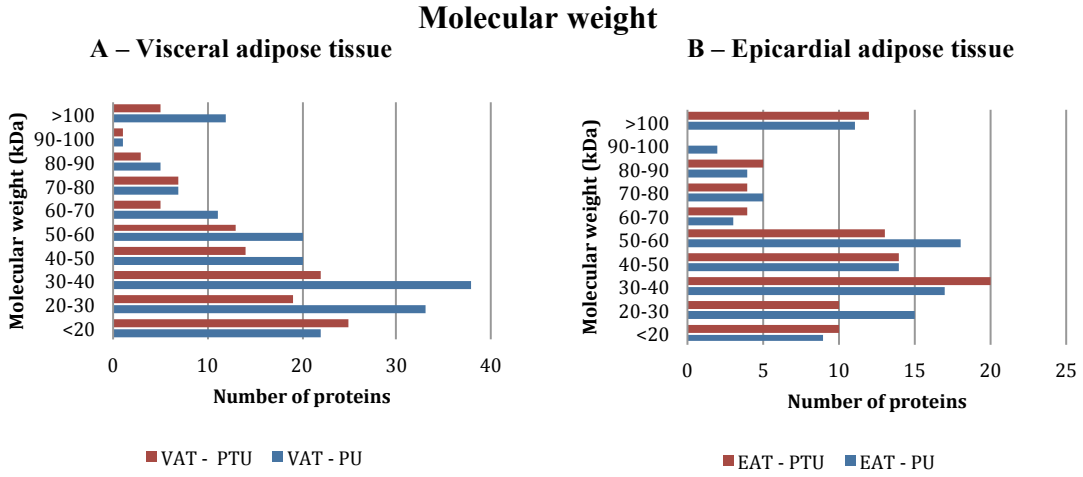

Figure 14 - Distribution of proteins of the epicardial and visceral adipose tissue according to their molecular weight in the different protocols. A – Protocol-urea and protocol-Tris and Urea of the visceral adipose tissue; B – Protocol -urea and protocol-Tris and Urea of the epicardial adipose tissue. VAT-PTU – Proteins extracted from Protocol-Tris and Urea of the visceral adipose tissue; EAT-PU – proteins extracted from Protocol-Urea of the epicardial adipose tissue; EAT-PTU – proteins extracted from protocol-Tris and Urea of the epicardial adipose tissue. Blue – protocol-Urea; Red – protocol – Tris and Urea.

Independently of the tissue or protocol, the most abundant proteins were below of a molecular weight of 60kDa (low-molecular-weight). Additionally the protocol-urea presents a greater number of proteins extracted and, as previously seen, it could cover a range of molecular weights equal or greater than PTU.

3.3 – Characterization of obese and lean ZSF1 epicardial and visceral adipose tissue proteome.

Subsequent to optimization of methodology of the proteins extraction in both tissues, we performed the evaluation of its expression in order to understand the metabolic changes involved in diastolic dysfunction. To achieve this, one-dimensional electrophoresis, nano-HPLC and MALDI-TOF/TOF were performed in order to separate and analyse proteins. To identify diastolic dysfunction-related proteins in epicardial and visceral adipose tissue, it was performed 1DE-LC-MS/MS approaches for quantitative comparison among subjects. Figure 15 shows the SDS-PAGE of epicardial and visceral adipose tissue proteins of obese and lean subjects with two replicates each and respective optical density (OD) bands analysis.

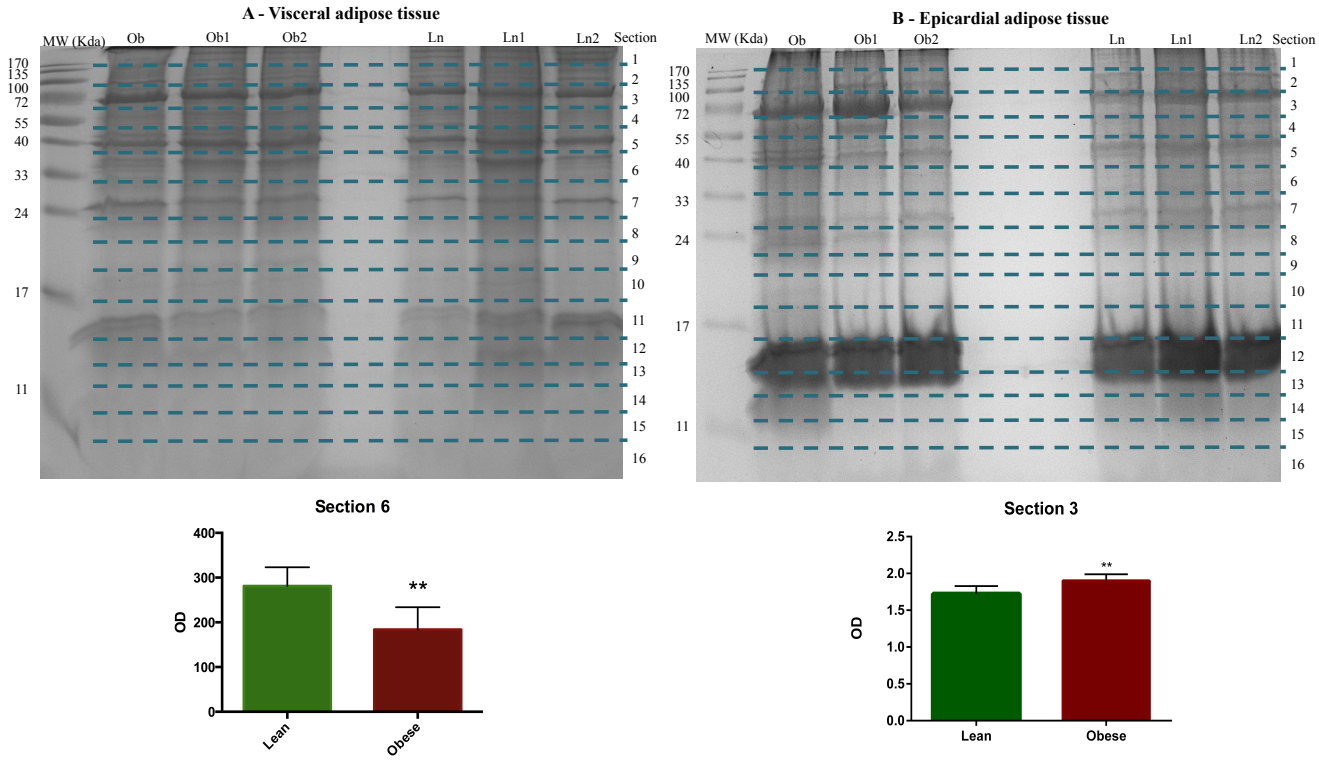

Figure 15 - Representation of the Sodium dodecylsulphate-polyacrylamide gel electrophoresis of (A) visceral and (B) epicardial adipose tissue of the obese and lean ZSF1 rats. The gel sections with significant optical density variations among groups are highlighted in the bottom graphs. **P ≤ 0.01 vs Lean ZSF1; ns – P > 0.05 vs Lean ZSF1. Ln – visceral adipose tissue of lean ZSF1 rat; Ob – visceral adipose tissue of obese ZSF1 rat; MW – molecular weight; OD – Optical density.

As described in Figure 15A, the band OD analysis only highlighted section 6 (estimated MW of 37-38 kDa), presenting significant variations between groups. LC-MS/MS analysis of this section retrieved 10 distinct proteins. From this 10 VAT proteins detected in section 6, heterogeneous nuclear ribonucleoproteins A2/B1, A1 and A2-annexin and lumican were the most prevalent (Appendix C – Supplemental Table C1 – C3). Likewise, in Figure 15B (in epicardial adipose tissue), the band OD analysis just highlights section 3 (estimated MW of 72-90 kDa) with significant variations between groups. LC-MS/MS analysis of this section recovered 19 distinct proteins (Appendix C – Supplemental Table C4 – C6). From these 19 proteins, the chaperone activity of bc1 complex-like, stress-70 protein, annexin-A6, serotransferrin, trifunctional enzyme subunit alpha, membrane primary amine oxidase, aconite hydratase and gelsolin were the most common proteins in all samples.

The large-scale LC-MS/MS analysis of all gel bands retrieved 195 and 260 proteins in visceral and epicardial adipose tissue, respectively (Appendix C). All identified proteins were distributed per group in a Venn diagram, as described in Figure 16A and 16B. From all visceral proteins detected, 126 were common to both types of adipose tissue studied

(Appendix C – Supplemental Table C3). On the other hand, 35 proteins were only identified in visceral of lean ZSF1 rats while 34 proteins were only identified in visceral of obese ZSF1 (Appendix C – Supplemental Table C1 – C2). Regarding epicardial adipose tissue, 102 identified proteins were common between obese and lean ZSF1, while 99 and 59 proteins were only identified in obese and lean respectively (Appendix C – Supplemental Table C4 – C6).

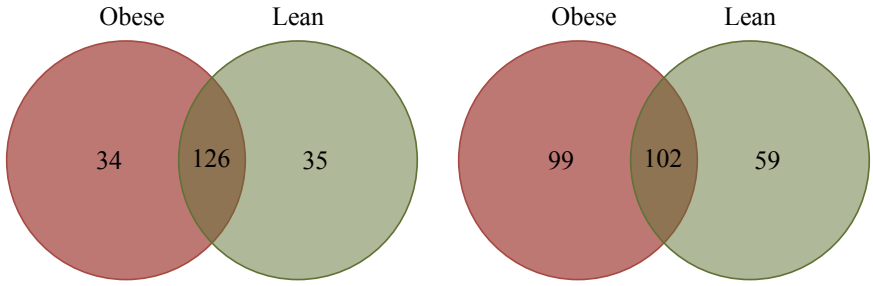

A - Visceral adipose tissue **B** - Epicardial adipose tissue

Figure 16 – Venn diagram representing the distribution of identified proteins per group evidencing the overlapped and unique proteins. A – Visceral adipose tissue; B – Epicardial adipose tissue; Lean – proteins identified in adipose tissue of lean ZSF1; Obese – Proteins identified in adipose tissue of obese ZSF1.

To understand the main differences between identified proteins of lean and obese ZSF1, the unique proteins of each tissue were assessed according to their biological processes and molecular function (Figure 17 and Figure 18) with PANTHER classification system.

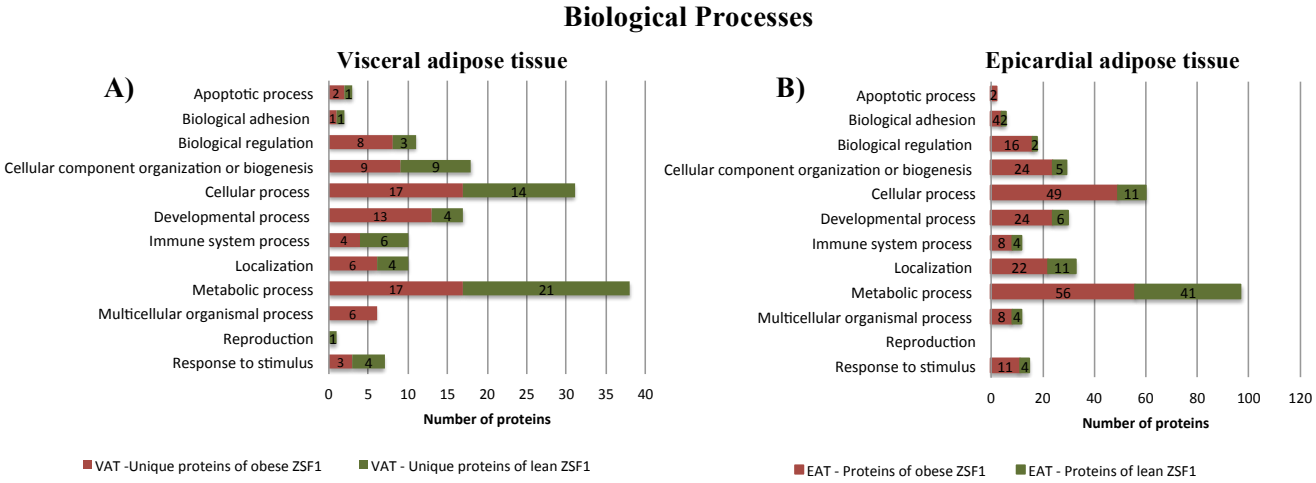

Figure 17 - Distribution of (A) visceral and (B) epicardial unique proteins identified in obese and lean ZSF1 rats according to its biological process. Bar chart represents the biological processes categories. Red –Proteins identified in obese ZSF1 model; Green –Proteins identified in lean ZSF1 model. VAT – Visceral adipose tissue; EAT – Epicardial adipose tissue

In biological process of VAT the main differences between obese and lean ZSF1 are in "multicellular organismal process" (6 proteins in obese and none in lean ZSF1), "metabolic process" (17 proteins in obese and 21 in lean ZSF1), "developmental process"

(13 proteins in obese and 4 in lean ZSF1) and biological regulation (8 proteins in obese and 3 in lean ZSF1) groups (Figure 17A). Moreover, these last three groups are the more prevalent of the biological processes involving majority of the identified proteins (Figure 17A). Observing Figure 17A the "developmental processes" and "biological regulation" seem to be the main groups involved in metabolism dysfunction in VAT of obese ZSF1.

The EAT analysis stand out four groups in obesity, "developmental process" (24 proteins in obese and 6 in lean ZSF1), "cellular process" (49 proteins in obese and 11 in lean ZSF1), "biological regulation" (16 proteins in obese and 2 in lean ZSF1) and "cellular component organization" (24 proteins in obese and 5 in lean ZSF1) (Figure 17B). However, observing the Figure 17B, the principal groups involved in metabolism dysfunction seem to be the cellular and developmental processes.

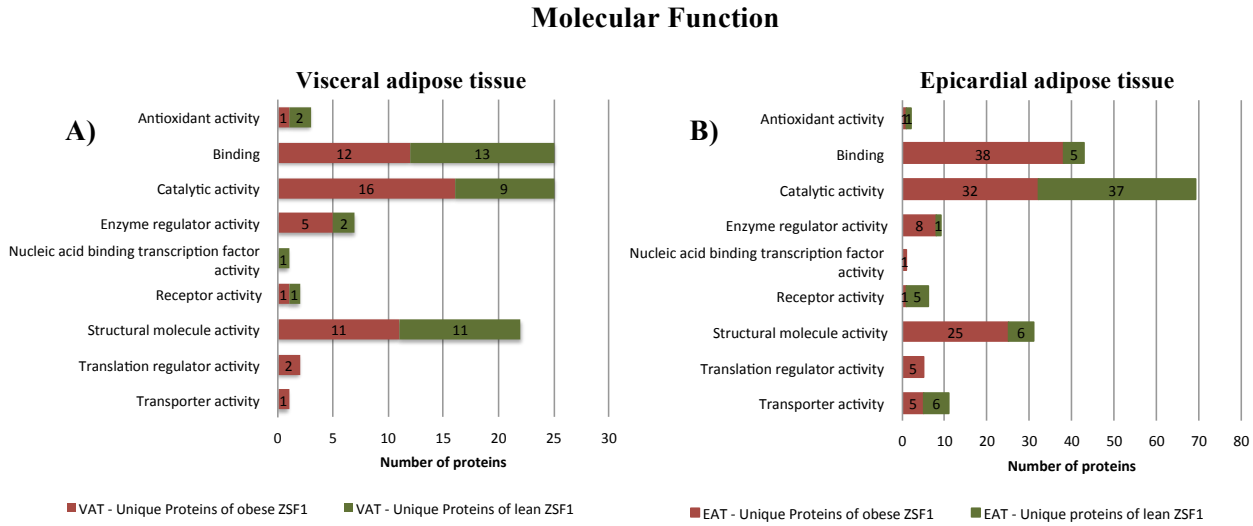

Figure 18 - Distribution of (A) visceral and (B) epicardial unique proteins identified in obese and lean ZSF1 model according to its molecular function. Bar chart represents the molecular function categories. Red –Proteins identified in obese ZSF1 model; Green –Proteins identified in lean ZSF1 model. VAT – Visceral adipose tissue; EAT – Epicardial adipose tissue

PANTHER classification of proteins by molecular function (Figure 18) revealed that in VAT, the majority of proteins are involved in "binding", "catalytic activity", "structural molecule activity" groups and "enzyme regulatory activity" (Figure 18A). However, the main distinctions between obese and lean ZSF1 model are in "catalytic activity" (16 proteins in obese and 9 in lean ZSF1) and "enzyme regulatory activity" (5 proteins in obese and 2 in lean ZSF1) (Figure 18A).

Observing the Figure 18B, in EAT the main groups of molecular function are "binding", "catalytic activity", "structural molecule activity" groups and "enzyme regulatory activity" (Figure 18B). Nevertheless, the major differences between obese and lean subjects are in "enzyme regulatory activity" (8 proteins in obese and 1 in lean ZSF1), "structural molecule activity" (25 proteins in obese and 6 in lean ZSF1) and "binding" (38 proteins in obese and 5 in lean ZSF1) groups (Figure 18B). Taken together, figure 21 shows that there are three groups involving the most proteins, "catalytic activity", "binding" and "structural molecule activity". Indeed, a research showed that these groups are typical signs of cardiac hypertrophy [134]. In addition to these analyzes, it was also performed a graphical presentation of the cellular components of all proteins identified in obese and lean ZSF1 (Figure 19).

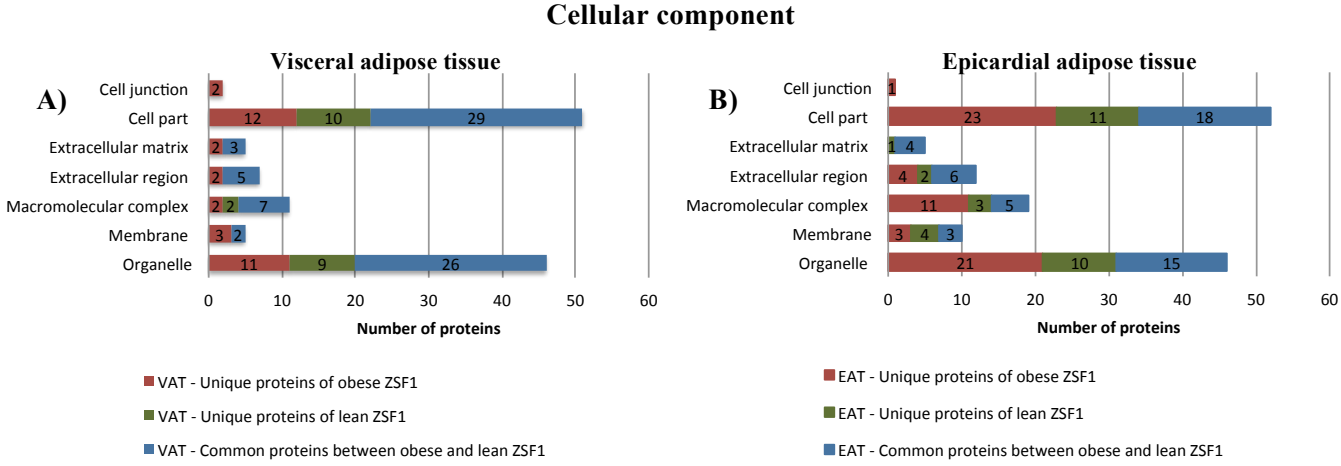

Figure 19 - Distribution of (A) visceral and (B) epicardial proteins identified in obese and lean ZSF1 model according to its cellular component. Bar chart represents the cellular component categories. Red – unique proteins of obese ZSF1 model; Green – unique proteins of lean ZSF1 model; Blue – common proteins of lean and obese ZSF1 model; EAT – epicardial adipose tissue; VAT – Visceral adipose tissue

In visceral adipose tissue, PANTHER classification showed that the majority of expressed proteins comprised "organelle group" in which 95.5% are cytoskeletal and 4.5% are mitochondrial proteins, and "cell part" group in which 94% are intracellular and 6% are plasma membrane proteins (Figure 19A). In the same way, in epicardial adipose tissue the main groups in cellular components are also "organelle" in which 80% are cytoskeletal and 20% are mitochondrial, and "cell part" in which 6% are plasma membrane and 94% intracellular (Figure 19B). The cytoskeletal proteins are quite typical of myocardium, however, as already observed in Chapter 3.2, observing the graphical presentation of the cellular components of the proteins identified in the studies of Table 4 in Subchapter 1.5.1

(Appendix A – Supplemental Figure A1), it is possible to conclude that these percentages are expected.

The comparison of abundances of the 126 and 102 proteins common between obese and lean ZSF1 in visceral and epicardial adipose tissue, respectively, was performed based on the normalization of the exponentially modified protein abundance index (emPAI) (Figure 20 and Figure 22, respectively). The normalized abundance analysis in VAT evidence nucleoside diphosphate kinase-B, collagen-alpha-2(I) chain and serotransferrin as the top 3 most abundant proteins in obese ZSF1 and alpha-enolase, ubiquitin-conjugating enzyme E2 N and perilipin-1 as the less abundant ones (Figure 20). On the other hand, EAT highlights fibrinogen-beta chain, heterogeneous nuclear ribonucleoproteins A2/B1 and alpha-1-macroglobulin as the top 3 most abundant proteins in obese ZSF1 and 2-oxoglutarate dehydrogenase mitochondrial, aconitate hydratase mitochondrial and electron transfer flavoprotein subunit alpha mitochondrial as the less abundant ones (Figure 22).

To evaluate the protein-protein interaction, the ClueGo and CluePedia program was performed, considering the threshold emPAI ratios values higher than 0.5 and lower than -0.5 (Figure 21 and Figure 23). In VAT, the protein-protein interaction evidences in obese ZSF1 the prevalence of processes involved in "negative regulation of interleukin-8 secretion" involving the annexin-A1 and A4, "response to oxidative stress", "cellular response to oxygen containing compound" and other processes related to oxidative metabolism (Figure 21 and Appendix C – Supplemental Figure C1). The main proteins involved in these last processes are aldehyde dehydrogenase, nucleoside diphosphate kinase B, 14.3.3 protein gamma, collagen alpha-1 chain, tropomyosin alpha-1 chain, serotransferrin, superoxide dismutase, peroxiredoxin-1, annexin A1, alpha-antiproteinase and heat shock protein beta-1 (Appendix C – Supplemental Figure C1). Regarding EAT of the obese ZSF1, the most abundant proteins relate to "collagen fibril organization", comprising annexin-A2, lumican and collagen alpha-1(I) chain proteins. Also, protein-protein interaction in EAT highlights decreased proteins involved in oxidative (mainly lipid and fatty acid oxidation) and metabolic processes (mainly catabolic) such as long-chain specific acyl-CoA dehydrogenase, 3-ketoacyl-CoA thiolase, Acyl-coenzyme A thioesterase 2, Enoyl-CoA hydratase, trifunctional enzyme subunit alpha and hydroxyacyl-coenzyme A dehydrogenase (Figure 23 and Appendix C – Supplemental Figure C2).

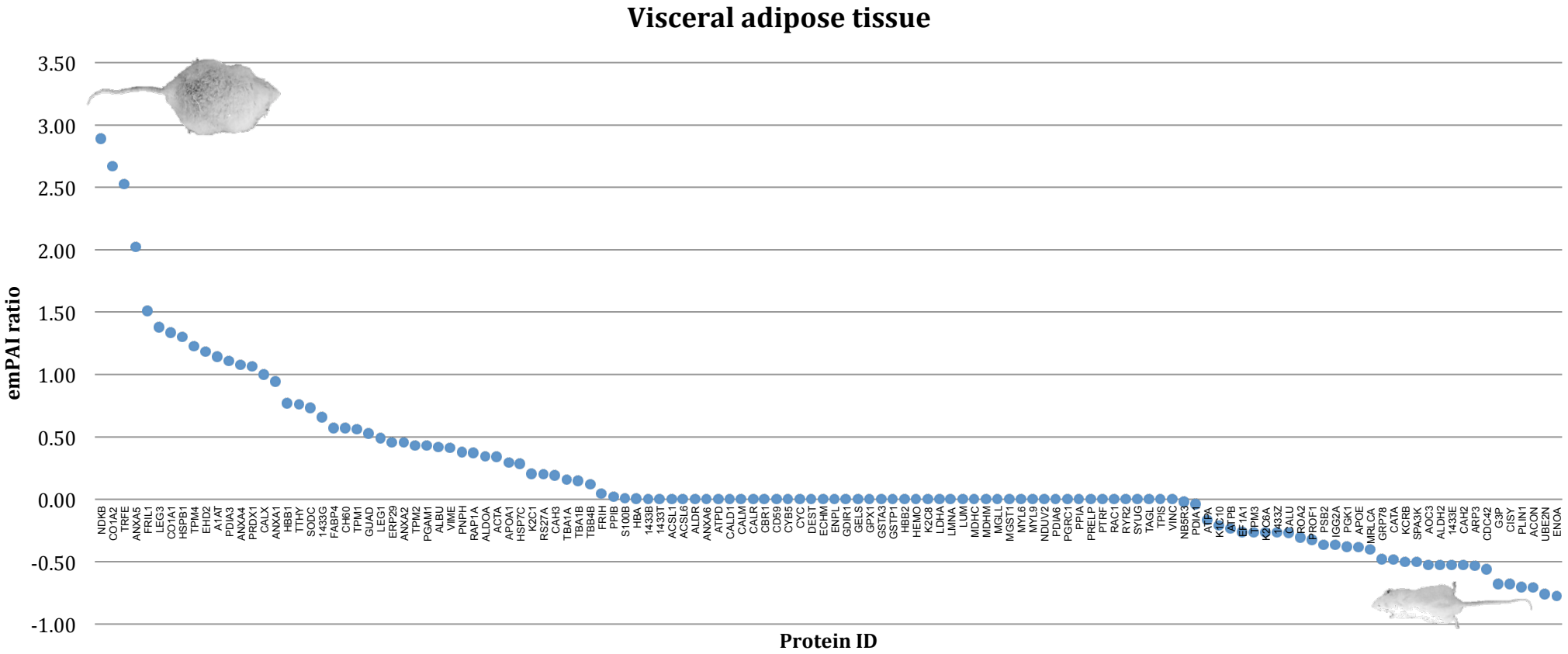

Figure 20 - Distribution of normalized emPAI values of visceral adipose tissue proteins in obese and lean groups highlighting different protein abundance distribution. Entry name has correspondence to protein name at Appendix D – Supplemental Table D3. Values above zero correspond to values of up-regulated proteins in obese ZSF1; Values below zero correspond to values down-regulated proteins in obese ZSF1.

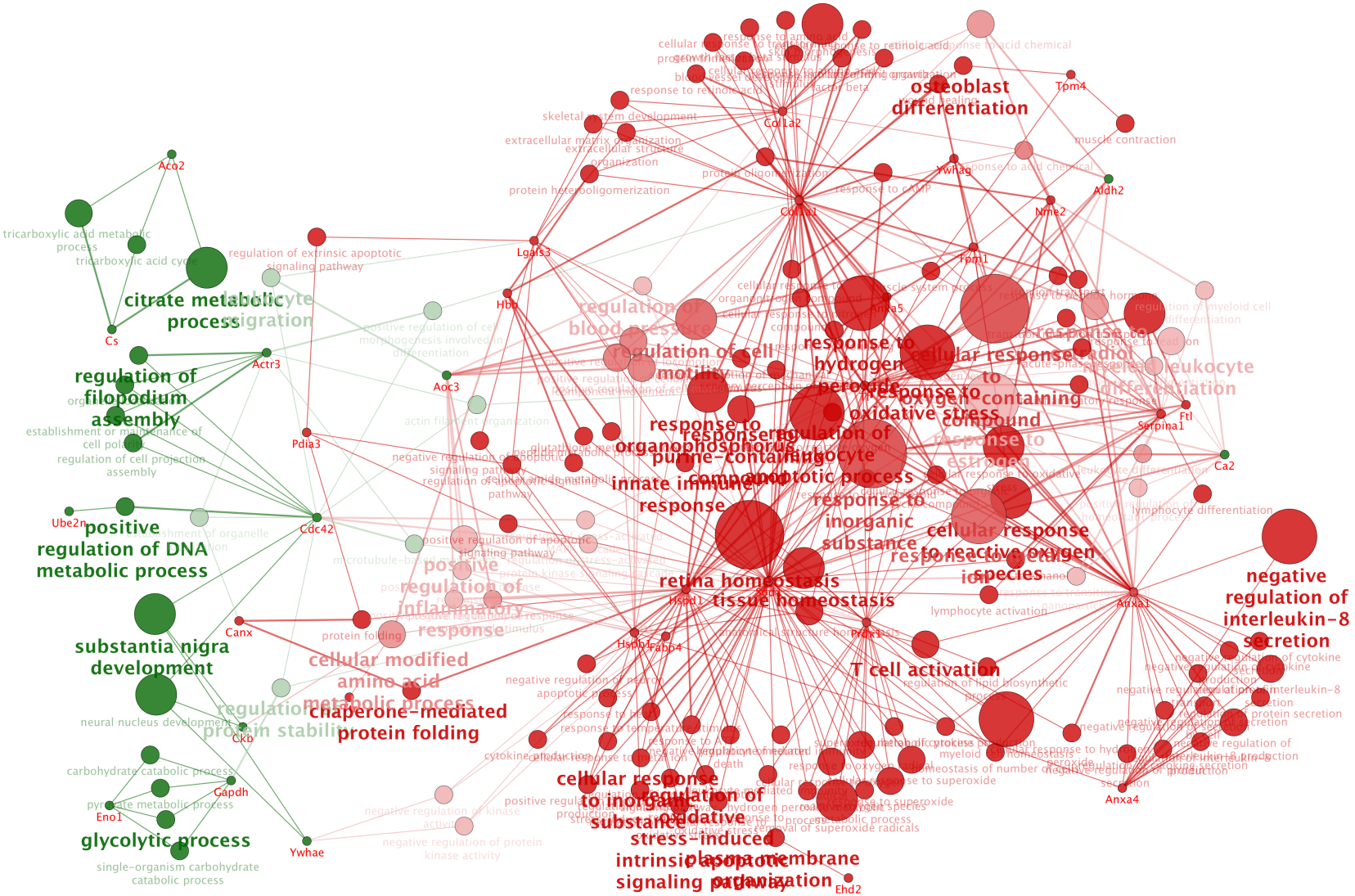

Figure 21 - ClueGo and CluePedia analysis of protein-protein interaction considering common proteins present in significant distinct levels (based on emPAI values) in visceral adipose tissue of obese and lean ZSF1 rats. Green nodes - biological processes negatively regulated (down-regulated) in obese subjects; Red nodes – biological processes positively regulated (up-regulated) in obese subjects.

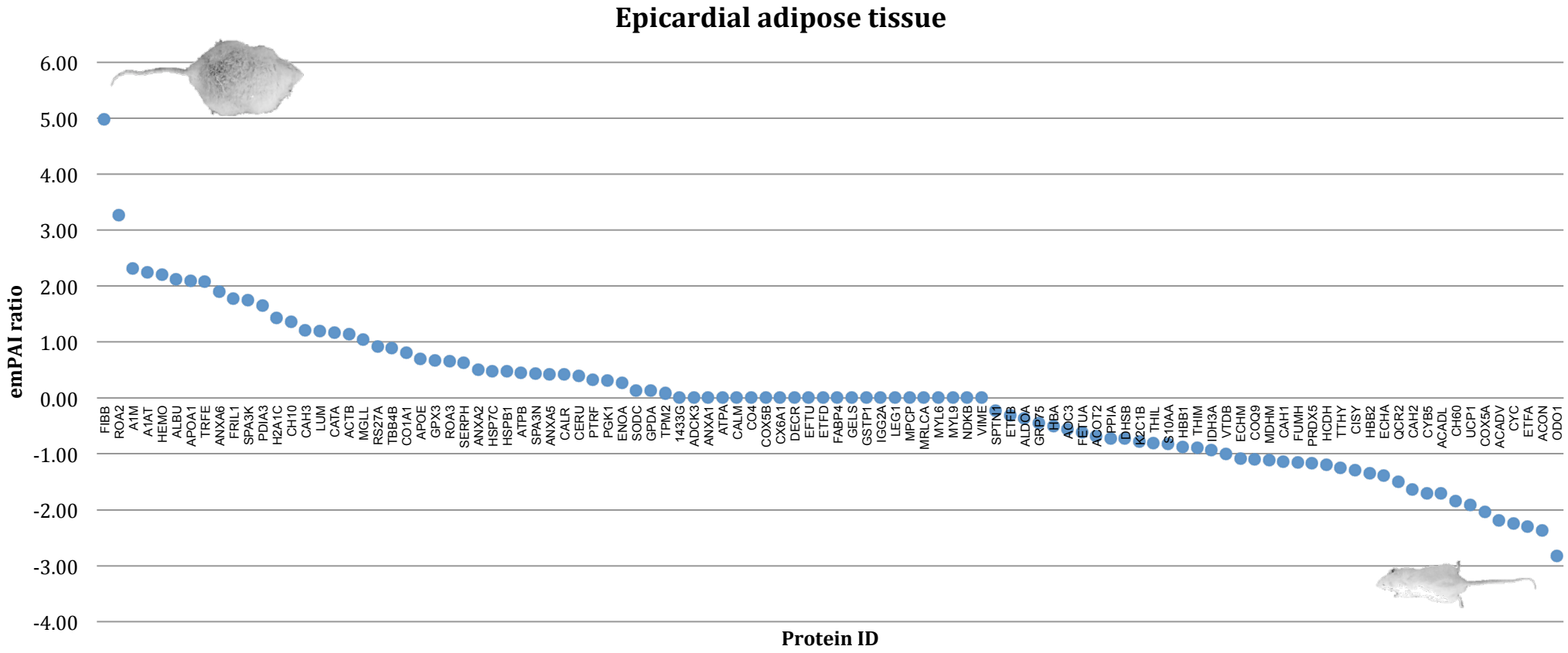

Figure 22 - Distribution of normalized emPAI values of epicardial adipose tissue proteins in obese and lean groups highlighting different protein abundance distribution. Entry name has correspondence to protein name at Appendix D – Supplemental Table D6. Values above zero correspond to values of up-regulated proteins in obese ZSF1; Values below zero correspond to values down-regulated proteins in obese ZSF1.

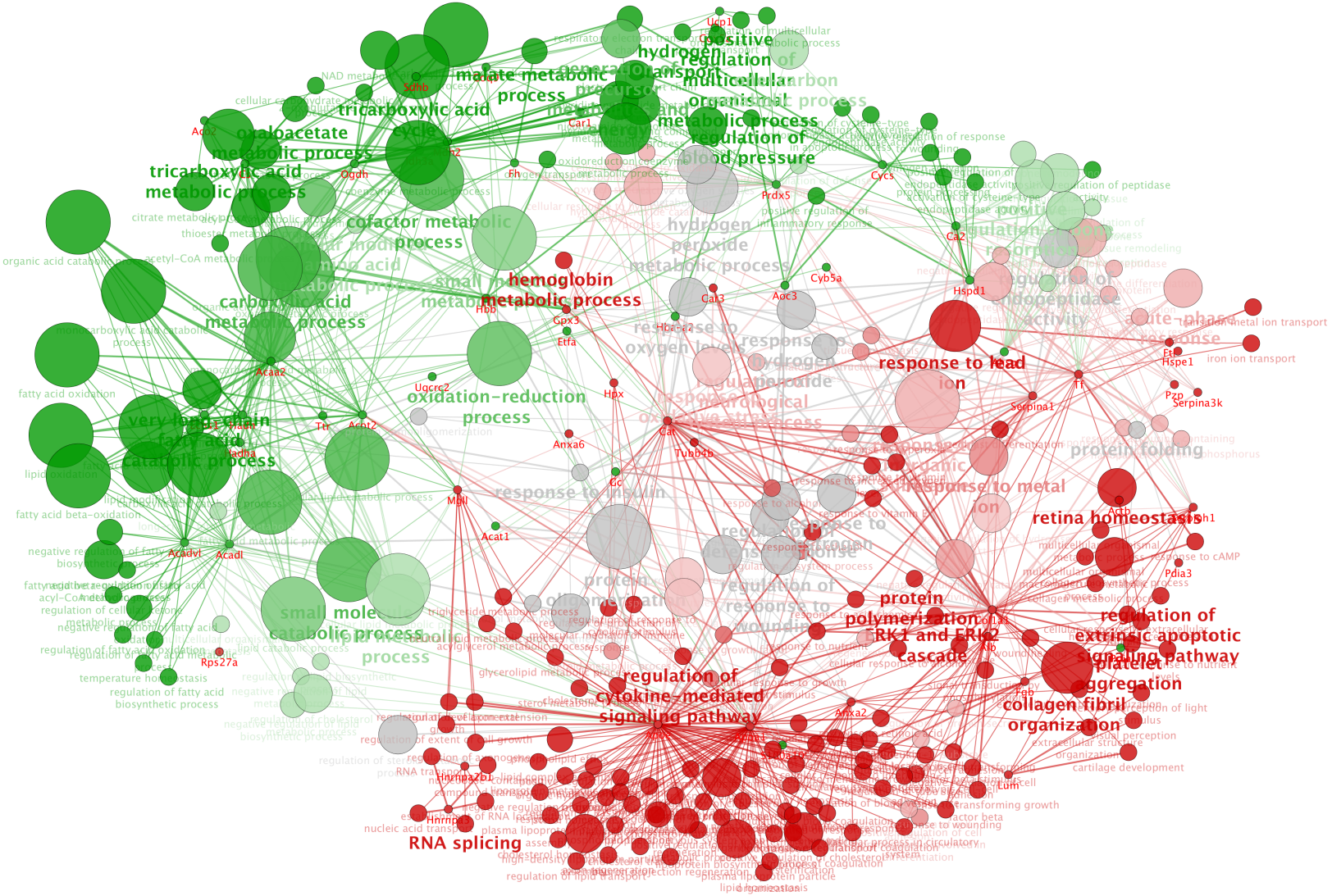

Figure 23 - ClueGo and CluePedia analysis of protein-protein interaction considering common proteins present in significant distinct levels (based on emPAI values) in epicardial adipose tissue of obese and lean ZSF1. Green nodes - biological processes negatively regulated (down-regulated); Red nodes – biological processes positively regulated (up-regulated) in obese subjects.

Evaluating Table 5 of the subchapter 1.5.1 and figure 21 it is possible to see the overexpression of Fabp4 in obese subjects. Indeed recent studies showed that Fabp4 has a positive association with heart failure and obesity [77, 79]. Therefore, it was assessed the interaction of this protein with other possible proteins with a String V9.1 program (Figure 24).

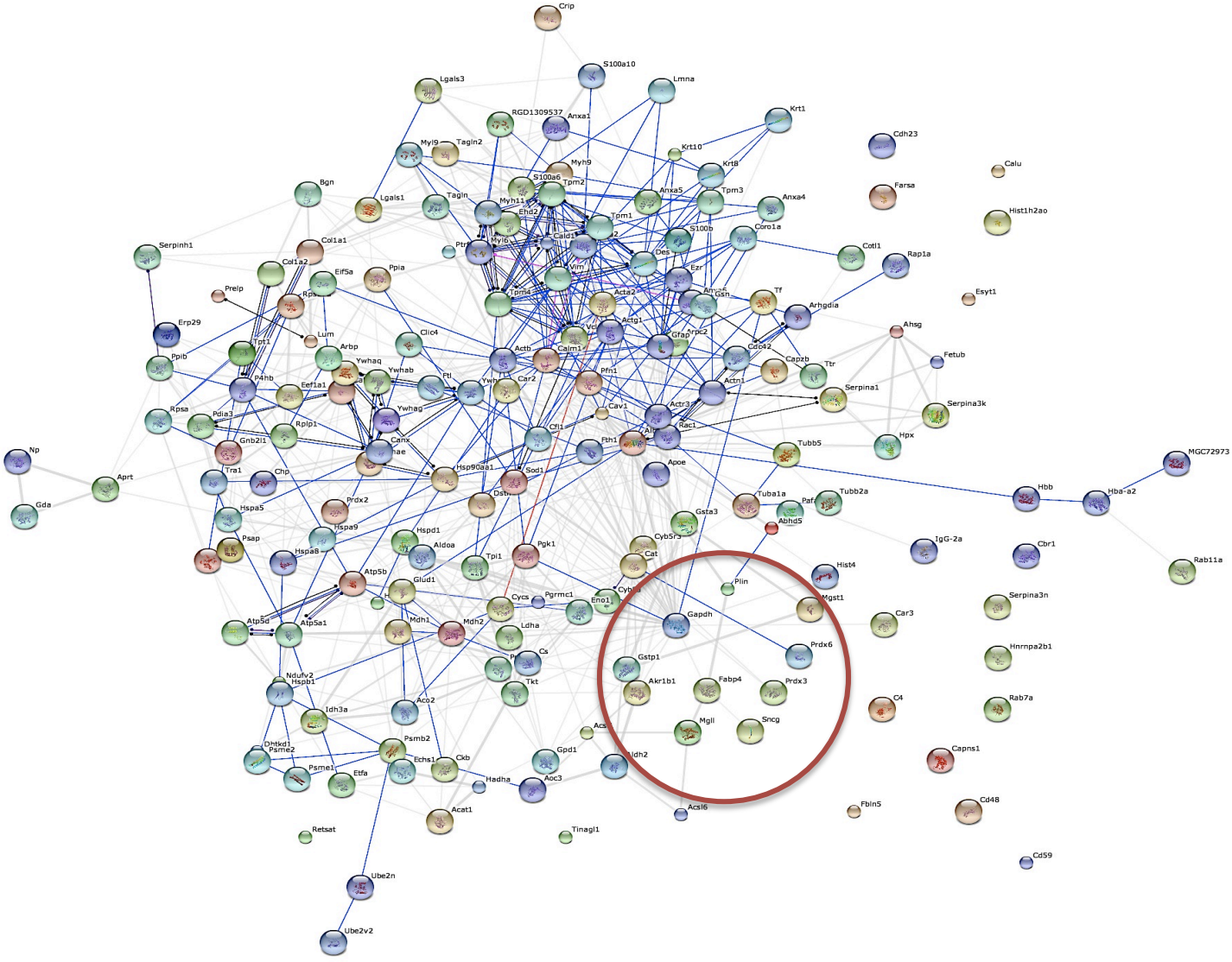

Figure 24 - String V9.1 analysis of protein-protein interaction considering common proteins present in obese and lean ZSF1 model. Red circle – show the interaction of the fabp4 with others proteins. Connections: Dark blue – Binding; Light blue – phenotype; Purple – catalysis; Red – inhibition; Black – reaction; Pink – Post-translational modification.

From figure 27, it is possible to conclude that Fabp4 interacts with others identified proteins as Perilipin-1 (Plin), Monoglyceride lipase (Mgll), Gamma-synuclein (Sncg) and Glyceraldehyde-3-phosphate dehydrogenase (Gapdh). Analysing its biological processes, they share mainly cellular and metabolic processes. The Plin and Fabp4 are involved in

lipid and primary metabolic processes, while Gapdh and Fabp4 are implicated in directly interact monocarboxylic, carboxylic and oxo acid metabolic processes However, as described in Figure 24 (red circle) there is not any direct relationship between them, so they do not directly interact.

3.4 – Characterization and comparison of epicardial and visceral adipose tissue proteome

Although epicardial and visceral adipose tissue share the same embryological origin, there are no studies that compare the adipocytes-derived substances secreted and the differences of expression among these tissues. Therefore the present work aimed to present the differences between epicardial and visceral adipose tissue proteome. The proteins identified in epicardial and visceral adipose tissue of obese and lean subjects were distributed per group in a Venn diagram (Figure 25).

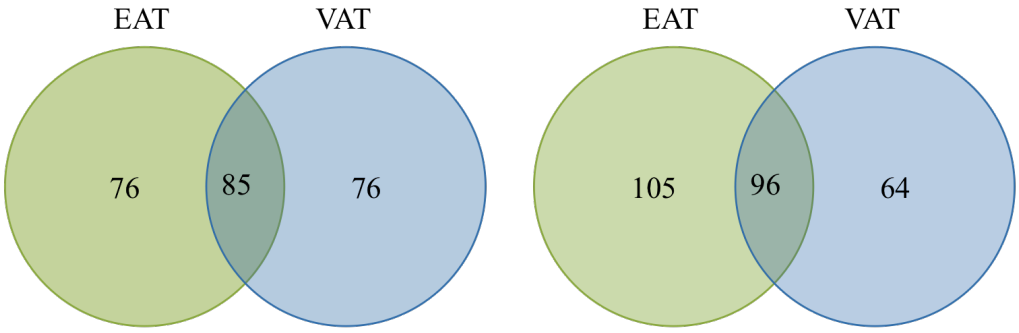

A – Lean ZSF1 animal model **B** – Obese ZSF1 animal model

Figure 25 –Venn diagram representing the distribution of identified proteins per subject evidencing the overlapped and unique proteins. A – Proteins identified in lean ZSF1 animal model; B – Proteins identified in obese ZSF1 animal model; EAT – Proteins identified in epicardial adipose tissue; VAT – Proteins identified in visceral adipose tissue.

From all visceral and epicardial adipose tissue of lean ZSF1 proteins, 85 of them were common to both tissues (Figure 25A), whereas 76 of them were identified as unique in each tissue, epicardial and visceral. On the other hand, in obese ZSF1 96 proteins were common between EAT and VAT, while 105 and 64 were unique in each tissue, respectively.

In order to understand the differences between unique proteins of epicardial and visceral adipose tissue, they were separated according to their biological process (Figure 26) and molecular function (Figure 27).

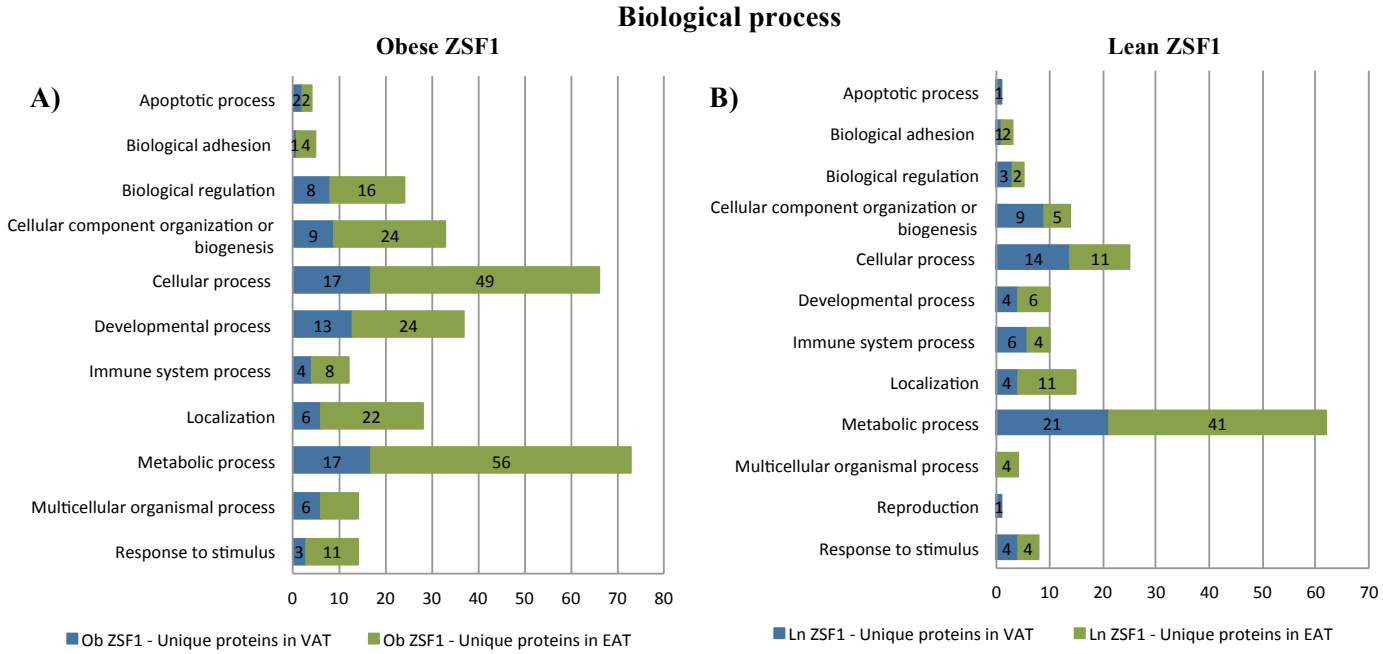

Figure 26 - Distribution of unique proteins identified in visceral and epicardial adipose tissue of obese (A) and lean (B) ZSF1 according to its biological processes. A) – Unique proteins in obese ZSF1; B) – Unique proteins in lean ZSF1; Blue bar – Proteins identified in visceral adipose tissue; Green bar – Proteins identified in epicardial adipose tissue.

Comparing both tissues in obese ZSF1 (Figure 26A), it is possible to observe that they share the same groups of biological processes with similar abundance of proteins. On the other hand, comparing VAT with EAT from lean ZSF1 (Figure 26B), the main difference between them is the presence of two exclusive groups in the VAT, "reproduction" and "apoptotic process". However, each one of these groups presents a single protein, being an insignificant difference. Moreover, the EAT from lean ZSF1 displays an additional group when compared to VAT, which is "multicellular organismal process".

PANTHER classification allows to compare the molecular function of the unique proteins in both tissues (Figure 27).

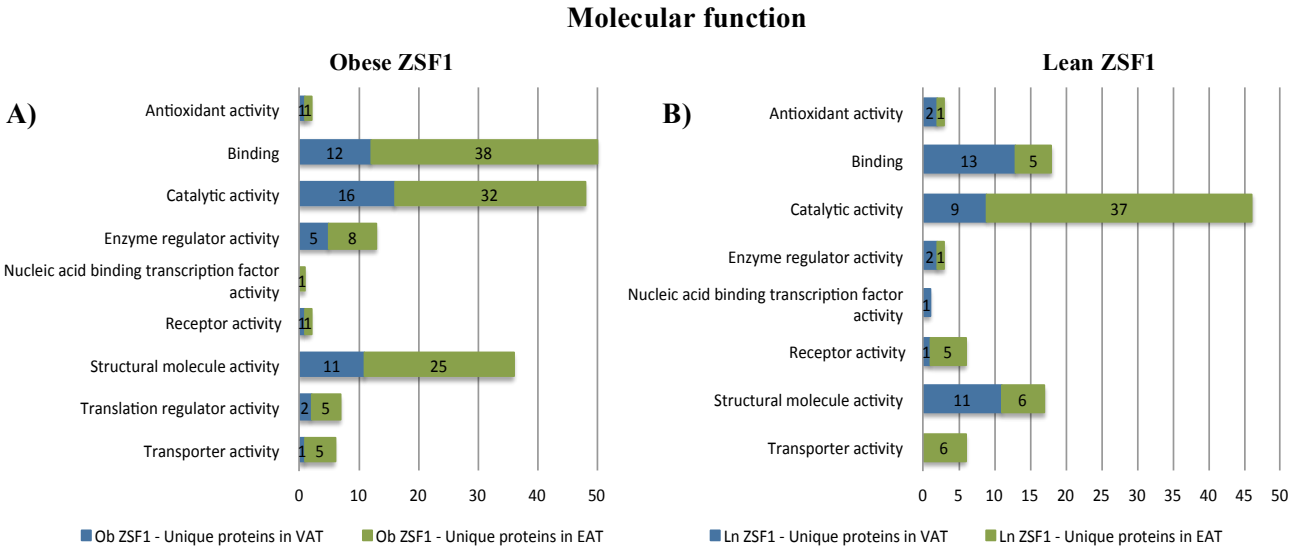

Figure 27 - Distribution of unique proteins identified in visceral and epicardial adipose tissue of obese (A) and lean (B) ZSF1 according to its molecular function. A) – Unique proteins in obese ZSF1; B) – Unique proteins in lean ZSF1; Blue bar – Proteins identified in visceral adipose tissue; Green bar – Proteins identified in epicardial adipose tissue

Taken together, the figure 27 shows that there are three dominant groups, in both visceral and epicardial adipose tissue, "catalytic activity", "binding" and "structural molecule activity".

Comparing EAT to VAT in obese ZSF1 (Figure 27A), the main difference lies in the existence of an exclusive molecular function group in EAT, "nucleic acid binding transcription factor activity". On the other hand, figure 27B highlights that lean ZSF1 present two distinct groups, "nucleic acid binding transcription factor activity" exclusive of VAT (1 protein) and "transporter activity" exclusive of EAT (6 protein).

Figure 28 displays a graphical representation of the distribution of unique and common proteins according to their cellular component group between obese and lean ZSF1.

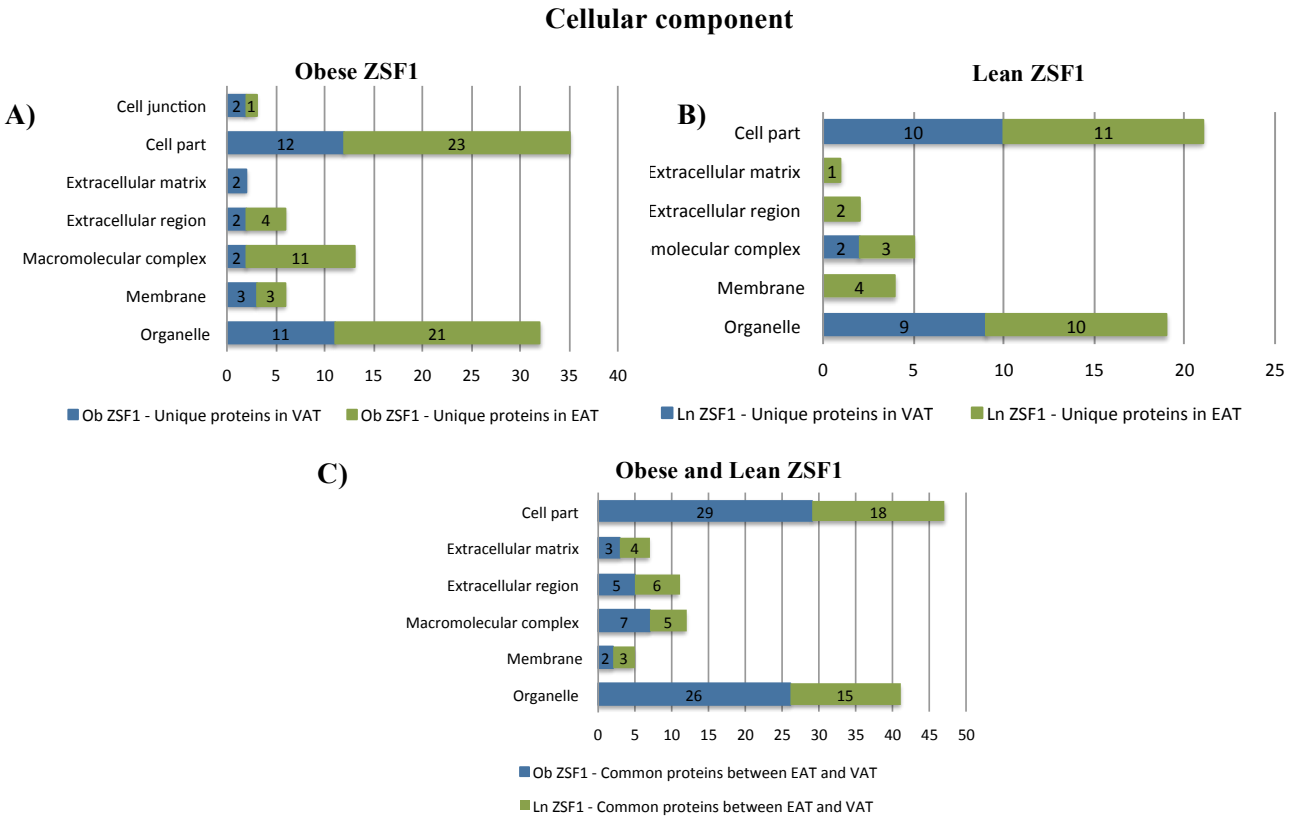

Figure 28 - Distribution of unique proteins identified in visceral and epicardial adipose tissue of obese (A) and lean (B) ZSF1 and (C) common proteins between both subjects according to its cellular component. A) – Unique proteins in obese ZSF1; B) – Unique proteins in lean ZSF1; C) – Common proteins between obese and lean in each tissue; Blue bar – Proteins identified in visceral adipose tissue; Green bar – Proteins identified in epicardial adipose tissue.

The unique proteins of obese ZSF1 in EAT and VAT share the same groups of the cellular components in similar abundance (Figure 28A). In the same way the common proteins between EAT and VAT of each subject are distributed in the same groups in similar abundance (Figure 28C). On the other hand, observing the Figure 28B, it is possible to see that the unique proteins of lean ZSF1 VAT are not present in some groups of the cellular component, namely "extracellular matrix", "extracellular region" and "membrane".

Figure 28 highlights that "cell part" group (mainly intracellular proteins) and "organelle" groups (mainly cytoskeletal) comprise the highest number of proteins in VAT and EAT. Although cytoskeletal proteins are quite typical of myocardium, as stated before, these results were expected.

The common proteins between tissues were analysed through its abundance ratio (based on emPAI ratio values) (Figure 29 and 31). Figure 29 represents the proteins identified in lean ZSF1 where it is possible to visualise that few proteins with significant

changes on its abundance. The proteins aconitate hydratase, mitochondrial, 60 kDa heat shock protein, mitochondrial and hemoglobin subunit beta-1 are the top three most abundant proteins in epicardial adipose tissue, while in visceral adipose tissue the proteins most abundant were carbonic anhydrase 3, annexin A1 and galectin-1 (Figure 31).

The comparison of abundances of the proteins common between epicardial and visceral adipose tissue in lean ZSF1 were performed with ClueGo and CluePedia program, considering a threshold emPAI ratios value higher than 0.5 and lower than -0.5. Figure 30 shows that the proteins up-regulated in epicardial adipose tissue are involved mainly in "tricarboxylic acid cycle", "protein oligomerization" and "gas transport" (Appendix D – Supplemental figure D1). On the other hand, the proteins of visceral adipose tissue highlight just one group, positive "regulation of vesicle function" (Appendix D – Supplemental figure D1).

Regarding to proteins identified in obese ZSF1 epicardial and visceral adipose tissue, the Figure 31 shows that EAT highlights aconitate hydratase, mitochondrial, citrate synthase, mitochondrial and alpha-enolase as the top three most abundance proteins in obese ZSF1 when compared with VAT. On the other hand, VAT highlights as the top three most abundance proteins the profilin-1, annexin A1 and galectin-1. Likewise the lean ZSF1, the proteins identified in VAT and EAT of the obese ZSF1 were assessed in the ClueGo and CluePedia program in order to evaluate the interaction of the corresponding proteins, considering a threshold emPAI ratios value higher than 0.5 and lower than -0.5. Figure 32 and Appendix D – Supplemental Figure D2 displays that proteins up-regulated in VAT are mainly involved in "negative regulation of blood coagulation" and "positive regulation of vesicle fusion", while the proteins of the EAT highlights "response to inorganic substance", "response to hydrogen peroxide", "tricarboxylic acid cycle" and "metabolic processes".

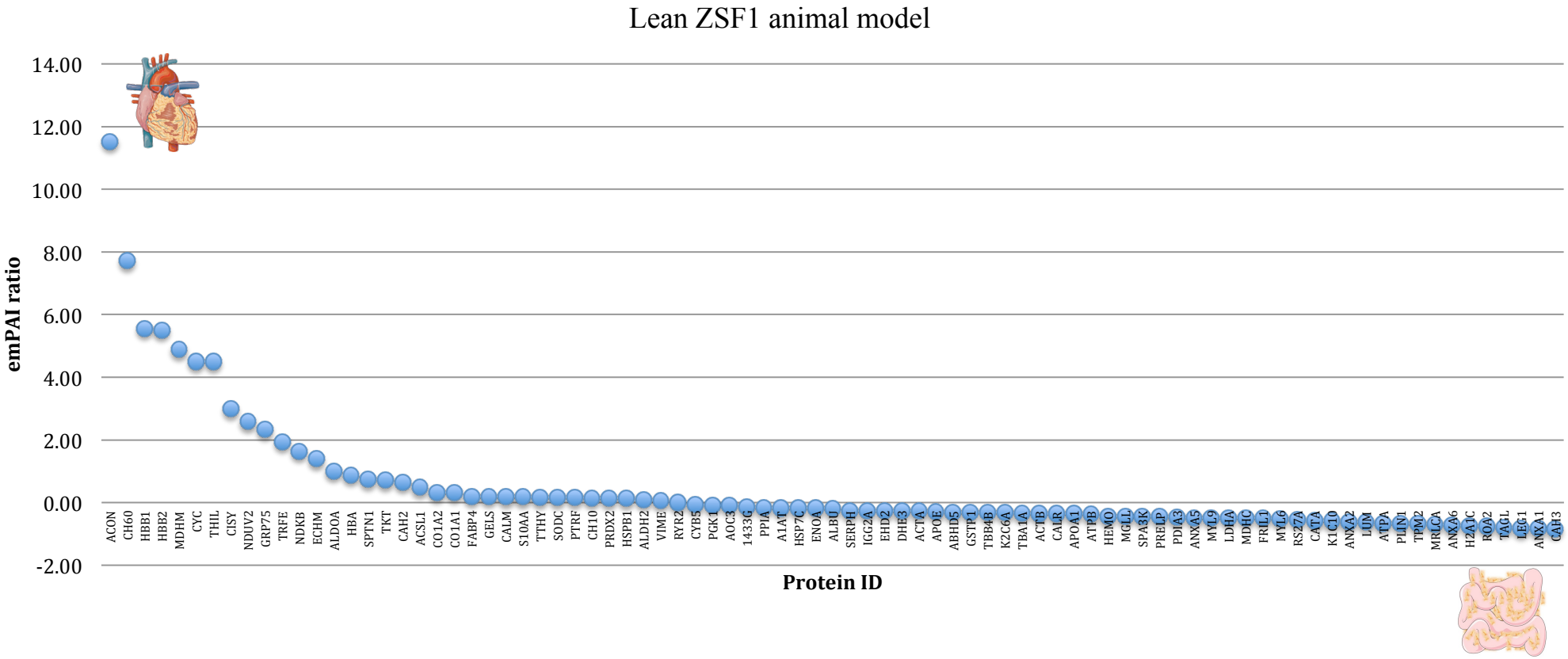

Figure 29 - Distribution of normalized emPAI values of visceral and epicardial adipose tissue proteins in lean groups. Entry name has correspondence to protein name in Appendix D – Supplemental Table D1. Values above zero correspond to values of up-regulated proteins in epicardial adipose tissue in lean ZSF1; Values below zero correspond to values up-regulated in visceral adipose tissue in lean ZSF1.

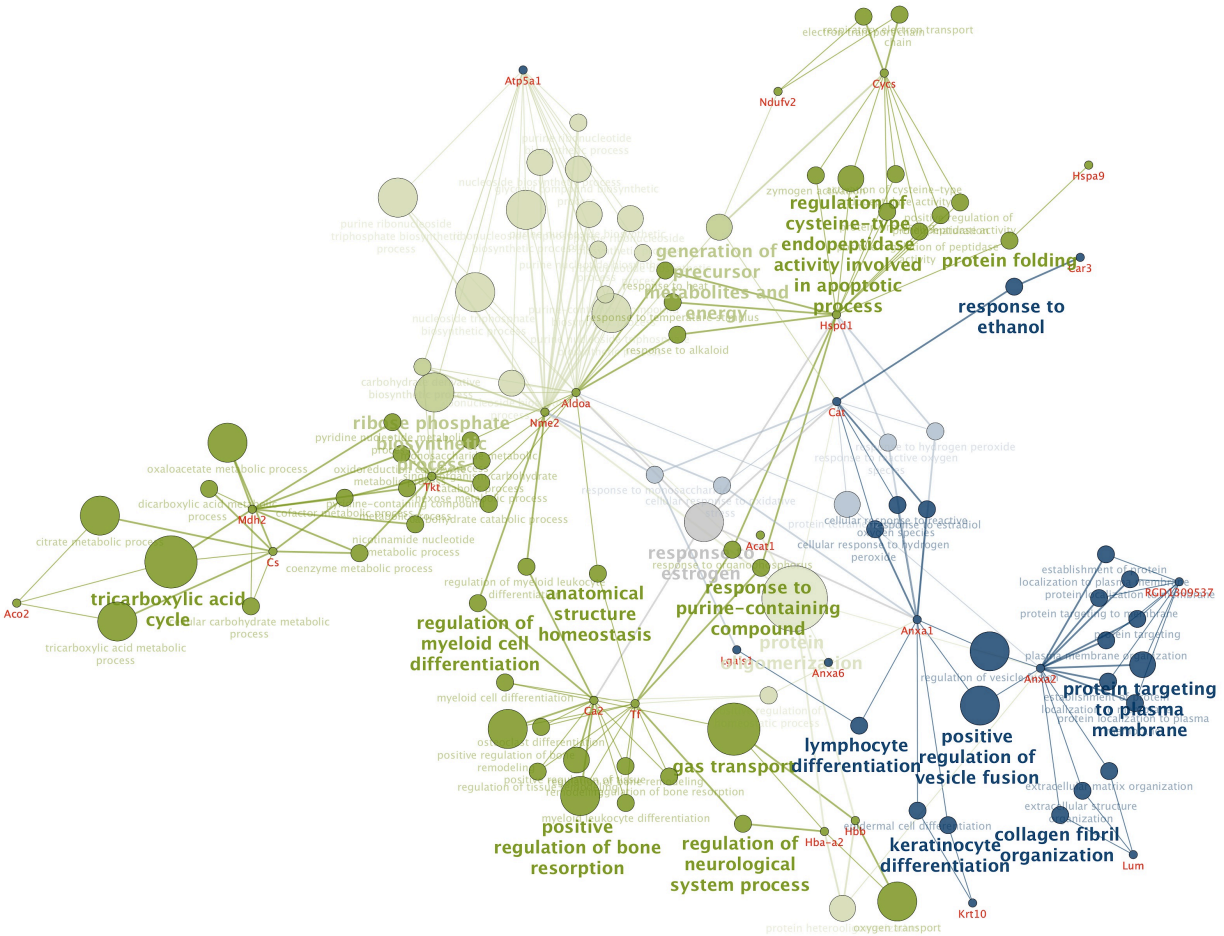

Figure 30 - ClueGo and CluePedia analysis of protein-protein interaction considering up-regulated proteins identified in visceral (blue nodes) and epicardial (green nodes) adipose tissue of lean ZSF1 animal model (based on emPAI values). Blue nodes – Proteins up-regulated in visceral adipose tissue in lean ZSF1; Green nodes – Proteins up-regulated in proteins of epicardial adipose tissue in lean ZSF1.

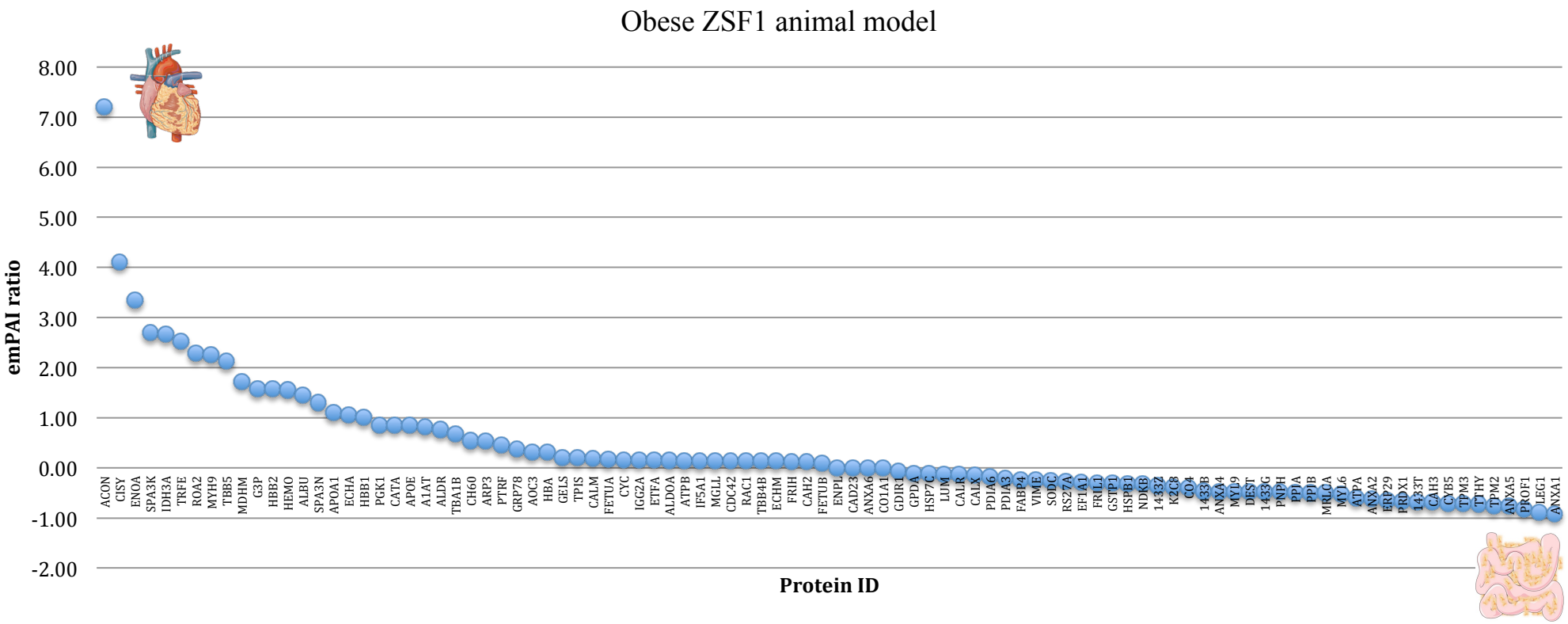

Figure 31 - Distribution of normalized emPAI values of visceral and epicardial adipose tissue proteins in obese groups. Entry name has correspondence to protein name in Appendix D – Supplemental Table D2. Values above zero correspond to values of up-regulated proteins in epicardial adipose tissue in obese ZSF1; Values below zero correspond to values up-regulated in visceral adipose tissue in obese ZSF1.

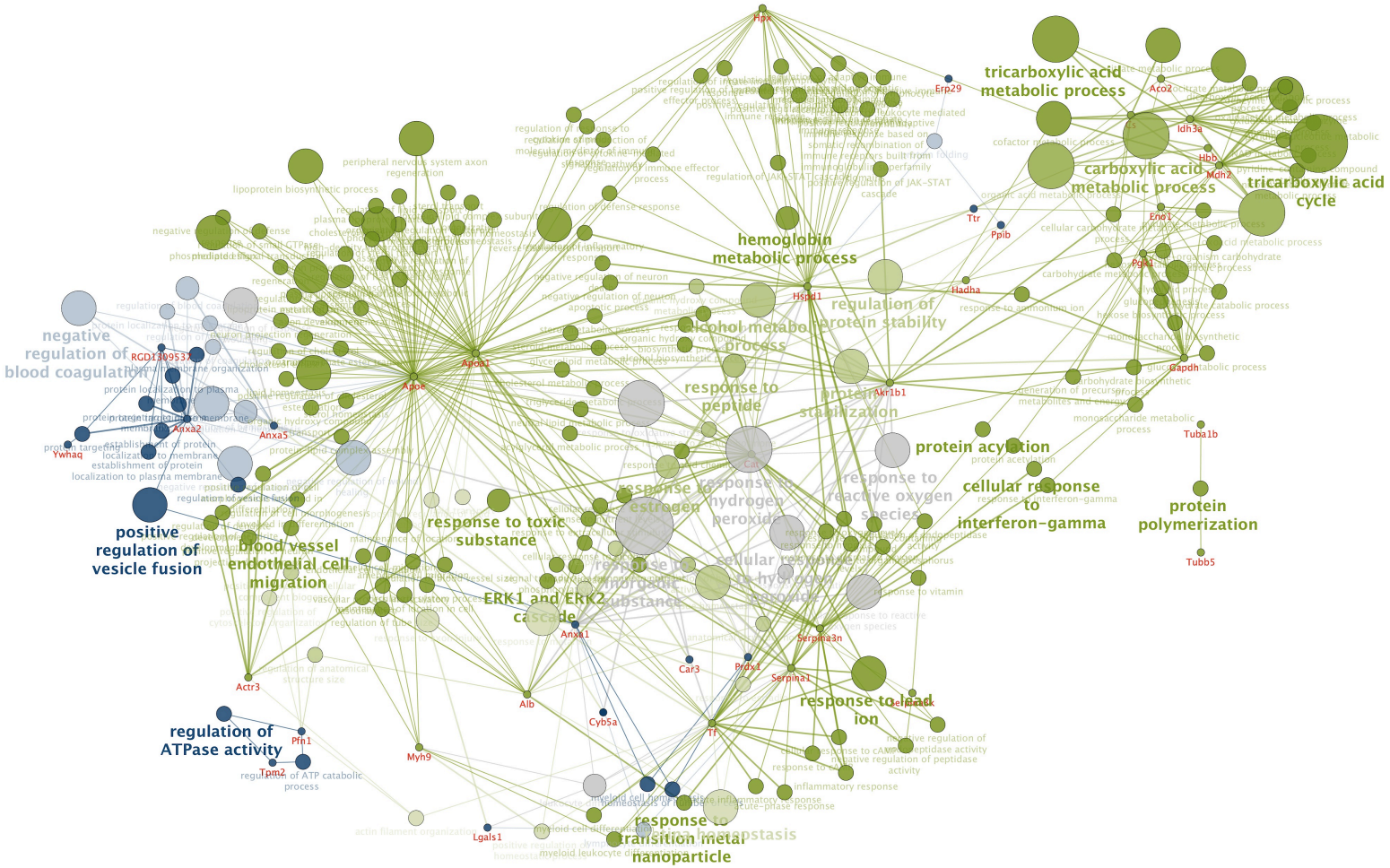

Figure 32 - ClueGo and CluePedia analysis of protein-protein interaction considering up-regulated proteins identified in visceral (blue nodes) and epicardial (green nodes) adipose tissue of obese ZSF1 animal model (based on emPAI values). Blue nodes – Proteins up-regulated in visceral adipose tissue of obese ZSF1; Green nodes – Proteins up-regulated in proteins of epicardial adipose tissue of obese ZSF1.

CHAPTER 4

DISCUSSION

The present study reveals the main differences of epicardial and visceral adipose tissue proteome from obese rats presenting diastolic heart failure and compares it to lean controls. A subsequent bioinformatic approach highlighted the most important signalling pathways that are altered in the presence of DHF associated to obesity, amongst other risk factors. This information might become very helpful for the diagnosis and prognosis of patients with this cardiac dysfunction and to clarify the pathophysiology of this disease.

According to the literature, there are no studies about changes in proteome profile of adipose tissue in diastolic dysfunction. Thus, in this study the optimization of methodology for analysis of visceral and epicardial adipose tissue proteome was performed. The differences between protocols were essentially the extraction solution of proteins. In the literature, VAT and EAT tissue proteome analyses are mainly based on 2DE technique [107, 111-113]. In these studies the protein extraction solutions are similar to PTU [111] and PU [112, 113]. However, they present a small number of extracted proteins (8 – 106 identified proteins) suggesting the need for improving these protocols. In fact, 2DE is very restricted in the detection of low abundance, very hydrophobic, extreme molecular weight and extreme *pI* proteins [118]. This suggests that it would be interesting to test different protein extraction protocols in order to maximize the amount of extracted proteins namely PU, PT and PTU. More recent studies managed to extract a large number of proteins using 1DE and LC-MS/MS [122, 123]. Therefore, in this study, a 1DE-LC-MALDI-TOF/TOF approach was used to test different proteins extraction solutions. Evaluating the reduced number of unique proteins extracted, the PT was immediately excluded. Regarding PU and PTU the main differences relied on protein distribution by the biological process groups, particularly in EAT. While PTU displayed “Reproduction” as an exclusive group in EAT, PU presented unique proteins belonging to “biological regulation” group. “Reproduction” means the production of new individuals that contain some portion of genetic material inherited from one or more parent organisms, while “biological regulation” is any process that modulates a measurable attribute of any biological process, quality or function [135, 136]. For this study the information of the “biological regulation” may be more useful, since an incorrect biological regulation might cause changes in modulation of protein expression resulting in a maladaptive cardiac remodelling and subsequently in diastolic dysfunction. The molecular function analysis shows that PU extracted a large number of proteins both in VAT and EAT, thus covering

the same molecular function groups that PTU. It is possible to conclude that the best protocol to extract proteins in the scope of this study is PU, since it displays no significant differences in cellular component protein distribution, gravy score, molecular weight and considering that it extracted more proteins, covering almost the same protein groups when compared to PTU.

To study diastolic dysfunction, a well-characterized animal model was used, the obese ZSF1 rat. Both obese and lean ZSF1 rats are hypertensive, as assessed by increased EAI and SAP, and present normal systolic function as observed by preserved ejection fraction and normal cardiac index values. However, only the obese ZSF1 rats present diastolic abnormalities displaying increased stiffness (EDP and EDPVR) and impaired relaxation (prolonged constant time of isovolumic relaxation). Moreover, the obese ZSF1 rat has been considered a good model of metabolic syndrome, presenting an impressive amount of fat tissue depots, hyperlipidaemia, proteinuria, impaired glucose tolerance and insulin resistance. Indeed, the initial hypothesis of this study was that the different pattern of adipokines expression in adipose tissue would impose different cardiac actions in obese ZSF1 rats, namely diastolic dysfunction [33, 61, 74, 76, 80, 88, 89]. However, maybe due to the low concentration and small size of adipokines it was not possible to detect them by the used techniques. Therefore, the systemic/paracrine effects of adipokine in D.D will not be addressed. Instead, fat tissue metabolic changes in obesity will be the main focus throughout this discussion. The only adipokine found was fatty acid-binding protein (Fabp4), presenting an overexpression in VAT of obese ZSF1 animals. According to our findings, the overexpression of this adipokine has been strongly associated to obesity, metabolic syndrome and cardiovascular diseases, including the DHF [77, 78, 137, 138]. Considering that obese ZSF1 presents obesity and hyperlipidaemia and that Fabp4 serves as a carrier protein for fatty acids and other lipophilic substances between extra- and intracellular membranes, its increase is expected [79]. However, it raises a question, not yet answered in the literature, whether Fabp4 is involved in causative links between obesity, the metabolic syndrome and related cardiovascular complications, such as DHF.

In obese ZSF1 epicardial adipose tissue a significant down-regulation of proteins involved in catabolic and metabolic processes, mainly associated to lipid and fatty acid oxidation, was observed. Obesity develops when energy production/intake exceed energy expenditure [139]. When the balance between energy supply and demand is perturbed, the

adipose tissue stores the excess of energy in form of TG. Moreover, when adipocyte size is greatly increased, there is a "spill-over" of lipids, such that circulating free fatty acids or TG are elevated [140]. These elevated levels can contribute to hyperlipidaemia like obese ZSF1 presents [141]. Studies have demonstrated that excess of adipose tissue as in obesity increases cardiac dependency on fatty acid oxidation for energy production [142, 143]. However, it has been proposed that elevated availability of fatty acid and TG to the myocardium may contribute to the development of cardiac dysfunction and heart failure [144, 145]. Therefore, as in present work these processes are decreased, it seems to exist a cardiac defensive mechanism in order to decrease the metabolism stabilizing the balance between anabolic and catabolic processes and consequently improving contractile function. Thus, the inhibition of proteins involved in these processes (long-chain acyl-CoA dehydrogenase, enoyl-CoA hydratase and 3-ketoacyl-CoA thiolase) may be used as therapeutic pathways to restrain fatty acid oxidation and improve diastolic dysfunction. In this regard, the inhibition of 3-ketoacyl-CoA thiolase highlights its promising potential to improve diastolic function [146].

In opposite, the EAT emPAI analysis revealed proteins significantly up-regulated when compared with lean ZSF1. These proteins are involved in collagen fibril organization. The collagen alpha-1(I) chain and lumican are the highlighted proteins involved in this process. In obesity, the connective fibre content of adipose tissue increases dramatically, due to up-regulated of several collagens, including collagen alpha-1. In adipose tissue, fibrosis appears to be initiated in response to adipocyte hypertrophy, which occurs as the initial step toward fat pad expansion through enlargement of the lipid droplet size in existing adipocytes [147]. The extracellular matrix in adipose tissue is particularly crucial for maintaining structural integrity of adipocytes and plays a critical role in adipogenesis. There are specific sequential alterations in the extracellular matrix during adipocyte differentiation, with a cascade of activation and deactivation of various matrix metalloproteinases, complementing the creation and destruction of the collagen network [148, 149]. The lumican is an extracellular matrix-localized proteoglycan associated with inflammation and known to bind collagens [150, 151]. Moreover, a study showed that lumican accelerates fibril formation [150] suggesting that inflammation associated to obesity and the adipose tissue enlargement increases lumican and thus collagen content in the extracellular matrix in order to accommodate the expansion of the adipose tissue.

Visceral adipose tissue of obese rats present increased response to oxidative metabolism including, up-regulation of proteins such as superoxide dismutase, an antioxidant enzyme and one of the first defences against reactive oxygen species (ROS)-mediated cardiac injury [152]; peroxiredoxin-1, which belong to an ubiquitous family of thiol-based antioxidant proteins involved in controlling cellular peroxide levels and in redox regulation of signal transduction [153], and annexin-1 that has been proposed to be involved in the regulation of cell growth and differentiation, apoptosis, and inflammation [154] hinting at a relationship between oxidative stress processes and inflammatory response of adipose tissue. Contrarily, other antioxidant enzymes involved in the above mentioned processes were shown to be a down-regulated namely catalase and aldehyde dehydrogenase (Aldh2). Its decreased expression contributes to mitochondrial impairment and increased oxidative stress [155, 156]. Similar changes in these enzymes' expression have been described in the heart resulting in diastolic dysfunction. These results suggest that obesity and inflammation are associated to increase of oxidative stress. Indeed, when obesity persists, the antioxidant sources, as catalase, can be depleted increasing the formation of ROS [165], which seems to be taking place in this work. However, as described above the increase of previous proteins suggests that this response may represent a compensatory mechanism to prevent the formation of ROS. Moreover, decrease of Aldh2 is inversely related to oxidative stress, suggesting that its up-regulation might become a potential therapeutic target in obesity.

In addition to these over-regulated processes, the negative regulation of interleukin-8 secretion, a pro-inflammatory cytokine, is also highlighted and it involves proteins A4 and annexin-A1. Interleukin-8 is produced by a variety of cells, including adipocytes [157]. This pro-inflammatory cytokine plays a crucial role in the recruitment of inflammatory cells such as neutrophils and lymphocytes into tissues [158]. However, the A4 and A1-annexin are anti-inflammatory proteins and were detected in the surface of apoptotic human neutrophils [159, 160]. In fact, a recent study showed that these anti-inflammatory proteins suppress IL-8 production by macrophages [160] suggesting, the presence of defensive mechanisms in visceral adipose tissue in order to improve the inflammation and possible the deleterious consequences associated to obese.

Thereby, all changes that occur in VAT leads to think that the main cause of development/progression obesity complications is oxidative stress, whereas in EAT seems

to be increase of catabolism and adipose tissue expansion. However, to compensate all these deregulations, fat metabolism seems to develop compensatory mechanisms, namely increasing antioxidants and anti-inflammatory proteins as well as inhibiting fatty acid oxidation. Thus, in addition of increase the Aldh2, the increase of proteins and inhibitors stated above may become an interesting therapeutic pathway to explore. However, additional studies on these relationships are needed to clarify the underlying pathways.

An unexpected finding of the present study is related to the fact that the proteome changes in adipose tissue seems to mirror well-described myofilamentary changes associated to DHF myocardium. Interestingly, the cellular component analysis of these proteins shows that, likewise the myocardium, epicardial and visceral adipose tissue express cytoskeletal proteins. Desmin, alpha-actinin-1 and tubulin beta-2A and 5 chain are some of the cytoskeletal proteins found in VAT, while tubulin alpha-1B and beta-3 chain, alpha-actinin-4 and actin alpha cardiac muscle 1 are present in EAT. The cardiomyocytes cytoskeleton is composed of microtubules (tubulin), intermediate filaments (desmin), microfilaments (actin) and endosarcomeric proteins (alpha-actinin and titin) [15]. Myocardial changes in some of these cytoskeletal proteins, such as titin or desmin [161], or on its phosphorylation status have been shown to alter diastolic function [162, 163]. Thus, despite in different locations, the cytoskeletal proteins present in EAT and VAT of obese subjects may be involved in development of diastolic dysfunction. Moreover, comparing the integration of the unique proteins exclusively assigned to VAT in obese and lean subjects in VAT we observed that the main difference between both subjects are in developmental and biological processes, while in EAT are developmental and cellular processes. All these processes comprise mainly structural constituents of cytoskeletal and actin-binding proteins as mentioned above. In the myocardium, previous studies described that the disarrangement and accumulation of desmin increases stiffness and decreases compliance contributing to diastolic dysfunction. In the same way, the increase of total tubulin has been associated to microtubule network density derived from cardiac hypertrophy [162, 164-166]. Moreover, defects in actin-alpha cardiac muscle 1 gene have been linked to impaired ventricular filling induced by dilated and hypertrophic cardiomyopathy [167, 168]. Thus, the results of the proteins found exclusively in the adipose tissue of obese subjects are consistent with several reported myofilamentary changes in DHF and which are responsible for increased of myocardial and chamber

stiffness and suggesting that, in obesity, the majority of proteins involved in development, cellular and biological processes in VAT and EAT, may lead to a disorganization of cardiac filament and cause a change in cardiac relaxation and impaired filling and consequently diastolic and contractile dysfunction. However, a study using non-muscle cells show that the cofilin-1 promotes actin dynamics by depolymerizing and severing actin filaments [169], which may improve the cardiac polymerization and decrease stiffness. So, if these increased levels of cofilin-1 in the adipose tissue of obese ZSF1 parallel its myocardial changes, then its up-regulation could represent an interesting adaptive mechanism to decrease myocardial stiffness and improve the diastolic function. Further studies are necessary to confirm this hypothesis.

Although EAT and VAT share the same embryological origin, there are no studies comparing either secreted adipocytes-derived substances or the differences between their expression levels. Previous studies have shown that, comparing to subcutaneous adipose tissue (SAT), the VAT is more prone to induce impaired fasting glucose [170, 171], diabetes [170, 172], insulin resistance [170, 173], hypertension [174, 175], lipids [176] and metabolic syndrome [177, 178]. However, it has become imperative to study EAT considering that it is the only fat depot that directly contacts with the myocardium. Studies showed that it presents: 1) higher number of adipocytes and their size is smaller, when compared with perirenal fat [59]; 2) different fatty acid composition comparing to SAT [179] and 3)distinct relative expression levels of adipokines when compared to subcutaneous or substernal fat [84, 180]. Despite all these findings only three studies have used proteomics to compare visceral and gonadal (GAT) and subcutaneous adipose tissue (SAT) [112] and EAT and SAT [107, 111] but none has provided such a broad general approach to the protein composition. In this study it was found that epicardial and visceral adipose tissue share 96 and 85 identified proteins in obese and lean ZSF1, respectively. There seems to be no significant differences between EAT and VAT regarding unique proteins distribution in biological processes, molecular function and cellular components, thus suggesting some similarities between both tissues. In this study, obese ZSF1 EAT presents increased ApoaI and catalase when compared with VAT. Contrastingly, previous studies comparing EAT and SAT report that apolipoprotein-AI (ApoaI) was increase in EAT, while catalase was decrease in this tissue [107, 111]. Moreover, enoyl-Coa hidratase, mitochondrial, 60kDa heat shock protein, mitochondrial and gesolin are increased in VAT

when compared with GAT and SAT [112]. Nevertheless, in present study these proteins are increased in obese ZSF1 EAT comparing with VAT. Altogether, data from the present study suggests that epicardial adipose tissue behaves differently from the others fat depots assessed, providing new information on epicardial adipose tissue metabolism. Furthermore, the comparison of shared proteins between epicardial and visceral adipose tissue show that there are up-regulated proteins identified in both tissues, either in lean as obese ZSF1, which are involved in different processes and responses. Differences between epicardial and visceral adipose tissue suggest that although they share some proteins in similar abundances, their functions may be different.

CHAPTER 5

CONCLUSION

Once analysed the changes in proteome of epicardial and visceral adipose tissue induced by obesity, it is possible to conclude that although the epicardial and visceral adipose tissue share the same embryological origin, its proteome and respective functions and processes seem to be different, being an important fact for future adipose tissue studies.

In EAT, the decreased proteins involved in catabolic and metabolic metabolism seem to be a compensatory mechanism in order to decrease the fatty acid oxidation associated to obesity and cardiac dysfunction, stabilizing the balance between anabolic and catabolic processes and consequently improve cardiac function.

The obesity and its associated inflammation causes changes in epicardial adipose tissue extracellular matrix increasing collagen content through increase of lumican in order to accommodate the expansion of the adipose tissue.

The decreased expression of catalase and Aldh2 may be one of the possible factors that lead to oxidative stress in obese subjects in VAT. However, the increase of others antioxidants and anti-inflammatory proteins seems to be a compensatory mechanisms developed by metabolism to prevent the increase of ROS and inflammation resultant of obesity. Therefore, the increase of Aldh2, antioxidants and anti-inflammatory agents in obesity may be a starting point for developing therapeutic ways to improve the oxidative stress derived from obesity.

The increased A4 and A1-annexin involved in negative regulation of IL-8 secretion suggest defensive mechanisms in visceral adipose tissue in order to improve the inflammation and potential obesity-induced consequence.

The increase of contractile proteins found exclusively in obese ZSF1 adipose tissue are consistent with several reported myofilamentary changes in DHF suggesting that they may be a reflection of what happens in the heart. In fact, several studies in proteomic present these proteins in adipose tissue, raising a question that is not yet answered in the literature, how and why these cardiac contractile proteins go to adipose tissue.

Taken together, the obesity seems result in increase of energy production, oxidative stress and inflammation that may change expression, function and phosphorylation of proteins involved in cardiac function. Thus, future work should focus on therapeutic strategies to counteract these deleterious/compensatory processes in obesity aiming to improve patients' quality of life. This work is a general approach to the protein

composition of visceral and epicardial adipose tissue, helping the future development in researches more specifics about diastolic dysfunction.

As stated in the discussion, the cardiac contractile proteins changes seem to be, in partly, caused by oxidative stress. This stress can impair the function and/or phosphorylation of these proteins and consequently cause changes in cardiac relaxation, thus leading to diastolic dysfunction. Therefore, in the future, a study about phosphoproteomics changes and its acute modulation in cardiac diastolic dysfunction would be interesting to elucidate the mechanisms involved in this disease.

Another possible study, to understand the mechanisms involved in diastolic dysfunction, would be to analyse the secretome using conditioned medium obtained by incubating the fat samples in a medium without serum. This conditioned medium would reflect the secretome that is released from fat tissue.

Lastly, once the present study was based on proteome of ZSF1 animal model, it would be useful and interesting to analyse samples from obese and lean human heart with cardiac diastolic dysfunction.

REFERENCES

1. McMurray J.J., Adamopoulos S., Anker S.D., Auricchio A., Bohm M., Dickstein K., Falk V., Filippatos G., Fonseca C., Gomez-Sanchez M.A., Jaarsma T., Kober L., Lip G.Y., Maggioni A.P., Parkhomenko A., Pieske B.M., Popescu B.A., Ronnevik P.K., Rutten F.H., Schwitter J., Seferovic P., Stepinska J., Trindade P.T., Voors A.A., Zannad F., Zeiher A. ESC Guidelines for the diagnosis and treatment of acute and chronic heart failure 2012: The Task Force for the Diagnosis and Treatment of Acute and Chronic Heart Failure 2012 of the European Society of Cardiology. Developed in collaboration with the Heart Failure Association (HFA) of the ESC. Eur Heart J. 2012;33(14):1787-1847.
2. López-Sendón J. The heart failure epidemic. Medicographia. 2011;33(4):363-369.
3. Owan T.E., Redfield M.M. Epidemiology of diastolic heart failure. Progress in cardiovascular diseases. 2005;47(5):320-332.
4. Yturralde R.F., Gaasch W.H. Diagnostic criteria for diastolic heart failure. Progress in cardiovascular diseases. 2005;47(5):314-319.
5. Katz A.M., Zile M.R. New molecular mechanism in diastolic heart failure. Circulation. 2006;113(16):1922-1925.
6. Owan TE, Hodge DO, Herges RM, Jacobsen SJ, Roger VL, MM R. Trends in prevalence and outcome of heart failure with preserved ejection fraction. N Engl J Med. 2006;355:251-259.
7. Zile M.R., Brutsaert D.L. New concepts in diastolic dysfunction and diastolic heart failure: Part I: diagnosis, prognosis, and measurements of diastolic function. Circulation. 2002;105(11):1387-1393.
8. Jurgens C.Y., Moser D.K., Armola R., Carlson B., Sethares K., Riegel B. Symptom clusters of heart failure. Research in nursing & health. 2009;32(5):551-560.
9. Association A.H. What is Heart Failure? 2012 [cited 2013 November 4]; Available from: http://www.heart.org/idc/groups/heart-public/@wcm/@hcm/documents/downloadable/ucm_300315.pdf.
10. Ashley E.A., Niebaue J. Cardiology Explained: London: Remedica; 2004.
11. Gary R., Davis L. Diastolic heart failure. Heart & lung : the journal of critical care. 2008;37(6):405-416.
12. Zile M.R., Baicu C.F., Gaasch W.H. Diastolic heart failure--abnormalities in active relaxation and passive stiffness of the left ventricle. The New England journal of medicine. 2004;350(19):1953-1959.
13. Aziz F., Tk L.A., Enweluzo C., Dutta S., Zaeem M. Diastolic heart failure: a concise review. Journal of clinical medicine research. 2013;5(5):327-334.
14. Galderisi M. Diastolic dysfunction and diastolic heart failure: diagnostic, prognostic and therapeutic aspects. Cardiovasc Ultrasound. 2005;3:9.
15. Leite-Moreira A.F. Heart failure - Current perspectives in diastolic dysfunction and diastolic heart failure. Heart. 2006;92(5):712-718.
16. Paulus W.J., Brutsaert D.L., Gillebert T.C., Rademakers F.E., Stanislas U., Leite-Moreira A.F., Hess O.M., Jiang Z.H., Kaufmann P., Mandinov L., Matter C., Marino P., Gibson D.G., Henein M.Y., Manolas J., Smiseth O.A., Stugaard M., Hatle L.K., Spirito P., Betocchi S., Villari B., Goetzsche O., Shah A.M., Failure E.S.G.D.H. How to diagnose diastolic heart failure. Eur Heart J. 1998;19(7):990-1003.
17. Vasan R.S., Benjamin E.J., Levy D. Prevalence, clinical features and prognosis of diastolic heart failure: an epidemiologic perspective. Journal of the American College of Cardiology. 1995;26(7):1565-1574.

18. Kuznetsova T., Herbots L., Lopez B., Jin Y., Richart T., Thijs L., Gonzalez A., Herregods M.C., Fagard R.H., Diez J., Staessen J.A. Prevalence of Left Ventricular Diastolic Dysfunction in a General Population. Circ-Heart Fail. 2009;2(2):105-112.
19. Kloch-Badelek M., Kuznetsova T., Sakiewicz W., Tikhonoff V., Ryabikov A., Gonzalez A., Lopez B., Thijs L., Jin Y., Malyutina S., Stolarz-Skrzypek K., Casiglia E., Diez J., Narkiewicz K., Kawecka-Jaszcz K., Staessen J.A., Genes E.P. Prevalence of left ventricular diastolic dysfunction in European populations based on cross-validated diagnostic thresholds. Cardiovasc Ultrasoun. 2012;10.
20. Wilhelmsen L., Rosengren A., Eriksson H., Lappas G. Heart failure in the general population of men--morbidity, risk factors and prognosis. Journal of internal medicine. 2001;249(3):253-261.
21. Kenchaiah S., Evans J.C., Levy D., Wilson P.W.F., Benjamin E.J., Larson M.G., Kannel W.B., Vasan R.S. Obesity and the risk of heart failure. New England Journal of Medicine. 2002;347(5):305-313.
22. Poirier P., Giles T.D., Bray G.A., Hong Y., Stern J.S., Pi-Sunyer F.X., Eckel R.H. Obesity and Cardiovascular Disease: Pathophysiology, Evaluation, and Effect of Weight Loss: An Update of the 1997 American Heart Association Scientific Statement on Obesity and Heart Disease From the Obesity Committee of the Council on Nutrition, Physical Activity, and Metabolism. Circulation. 2006;113(6):898-918.
23. Cetin M., Kocaman S.A., Durakoglugil M.E., Erdogan T., Ergul E., Dogan S., Canga A. Effect of epicardial adipose tissue on diastolic functions and left atrial dimension in untreated hypertensive patients with normal systolic function. Journal of cardiology. 2013;61(5):359-364.
24. Russo C., Jin Z., Homma S., Rundek T., Elkind M.S., Sacco R.L., Di Tullio M.R. Effect of obesity and overweight on left ventricular diastolic function: a community-based study in an elderly cohort. Journal of the American College of Cardiology. 2011;57(12):1368-1374.
25. Lavie C.J., Amodeo C., Ventura H.O., Messerli F.H. LEft atrial abnormalities indicating diastolic ventricular dysfunction in cardiopathy of obesity. CHEST Journal. 1987;92(6):1042-1046.
26. Powell B.D., Redfield M.M., Bybee K.A., Freeman W.K., Rihal C.S. Association of Obesity With Left Ventricular Remodeling and Diastolic Dysfunction in Patients Without Coronary Artery Disease. The American journal of cardiology. 2006;98(1):116-120.
27. Peterson L.R., Waggoner A.D., Schechtman K.B., Meyer T., Gropler R.J., Barzilai B., Davila-Roman V.G. Alterations in left ventricular structure and function in young healthy obese women: assessment by echocardiography and tissue Doppler imaging. Journal of the American College of Cardiology. 2004;43(8):1399-1404.
28. Cornier M.-A., Dabelea D., Hernandez T.L., Lindstrom R.C., Steig A.J., Stob N.R., Van Pelt R.E., Wang H., Eckel R.H. The Metabolic Syndrome. Endocrine Reviews. 2008;29(7):777-822.
29. Eckel R.H., Grundy S.M., Zimmet P.Z. The metabolic syndrome. The Lancet.365(9468):1415-1428.
30. Emanuela F., Grazia M., Marco de R., Maria Paola L., Giorgio F., Marco B. Inflammation as a Link between Obesity and Metabolic Syndrome. Journal of nutrition and metabolism. 2012;2012:476380.
31. Grundy S.M. Obesity, metabolic syndrome, and cardiovascular disease. The Journal of clinical endocrinology and metabolism. 2004;89(6):2595-2600.

32. Klein S. Is visceral fat responsible for the metabolic abnormalities associated with obesity?: implications of omentectomy. Diabetes Care. 2010;33(7):1693-1694.
33. Hajer G.R., van Haeften T.W., Visseren F.L. Adipose tissue dysfunction in obesity, diabetes, and vascular diseases. Eur Heart J. 2008;29(24):2959-2971.
34. Novo S., Balbarini A., Belch J.J., Bonura F., Clement D.L., Diamantopoulos E., Fareed J., Norgren L., Poredos P., Rotzocil K. The metabolic syndrome: definition, diagnosis and management. International angiology : a journal of the International Union of Angiology. 2008;27(3):220-231.
35. Alberti K.G., Zimmet P.Z. Definition, diagnosis and classification of diabetes mellitus and its complications. Part 1: diagnosis and classification of diabetes mellitus provisional report of a WHO consultation. Diabetic medicine : a journal of the British Diabetic Association. 1998;15(7):539-553.
36. Balkau B., Charles M.A. Comment on the provisional report from the WHO consultation. European Group for the Study of Insulin Resistance (EGIR). Diabetic medicine : a journal of the British Diabetic Association. 1999;16(5):442-443.
37. Grundy S.M., Cleeman J.I., Daniels S.R., Donato K.A., Eckel R.H., Franklin B.A., Gordon D.J., Krauss R.M., Savage P.J., Smith S.C., Jr., Spertus J.A., Costa F. Diagnosis and management of the metabolic syndrome: an American Heart Association/National Heart, Lung, and Blood Institute Scientific Statement. Circulation. 2005;112(17):2735-2752.
38. Zimmet P., Magliano D., Matsuzawa Y., Alberti G., Shaw J. The metabolic syndrome: a global public health problem and a new definition. Journal of atherosclerosis and thrombosis. 2005;12(6):295-300.
39. Laclaustra M., Corella D., Ordovas J.M. Metabolic syndrome pathophysiology: the role of adipose tissue. Nutrition, metabolism, and cardiovascular diseases : NMCD. 2007;17(2):125-139.
40. Forner F., Kumar C., Luber C.A., Fromme T., Klingenspor M., Mann M. Proteome Differences between Brown and White Fat Mitochondria Reveal Specialized Metabolic Functions. Cell Metabolism. 2009;10(4):324-335.
41. Vazquez-Vela M.E.F., Torres N., Tovar A.R. White Adipose Tissue as Endocrine Organ and Its Role in Obesity. Arch Med Res. 2008;39(8):715-728.
42. Gnacinska M., Malgorzewicz S., Stojek M., Lysiak-Szydlowska W., Sworczak K. Role of adipokines in complications related to obesity: a review. Advances in medical sciences. 2009;54(2):150-157.
43. Trayhurn P., Wood I.S. Adipokines: inflammation and the pleiotropic role of white adipose tissue. The British journal of nutrition. 2004;92(3):347-355.
44. Trayhurn P., Bing C., Wood I.S. Adipose tissue and adipokines--energy regulation from the human perspective. The Journal of nutrition. 2006;136(7 Suppl):1935S-1939S.
45. Maury E., Brichard S.M. Adipokine dysregulation, adipose tissue inflammation and metabolic syndrome. Molecular and Cellular Endocrinology. 2010;314(1):1-16.
46. Harwood H.J. The adipocyte as an endocrine organ in the regulation of metabolic homeostasis. Neuropharmacology. 2012;63(1):57-75.
47. Deng Y.F., Scherer P.E. Adipokines as novel biomarkers and regulators of the metabolic syndrome. Year in Diabetes and Obesity. 2010;1212:E1-E19.
48. Stastna M., Van Eyk J.E. Investigating the Secretome Lessons About the Cells That Comprise the Heart. Circ-Cardiovasc Gene. 2012;5(1):O8-O18.

49. Baker A.R., da Silva N.F., Quinn D.W., Harte A.L., Pagano D., Bonser R.S., Kumar S., McTernan P.G. Human epicardial adipose tissue expresses a pathogenic profile of adipocytokines in patients with cardiovascular disease. Cardiovasc Diabetol. 2006;5.
50. Ouchi N., Parker J.L., Lugus J.J., Walsh K. Adipokines in inflammation and metabolic disease. Nature reviews Immunology. 2011;11(2):85-97.
51. Lima-Martínez M.M., Iacobellis G. Grasa epicárdica: una nueva herramienta para la evaluación del riesgo cardiometabólico. Hipertensión y Riesgo Vascular. 2011;28(2):63-68.
52. Fain J.N. Release of inflammatory mediators by human adipose tissue is enhanced in obesity and primarily by the nonfat cells: a review. Mediators of inflammation. 2010;2010:513948.
53. Vanderkooy K., Leenen R., Seidell J.C., Deurenberg P., Visser M. Abdominal Diameters as Indicators of Visceral Fat - Comparison between Magnetic-Resonance-Imaging and Anthropometry. Brit J Nutr. 1993;70(1):47-58.
54. Iacobellis G., Assael F., Ribaudo M.C., Zappaterreno A., Alessi G., Di Mario U., Leonetti F. Epicardial fat from echocardiography: A new method for visceral adipose tissue prediction. Obes Res. 2003;11(2):304-310.
55. Iacobellis G., Ribaudo M.C., Assael F., Vecci E., Tiberti C., Zappaterreno A., Di Mario U., Leonetti F. Echocardiographic epicardial adipose tissue is related to anthropometric and clinical parameters of metabolic syndrome: A new indicator of cardiovascular risk. J Clin Endocr Metab. 2003;88(11):5163-5168.
56. Iacobellis G., Corradi D., Sharma A.M. Epicardial adipose tissue: anatomic, biomolecular and clinical relationships with the heart. Nature clinical practice Cardiovascular medicine. 2005;2(10):536-543.
57. Sengul C., Ozveren O. Epicardial adipose tissue: a review of physiology, pathophysiology, and clinical applications. Anadolu kardiyoloji dergisi : AKD = the Anatolian journal of cardiology. 2013;13(3):261-265.
58. Iacobellis G., Bianco A.C. Epicardial adipose tissue: emerging physiological, pathophysiological and clinical features. Trends in endocrinology and metabolism: TEM. 2011;22(11):450-457.
59. Marchington J.M., Mattacks C.A., Pond C.M. Adipose-Tissue in the Mammalian Heart and Pericardium - Structure, Fetal Development and Biochemical-Properties. Comp Biochem Phys B. 1989;94(2):225-232.
60. Smith H.L., Willius F.A. Adiposity of the heart - A clinical and pathologic study of one hundred and thirty-six obese patients. Archives of internal medicine. 1933;52(6):911-931.
61. Cherian S., Lopaschuk G.D., Carvalho E. Cellular cross-talk between epicardial adipose tissue and myocardium in relation to the pathogenesis of cardiovascular disease. Am J Physiol-Endoc M. 2012;303(8):E937-E949.
62. Sacks H.S., Fain J.N. Human epicardial adipose tissue: a review. Am Heart J. 2007;153(6):907-917.
63. Ibrahim M.M. Subcutaneous and visceral adipose tissue: structural and functional differences. Obesity reviews : an official journal of the International Association for the Study of Obesity. 2010;11(1):11-18.
64. Cook K.S., Min H.Y., Johnson D., Chaplinsky R.J., Flier J.S., Hunt C.R., Spiegelman B.M. Adipsin: a circulating serine protease homolog secreted by adipose tissue and sciatic nerve. Science. 1987;237(4813):402-405.

65. Hotamisligil G.S., Shargill N.S., Spiegelman B.M. Adipose expression of tumor necrosis factor-alpha: direct role in obesity-linked insulin resistance. Science. 1993;259(5091):87-91.
66. Zhang Y., Proenca R., Maffei M., Barone M., Leopold L., Friedman J.M. Positional cloning of the mouse obese gene and its human homologue. Nature. 1994;372(6505):425-432.
67. Alessi M.C., Peiretti F., Morange P., Henry M., Nalbone G., Juhan-Vague I. Production of plasminogen activator inhibitor 1 by human adipose tissue: possible link between visceral fat accumulation and vascular disease. Diabetes. 1997;46(5):860-867.
68. Fernandes T.M., Jr R.R.A., Moreira A.F.L. Acções cardiovasculares da adiponectina: implicações fisiopatológicas. Revista portuguesa de cardiologia : orgão oficial da Sociedade Portuguesa de Cardiologia. 2008.
69. Falcao-Pires I., Castro-Chaves P., Miranda-Silva D., Lourenco A.P., Leite-Moreira A.F. Physiological, pathological and potential therapeutic roles of adipokines. Drug discovery today. 2012;17(15-16):880-889.
70. Thalmann S., Meier C.A. Local adipose tissue depots as cardiovascular risk factors. Cardiovascular research. 2007;75(4):690-701.
71. Hopkins T.A., Ouchi N., Shibata R., Walsh K. Adiponectin actions in the cardiovascular system. Cardiovascular research. 2007;74(1):11-18.
72. Sam F., Duhaney T.A.S., Sato K., Wilson R.M., Ohashi K., Sono-Romanelli S., Higuchi A., De Silva D.S., Qin F.Z., Walsh K., Ouchi N. Adiponectin Deficiency, Diastolic Dysfunction, and Diastolic Heart Failure. Endocrinology. 2010;151(1):322-331.
73. Kralisch S., Fasshauer M. Adipocyte fatty acid binding protein: a novel adipokine involved in the pathogenesis of metabolic and vascular disease? Diabetologia. 2013;56(1):10-21.
74. Tuncman G., Erbay E., Hom X., De Vivo I., Campos H., Rimm E.B., Hotamisligil G.S. A genetic variant at the fatty acid-binding protein aP2 locus reduces the risk for hypertriglyceridemia, type 2 diabetes, and cardiovascular disease. P Natl Acad Sci USA. 2006;103(18):6970-6975.
75. Stejskal D., Karpisek M. Adipocyte fatty acid binding protein in a Caucasian population: a new marker of metabolic syndrome? Eur J Clin Invest. 2006;36(9):621-625.
76. Cabre A., Lazaro I., Girona J., Manzanares J.M., Marimon F., Plana N., Heras M., Masana L. Plasma fatty acid binding protein 4 is associated with atherogenic dyslipidemia in diabetes. J Lipid Res. 2008;49(8):1746-1751.
77. Lamounier-Zepter V., Look C., Alvarez J., Christ T., Ravens U., Schunck W.H., Ehrhart-Bornstein M., Bornstein S.R., Morano I. Adipocyte Fatty Acid-Binding Protein Suppresses Cardiomyocyte Contraction A New Link Between Obesity and Heart Disease. Circ Res. 2009;105(4):326-U334.
78. Djousse L., Bartz T.M., Ix J.H., Kochar J., Kizer J.R., Gottdiener J.S., Tracy R.P., Mozaffarian D., Siscovick D.S., Mukamal K.J., Zieman S.J. Fatty acid-binding protein 4 and incident heart failure: the Cardiovascular Health Study. European journal of heart failure. 2013;15(4):394-399.
79. Djousse L., Bartz T.M., Ix J.H., Kochar J., Kizer J.R., Gottdiener J.S., Tracy R.P., Mozaffarian D., Siscovick D.S., Mukamal K.J., Zieman S.J. Fatty acid-binding protein 4 and incident heart failure: the Cardiovascular Health Study. European journal of heart failure. 2013;15(4):394-399.
80. Malavazos A.E., Corsi M.M., Ermetici F., Coman C., Sardanelli F., Rossi A., Morricone L., Ambrosi B. Proinflammatory cytokines and cardiac abnormalities in

uncomplicated obesity: Relationship with abdominal fat deposition. Nutr Metab Cardiovas. 2007;17(4):294-302.
81. Iacobellis G., Ribaudo M.C., Zappaterreno A., Iannucci C.V., Leonetti F. Relation between epicardial adipose tissue and left ventricular mass. American Journal of Cardiology. 2004;94(8):1084-1087.
82. Iacobellis G., Pond C.M., Sharma A.M. Different "weight" of cardiac and general adiposity in predicting left ventricle morphology. Obesity (Silver Spring). 2006;14(10):1679-1684.
83. Iacobellis G., Leonetti F., Singh N., A M.S. Relationship of epicardial adipose tissue with atrial dimensions and diastolic function in morbidly obese subjects. International journal of cardiology. 2007;115(2):272-273.
84. Mazurek T., Zhang L.F., Zalewski A., Mannion J.D., Diehl J.T., Arafat H., Sarov-Blat L., O'Brien S., Keiper E.A., Johnson A.G., Martin J., Goldstein B.J., Shi Y. Human epicardial adipose tissue is a source of inflammatory mediators. Circulation. 2003;108(20):2460-2466.
85. Iacobellis G., Pistilli D., Gucciardo M., Leonetti F., Miraldi F., Brancaccio G., Gallo P., di Gioia C.R.T. Adiponectin expression in human epicardial adipose tissue in vivo is lower in patients with coronary artery disease. Cytokine. 2005;29(6):251-255.
86. Bahia L., Aguiar L.G., Villela N., Bottino D., Godoy-Matos A.F., Geloneze B., Tambascia M., Bouskela E. Relationship between adipokines, inflammation, and vascular reactivity in lean controls and obese subjects with metabolic syndrome. Clinics (Sao Paulo, Brazil). 2006;61(5):433-440.
87. Ohmori R., Momiyama Y., Kato R., Taniguchi H., Ogura M., Ayaori M., Nakamura H., Ohsuzu F. Associations between serum resistin levels and insulin resistance, inflammation, and coronary artery disease. Journal of the American College of Cardiology. 2005;46(2):379-380.
88. Piestrzeniewicz K., Luczak K., Maciejewski M., Goch J.H. Impact of obesity and adipokines on cardiac structure and function in men with first myocardial infarction. Arch Med Sci. 2008;4(2):152-160.
89. Barouch L.A., Berkowitz D.E., Harrison R.W., O'Donnell C.P., Hare J.M. Disruption of leptin signaling contributes to cardiac hypertrophy independently of body weight in mice. Circulation. 2003;108(6):754-759.
90. Hong S.J., Park C.G., Seo H.S., Oh D.J., Ro Y.M. Associations among plasma adiponectin, hypertension, left ventricular diastolic function and left ventricular mass index. Blood Pressure. 2004;13(4):236-242.
91. Hamdani N., Franssen C., Lourenco A., Falcao-Pires I., Fontoura D., Leite S., Plettig L., Lopez B., Ottenheijm C.A., Becher P.M., Gonzalez A., Tschope C., Diez J., Linke W.A., Leite-Moreira A.F., Paulus W.J. Myocardial titin hypophosphorylation importantly contributes to heart failure with preserved ejection fraction in a rat metabolic risk model. Circulation Heart failure. 2013;6(6):1239-1249.
92. Zile M.R., Gottdiener J.S., Hetzel S.J., McMurray J.J., Komajda M., McKelvie R., Baicu C.F., Massie B.M., Carson P.E. Prevalence and significance of alterations in cardiac structure and function in patients with heart failure and a preserved ejection fraction. Circulation. 2011;124(23):2491-2501.
93. Tofovic S.P., Dubey R., Salah E.M., Jackson E.K. 2-Hydroxyestradiol attenuates renal disease in chronic puromycin aminonucleoside nephropathy. J Am Soc Nephrol. 2002;13(11):2737-2747.

94. Bilan V.P., Salah E.M., Bastacky S., Jones H.B., Mayers R.M., Zinker B., Poucher S.M., Tofovic S.P. Diabetic nephropathy and long-term treatment effects of rosiglitazone and enalapril in obese ZSF1 rats. The Journal of endocrinology. 2011;210(3):293-308.
95. Tofovic S.P., Kost C.K., Jr., Jackson E.K., Bastacky S.I. Long-term caffeine consumption exacerbates renal failure in obese, diabetic, ZSF1 (fa-fa(cp)) rats. Kidney Int. 2002;61(4):1433-1444.
96. Tofovic S.P., Kusaka H., Kost C.K., Jr., Bastacky S. Renal function and structure in diabetic, hypertensive, obese ZDFxSHHF-hybrid rats. Renal failure. 2000;22(4):387-406.
97. Joshi D., Gupta R., Dubey A., Shiwalkar A., Pathak P., Gupta R.C., Chauthaiwale V., Dutt C. TRC4186, a novel AGE-breaker, improves diabetic cardiomyopathy and nephropathy in Ob-ZSF1 model of type 2 diabetes. Journal of cardiovascular pharmacology. 2009;54(1):72-81.
98. Rafikova O., Salah E.M., Tofovic S.P. Renal and metabolic effects of tempol in obese ZSF1 rats--distinct role for superoxide and hydrogen peroxide in diabetic renal injury. Metabolism: clinical and experimental. 2008;57(10):1434-1444.
99. Zambad S.P., Munshi S., Dubey A., Gupta R., Busiello R.A., Lanni A., Goglia F., Gupta R.C., Chauthaiwale V., Dutt C. TRC150094 attenuates progression of nontraditional cardiovascular risk factors associated with obesity and type 2 diabetes in obese ZSF1 rats. Diabetes, metabolic syndrome and obesity : targets and therapy. 2011;4:5-16.
100. Zile M.R., Brutsaert D.L. New concepts in diastolic dysfunction and diastolic heart failure: Part II: causal mechanisms and treatment. Circulation. 2002;105(12):1503-1508.
101. Arrell D.K., Neverova I., Van Eyk J.E. Cardiovascular proteomics: evolution and potential. Circ Res. 2001;88(8):763-773.
102. White M.Y., Van Eyk J.E. Cardiovascular proteomics: past, present, and future. Molecular diagnosis & therapy. 2007;11(2):83-95.
103. Wilkins M.R., Pasquali C., Appel R.D., Ou K., Golaz O., Sanchez J.C., Yan J.X., Gooley A.A., Hughes G., HumpherySmith I., Williams K.L., Hochstrasser D.F. From proteins to proteomes: Large scale protein identification by two-dimensional electrophoresis and amino acid analysis. Bio-Technol. 1996;14(1):61-65.
104. Lamond A.I., Uhlen M., Horning S., Makarov A., Robinson C.V., Serrano L., Hartl F.U., Baumeister W., Werenskiold A.K., Andersen J.S., Vorm O., Linial M., Aebersold R., Mann M. Advancing cell biology through proteomics in space and time (PROSPECTS). Molecular & cellular proteomics : MCP. 2012;11(3):O112 017731.
105. Abdallah C., Dumas-Gaudot E., Renaut J., Sergeant K. Gel-based and gel-free quantitative proteomics approaches at a glance. International journal of plant genomics. 2012;2012:494572.
106. Chiou S.H., Wu C.Y. Clinical proteomics: current status, challenges, and future perspectives. The Kaohsiung journal of medical sciences. 2011;27(1):1-14.
107. Salgado-Somoza A., Teijeira-Fernandez E., Fernandez A.L., Gonzalez-Juanatey J.R., Eiras S. Changes in lipid transport-involved proteins of epicardial adipose tissue associated with coronary artery disease. Atherosclerosis. 2012;224(2):492-499.
108. Gauci V.J., Padula M.P., Coorssen J.R. Coomassie blue staining for high sensitivity gel-based proteomics. J Proteomics. 2013;90:96-106.
109. Zhao L., Ding Y.Q., Liang L., Li X., Li X.H., Wu L.S. [Two-dimensional polyacrylamide gel electrophoresis-based serum protein separation: comparison of two sample preparation methods]. Nan fang yi ke da xue xue bao = Journal of Southern Medical University. 2007;27(1):5-8.

110. Babnigg G., Giometti C.S. GELBANK: a database of annotated two-dimensional gel electrophoresis patterns of biological systems with completed genomes. Nucleic Acids Res. 2004;32(Database issue):D582-585.
111. Salgado-Somoza A., Teijeira-Fernandez E., Fernandez A.L., Gonzalez-Juanatey J.R., Eiras S. Proteomic analysis of epicardial and subcutaneous adipose tissue reveals differences in proteins involved in oxidative stress. Am J Physiol-Heart C. 2010;299(1):H202-H209.
112. Roca-Rivada A., Alonso J., Al-Massadi O., Castelao C., Peinado J.R., Seoane L.M., Casanueva F.F., Pardo M. Secretome analysis of rat adipose tissues shows location-specific roles for each depot type. J Proteomics. 2011;74(7):1068-1079.
113. Xie W.D., Wang H., Zhang J.F., Kung H.F., Zhao Y.N., Zhang Y.O. Proteomic profile of visceral adipose tissues between low-fat diet-fed obesity-resistant and obesity-prone C57BL/6 mice. Molecular medicine reports. 2010;3(6):1047-1052.
114. Bland A.M., Janech M.G., Almeida J.S., Arthur J.M. Sources of variability among replicate samples separated by two-dimensional gel electrophoresis. Journal of biomolecular techniques : JBT. 2010;21(1):3-8.
115. Beckett P. The basics of 2D DIGE. Methods Mol Biol. 2012;854:9-19.
116. Tonge R., Shaw J., Middleton B., Rowlinson R., Rayner S., Young J., Pognan F., Hawkins E., Currie I., Davison M. Validation and development of fluorescence two-dimensional differential gel electrophoresis proteomics technology. Proteomics. 2001;1(3):377-396.
117. Murri M., Insenser M., Bernal-Lopez M.R., Perez-Martinez P., Escobar-Morreale H.F., Tinahones F.J. Proteomic analysis of visceral adipose tissue in pre-obese patients with type 2 diabetes. Mol Cell Endocrinol. 2013;376(1-2):99-106.
118. Kupcova Skalnikova H. Proteomic techniques for characterisation of mesenchymal stem cell secretome. Biochimie. 2013;95(12):2196-2211.
119. Howes J.M., Keen J.N., Findlay J.B., Carter A.M. The application of proteomics technology to thrombosis research: the identification of potential therapeutic targets in cardiovascular disease. Diabetes Vasc Dis Re. 2008;5(3):205-212.
120. Amado F.M., Ferreira R.P., Vitorino R. One decade of salivary proteomics: current approaches and outstanding challenges. Clinical biochemistry. 2013;46(6):506-517.
121. Chi P.V., Dung N.T. 2D-NanoLC-ESI-MS/MS for Separation and Identification of Mouse Brain Membrane Proteins2012 2012-10-24.
122. Kim S.J., Chae S., Kim H., Mun D.G., Back S., Choi H.Y., Park K.S., Hwang D., Choi S.H., Lee S.W. A protein profile of visceral adipose tissues linked to early pathogenesis of type 2 diabetes mellitus. Molecular & cellular proteomics : MCP. 2014;13(3):811-822.
123. Alvarez-Llamas G., Szalowska E., de Vries M.P., Weening D., Landman K., Hoek A., Wolffenbuttel B.H., Roelofsen H., Vonk R.J. Characterization of the human visceral adipose tissue secretome. Molecular & cellular proteomics : MCP. 2007;6(4):589-600.
124. Rodriguez-Suarez E., Whetton A.D. The application of quantification techniques in proteomics for biomedical research. Mass Spectrom Rev. 2013;32(1):1-26.
125. Amado F., Domingues P., Domingues M.d.R., Ferreira R., Vitorino R. Análise de proteínas - Guia de laboratório. 100luz ed2013.
126. Henzel W.J., Watanabe C., Stults J.T. Protein identification: the origins of peptide mass fingerprinting. Journal of the American Society for Mass Spectrometry. 2003;14(9):931-942.

127. Lewis J.K., Wei J., Siuzdak G. Matrix-Assisted Laser Desorption/Ionization Mass Spectrometry in Peptide and Protein Analysis. Encyclopedia of Analytical Chemistry: John Wiley & Sons, Ltd; 2006.
128. Webster J., Oxley D. Protein identification by MALDI-TOF mass spectrometry. Methods Mol Biol. 2012;800:227-240.
129. Patterson S.D., Aebersold R.H. Proteomics: the first decade and beyond. Nature genetics. 2003;33:311-323.
130. Canas B., Lopez-Ferrer D., Ramos-Fernandez A., Camafeita E., Calvo E. Mass spectrometry technologies for proteomics. Briefings in functional genomics & proteomics. 2006;4(4):295-320.
131. Dakna M., He Z., Yu W.C., Mischak H., Kolch W. Technical, bioinformatical and statistical aspects of liquid chromatography-mass spectrometry (LC-MS) and capillary electrophoresis-mass spectrometry (CE-MS) based clinical proteomics: a critical assessment. Journal of chromatography B, Analytical technologies in the biomedical and life sciences. 2009;877(13):1250-1258.
132. Lowry O.H., Rosebrough N.J., Farr A.L., Randall R.J. Protein Measurement with the Folin Phenol Reagent. J Biol Chem. 1951;193(1):265-275.
133. EMBL-EBI. Localization (GO:0051179) 2014 [cited 2014 31 May]; Available from: http://www.ebi.ac.uk/QuickGO/GTerm?id=GO:0051179.
134. Fessart D., Martin-Negrier M.L., Claverol S., Thiolat M.L., Crevel H., Toussaint C., Bonneu M., Muller B., Savineau J.P., Delom F. Proteomic remodeling of proteasome in right heart failure. Journal of molecular and cellular cardiology. 2014;66:41-52.
135. EMBL-EBI. Reproduction (GO:0000003). 2014 [cited 2014 31 May]; Available from: http://www.ebi.ac.uk/QuickGO/GTerm?id=GO:0000003.
136. EMBL-EBI. Biological regulation (GO:0065007) 2014 [cited 2014 31 May]; Available from: http://www.ebi.ac.uk/QuickGO/GTerm?id=GO:0065007.
137. Vural B., Atalar F., Ciftci C., Demirkan A., Susleyici-Duman B., Gunay D., Akpinar B., Sagbas E., Ozbek U., Buyukdevrim A.S. Presence of fatty-acid-binding protein 4 expression in human epicardial adipose tissue in metabolic syndrome. Cardiovasc Pathol. 2008;17(6):392-398.
138. Baessler A., Lamounier-Zepter V., Fenk S., Strack C., Lahmann C., Loew T., Schmitz G., Bluher M., Bornstein S.R., Fischer M. Adipocyte fatty acid-binding protein levels are associated with left ventricular diastolic dysfunction in morbidly obese subjects. Nutr Diabetes. 2014;4.
139. Serra D., Mera P., Malandrino M.I., Mir J.F., Herrero L. Mitochondrial Fatty Acid Oxidation in Obesity. Antioxid Redox Sign. 2013;19(3):269-283.
140. Boden G. Obesity and Free Fatty Acids. Endocrin Metab Clin. 2008;37(3):635-+.
141. Lewis G.F., Uffelman K.D., Szeto L.W., Weller B., Steiner G. Interaction between Free Fatty-Acids and Insulin in the Acute Control of Very-Low-Density Lipoprotein Production in Humans. Journal of Clinical Investigation. 1995;95(1):158-166.
142. Jaswal J.S., Ussher J.R., Lopaschuk G.D. Myocardial fatty acid utilization as a determinant of cardiac efficiency and function. Clin Lipidol. 2009;4(3):379-389.
143. Peterson L.R., Herrero P., Schechtman K.B., Racette S.B., Waggoner A.D., Kisrieva-Ware Z., Dence C., Klein S., Marsala J., Meyer T., Gropler R.J. Effect of obesity and insulin resistance on myocardial substrate metabolism and efficiency in young women. Circulation. 2004;109(18):2191-2196.

144. Young M.E., Guthrie P.H., Razeghi P., Leighton B., Abbasi S., Patil S., Youker K.A., Taegtmeyer H. Impaired long-chain fatty acid oxidation and contractile dysfunction in the obese Zucker rat heart. Diabetes. 2002;51(8):2587-2595.
145. Sharma S., Adrogue J.V., Golfman L., Uray I., Lemm J., Youker K., Noon G.P., Frazier O.H., Taegtmeyer H. Intramyocardial lipid accumulation in the failing human heart resembles the lipotoxic rat heart. Faseb J. 2004;18(14):1692-1700.
146. Ussher J.R., Fillmore N., Keung W., Mori J., Beker D.L., Wagg C.S., Jaswal J.S., Lopaschuk G.D. Trimetazidine Therapy Prevents Obesity-Induced Cardiomyopathy in Mice. Can J Cardiol. 2014;30(8):940-944.
147. Khan T., Muise E.S., Iyengar P., Wang Z.V., Chandalia M., Abate N., Zhang B.B., Bonaldo P., Chua S., Scherer P.E. Metabolic Dysregulation and Adipose Tissue Fibrosis: Role of Collagen VI. Molecular and cellular biology. 2009;29(6):1575-1591.
148. Kubo Y., Kaidzu S., Nakajima I., Takenouchi K., Nakamura F. Organization of extracellular matrix components during differentiation of adipocytes in long-term culture. In Vitro Cell Dev-An. 2000;36(1):38-44.
149. Lilla J., Stickens D., Werb Z. Metalloproteases and adipogenesis: A weighty subject. American Journal of Pathology. 2002;160(5):1551-1554.
150. Neame P.J., Kay C.J., McQuillan D.J., Beales M.P., Hassell J.R. Independent modulation of collagen fibrillogenesis by decorin and lumican. Cellular and Molecular Life Sciences. 2000;57(5):859-863.
151. Engebretsen K.V.T., Lunde I.G., Strand M.E., Waehre A., Sjaastad I., Marstein H.S., Skrbic B., Dahl C.P., Askevold E.T., Christensen G., Bjornstad J.L., Tonnessen T. Lumican is increased in experimental and clinical heart failure, and its production by cardiac fibroblasts is induced by mechanical and proinflammatory stimuli. Febs Journal. 2013;280(10):2382-2398.
152. Shiomi T., Tsutsui H., Matsusaka H., Murakami K., Hayashidani S., Ikeuchi M., Wen J., Kubota T., Utsumi H., Takeshita A. Overexpression of glutathione peroxidase prevents left ventricular remodeling and failure after myocardial infarction in mice. Circulation. 2004;109(4):544-549.
153. Wood Z.A., Schroder E., Harris J.R., Poole L.B. Structure, mechanism and regulation of peroxiredoxins. Trends in biochemical sciences. 2003;28(1):32-40.
154. Rhee N.J., Kim G.Y., Huh J.W., Kim S.W., Na D.S. Annexin I is a stress protein induced by heat, oxidative stress and a sulfhydryl-reactive agent. European Journal of Biochemistry. 2000;267(11):3220-3225.
155. Chen C.H., Sun L.H., Mochly-Rosen D. Mitochondrial aldehyde dehydrogenase and cardiac diseases. Cardiovascular research. 2010;88(1):51-57.
156. Zhang Y.M., Mi S.L., Hu N., Doser T.A., Sun A.J., Ge J.B., Ren J. Mitochondrial aldehyde dehydrogenase 2 accentuates aging-induced cardiac remodeling and contractile dysfunction: role of AMPK, Sirt1, and mitochondrial function. Free Radical Bio Med. 2014;71:208-220.
157. Kobashi C., Asamizu S., Ishiki M., Iwata M., Usui I., Yamazaki K., Tobe K., Kobayashi M., Urakaze M. Inhibitory effect of IL-8 on insulin action in human adipocytes via MAP kinase pathway. J Inflamm-Lond. 2009;6.
158. Mackay C.R. Chemokines: immunology's high impact factors. Nature immunology. 2001;2(2):95-101.
159. Iwasa T., Takahashi R., Nagata K., Kobayashi Y. Suppression of MIP-2 or IL-8 production by annexins A1 and A4 during coculturing of macrophages with late apoptotic

human peripheral blood neutrophils. Biochimica et biophysica acta. 2012;1822(2):204-211.
160. Iwasa T., Takahashi R., Nagata K., Kobayashi Y. Suppression of MIP-2 or IL-8 production by annexins A1 and A4 during coculturing of macrophages with late apoptotic human peripheral blood neutrophils. Bba-Mol Basis Dis. 2012;1822(2):204-211.
161. Bishu K., Hamdani N., Mohammed S.F., Kruger M., Ohtani T., Ogut O., Brozovich F.V., Burnett J.C., Jr., Linke W.A., Redfield M.M. Sildenafil and B-type natriuretic peptide acutely phosphorylate titin and improve diastolic distensibility in vivo. Circulation. 2011;124(25):2882-2891.
162. Cooper G.t. Cardiocyte cytoskeleton in hypertrophied myocardium. Heart failure reviews. 2000;5(3):187-201.
163. Kostin S., Hein S., Arnon E., Scholz D., Schaper J. The cytoskeleton and related proteins in the human failing heart. Heart failure reviews. 2000;5(3):271-280.
164. Narishige T., Blade K.L., Ishibashi Y., Nagai T., Hamawaki M., Menick D.R., Kuppuswamy D., Cooper G.t. Cardiac hypertrophic and developmental regulation of the beta-tubulin multigene family. J Biol Chem. 1999;274(14):9692-9697.
165. Sequeira V., Nijenkamp L.L.A.M., Regan J.A., van der Velden J. The physiological role of cardiac cytoskeleton and its alterations in heart failure. Bba-Biomembranes. 2014;1838(2):700-722.
166. Cooper G.t. Cytoskeletal networks and the regulation of cardiac contractility: microtubules, hypertrophy, and cardiac dysfunction. American journal of physiology Heart and circulatory physiology. 2006;291(3):H1003-1014.
167. Laing N.G., Dye D.E., Wallgren-Pettersson C., Richard G., Monnier N., Lillis S., Winder T.L., Lochmuller H., Graziano C., Mitrani-Rosenbaum S., Twomey D., Sparrow J.C., Beggs A.H., Nowak K.J. Mutations and polymorphisms of the skeletal muscle alpha-actin gene (ACTA1). Human mutation. 2009;30(9):1267-1277.
168. McNally E.M., Golbus J.R., Puckelwartz M.J. Genetic mutations and mechanisms in dilated cardiomyopathy. The Journal of clinical investigation. 2013;123(1):19-26.
169. Hotulainen P., Paunola E., Vartiainen M.K., Lappalainen P. Actin-depolymerizing factor and cofilin-1 play overlapping roles in promoting rapid F-actin depolymerization in mammalian nonmuscle cells. Molecular biology of the cell. 2005;16(2):649-664.
170. Goodpaster B.H., Krishnaswami S., Resnick H., Kelley D.E., Haggerty C., Harris T.B., Schwartz A.V., Kritchevsky S., Newman A.B. Association between regional adipose tissue distribution and both type 2 diabetes and impaired glucose tolerance in elderly men and women. Diabetes Care. 2003;26(2):372-379.
171. Hayashi T., Boyko E.J., Leonetti D.L., McNeely M.J., Newell-Morris L., Kahn S.E., Fujimoto W.Y. Visceral adiposity and the risk of impaired glucose tolerance - A prospective study among Japanese Americans. Diabetes Care. 2003;26(3):650-655.
172. Kanaya A.M., Harris T., Goodpaster B.H., Tylavsky F., Cummings S.R., Study H.A.B.C. Adipocytokines attenuate the association between visceral adiposity and diabetes in older adults. Diabetes Care. 2004;27(6):1375-1380.
173. Tulloch-Reid M.K., Hanson R.L., Sebring N.G., Reynolds J.C., Premkumar A., Genovese D.J., Sumner A.E. Both subcutaneous and visceral adipose tissue correlate highly with insulin resistance in African Americans. Obes Res. 2004;12(8):1352-1359.
174. Hayashi T., Boyko E.J., Leonetti D.L., McNeely M.J., Newell-Morris L., Kahn S.E., Fujimoto W.Y. Visceral adiposity is an independent predictor of incident hypertension in Japanese Americans. Ann Intern Med. 2004;140(12):992-1000.

175. Sironi A.M., Gastaldelli A., Mari A., Ciociaro D., Positano V., Buzzigoli E., Ghione S., Turchi S., Lombardi M., Ferrannini E. Visceral fat in hypertension - Influence on insulin resistance and beta-cell function. Hypertension. 2004;44(2):127-133.
176. Nicklas B.J., Penninx B.W.J.H., Ryan A.S., Berman D.M., Lynch N.A., Dennis K.E. Visceral adipose tissue cutoffs associated with metabolic risk factors for coronary heart disease in women. Diabetes Care. 2003;26(5):1413-1420.
177. Mori Y., Hoshino K., Yokota K., Yokose T., Tajima N. Increased visceral fat and impaired glucose tolerance predict the increased risk of metabolic syndrome in Japanese middle-aged men. Exp Clin Endocr Diab. 2005;113(6):334-339.
178. Goodpaster B.H., Krishnaswami S., Harris T.B., Katsiaras A., Kritchevsky S.B., Simonsick E.M., Nevitt M., Holvoet P., Newman A.B. Obesity, regional body fat distribution, and the metabolic syndrome in older men and women. Archives of internal medicine. 2005;165(7):777-783.
179. Pezeshkian M., Noori M., Najjarpour-Jabbari H., Abolfathi A., Darabi M., Darabi M., Shaaker M., Shahmohammadi G. Fatty Acid Composition of Epicardial and Subcutaneous Human Adipose Tissue. Metab Syndr Relat D. 2009;7(2):125-131.
180. Fain J.N., Sacks H.S., Bahouth S.W., Tichansky D.S., Madan A.K., Cheema P.S. Human epicardial adipokine messenger RNAs: comparisons of their expression in substernal, subcutaneous, and omental fat. Metabolism-Clinical and Experimental. 2010;59(9):1379-1386.

APPENDIX

SUPPLEMENTARY DATA

Appendix A – Analysis of proteins resulting from the studies of the Table 4.

Supplemental Table A 1 - Genes of the proteins secreted by visceral and epicardial adipose tissue matching between studies of the Table 4. Genes in bold – most common genes

	Proteomic analysis of epicardial and subcutaneous adipose tissue reveals differences in proteins involved in oxidative stress	Secretome analysis of rat adipose tissues shows location-specific roles for each depot type.	Characterization of the Human Visceral Adipose Tissue Secretome	Changes in lipid transport-involved proteins of epicardial adipose tissue associated with coronary artery disease	A protein profile of visceral adipose tissues linked to early pathogenesis of type 2 diabetes mellitus		Proteomic analysis of visceral adipose tissue in pre-obese patients with type 2 diabetes	Proteomic profile of visceral adipose tissues between low-fat diet-fed obesity-resistant and obesity-prone C57BL/6 mice
Proteomic analysis of epicardial and subcutaneous adipose tissue reveals differences in proteins involved in oxidative stress		VIM	**ACTB**	-	**ACTB**		**ACTB**	-
Secretome analysis of rat adipose tissues shows location-specific roles for each depot type			**GSTP1** PGAM1 **FABP4** GSTO1 **LDHB** NID2 **PARK7** PRDX1 **PRDX2** **PRDX3**	**FABP4** MIF **PRDX2**	BPNT1 **GSTP1** CALR CAPZB GSTO1 HIBCH **LDHB** MIF NID2 NIT1	**PARK7** PDIA3 PDIA6 PDXK PGAM1 **PRDX2** **PRDX3** PRDX5 WDR1 NIT2	ALDH2 GSTM2	-

Supplemental Table A1 – (Continue...)

Characterization of the Human Visceral Adipose Tissue Secretome				**A2M**	**A2M**	CFB	FASN	LAMA4	**PRDX2**	**ACTB**	PRDX6
				CST3	ACAA2	COL12A1	FBLN1	**LDHB**	**PRDX3**	**ALDH1A1**	
				F13A1	ACOT1	COL15A1	FH	LGALS3	PRDX6	**IGKC**	
				FABP4	**ACTB**	COL1A1	FHL1	LGALS3BP	PSMA1		
				FAH	ACTN1	COL1A2	FN1	LRP1	PSMA3		
				GPI	ACTN4	COL4A2	GARS	LTA4H	PSMA4		
				HBA1	ACY1	COL4A4	GDI1	LTBP2	PSMA6		
				HBB	ADH5	COL6A1	GDI2	LYZ	PSMB3		
				LYZ	ADIPOQ	COL6A2	GLO1	MAN2C1	PSMB4		
				MDH1	AKR1A1	COL6A3	GOT1	MCAM	PSMB5		
				PEBP1	ALAD	CRYZ	GPD1	MDH1	PSMB7		
				PRDX2	ALB	CST3	GPI	ME1	PTX3		
				TF	**ALDH1A1**	CSTB	GPX3	MPO	PYGL		
				VIM	ALDOA	CTSD	GSN	MSN	QDPR		
				YWHAG	ANXA2	CTSZ	GSS	NID1	RBP4		
					APEH	DPP3	GSTO1	NID2	SERPINB1		
					APEX1	DPT	**GSTP1**	NQO2	SERPINB6		
					ARHGDIA	ECH1	GSTT1	NRP1	SERPINF1		
					AZU1	ECM1	HBA1	OGN	SH3BGRL		
					C19orf10	EFEMP1	HBB	OLFML1	SOD1		
					C1S	EHD2	HIST1H2BK	P4HB	SOD2		
					C7	ELANE	HSP90AB1	PAFAH1B1	SOD3		
					CA1	EMILIN1	HSPA1A	**PARK7**	SPARC		
					CA3	ENO1	HSPA4	PEBP1	SPON1		
					CALB2	ERAP1	HSPG2	PEPD	SPTAN1		
					CAPN1	F13A1	IDH1	PGAM1	SPTBN1		
					CD14	**FABP4**	IGFBP7	PGD	TAGLN		
					CD44	FABP5	IGHM	PGLS	TF		
					CDH5	FAH	IGHM	PLXNB2	TFRC		
					CES1	FAM49B	**IGKC**	PPIB	TGFBI		
					TKT	TXNRD1	VCP	YWHAE	THBS1		

Supplemental Table A1 – (Continue...)

Changes in lipid transport-involved proteins of epicardial adipose tissue associated with coronary artery disease					**A2M** ACTBL2 APOA1 CST3 F13A1	**FABP4** FAH FGB GPI HBA1	HBB HBD HBG1 HSPE1 LYZ	MDH1 MIF PEBP1 **PRDX2** S100A8	TF TTR UGP2 VCL	-	-
A protein profile of visceral adipose tissues linked to early pathogenesis of type 2 diabetes mellitus										**ACTB** **ALDH1A1** ANXA1 APOA4 **IGKC**	SERPINC1	MGLL PRDX6 TPM2
Proteomic analysis of visceral adipose tissue in pre-obese patients with type 2 diabetes												-
Proteomic profile of visceral adipose tissues between low-fat diet-fed obesity-resistant and obesity-prone C57BL/6 mice												

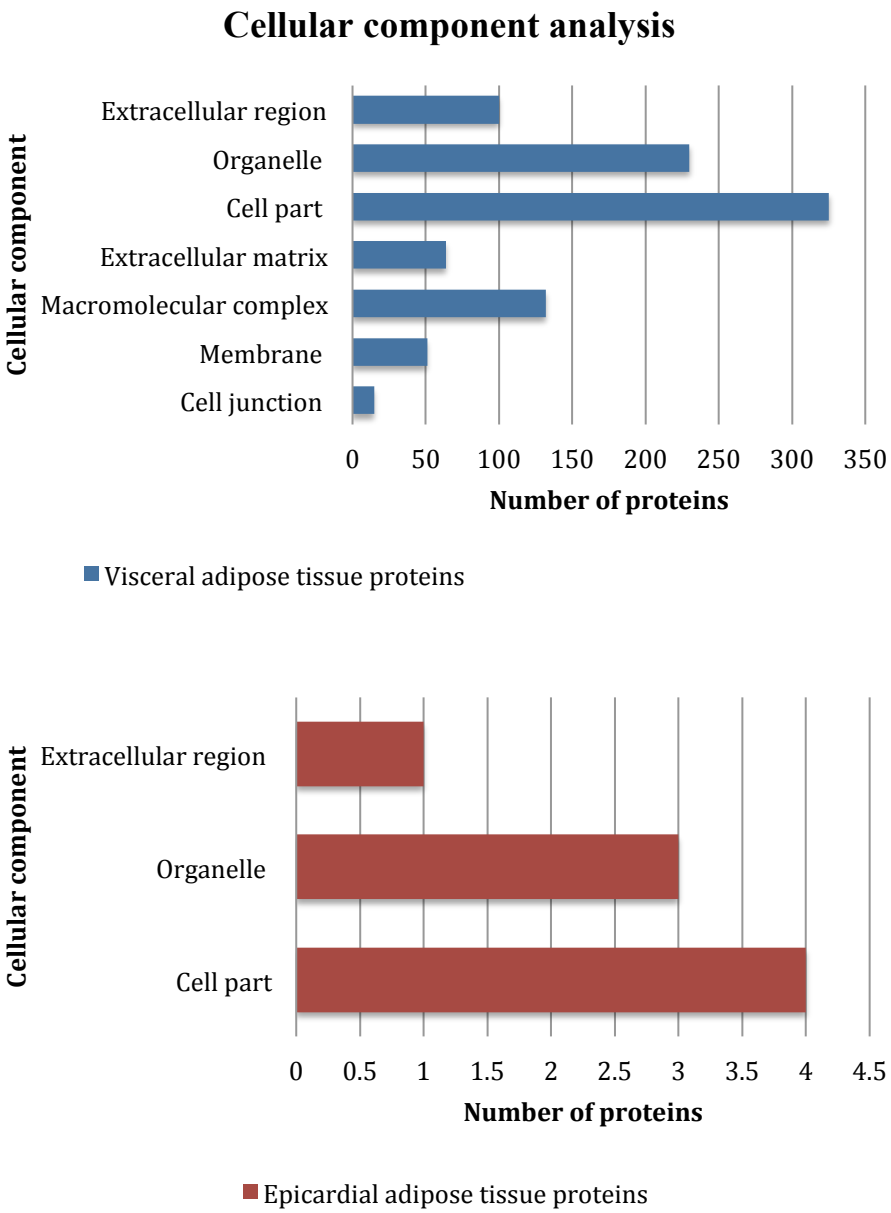

Supplemental Figure A 1 - Distribution of visceral and epicardial proteins resulting from the studies of the Table 4 according to cellular component with the PANTHER classification system (http://www.pantherdb.org). Blue – visceral adipose tissue; Red – epicardial adipose tissue

Appendix B – Proteins resulting of optimization of methodology for analysis of the both tissues

Supplemental Table B 1 - Proteins of visceral adipose tissue extracted from protocol - Tris

Protein name	Gene name	Entry name	Accession number	Mascot score	Matching peptides	Sequence coverage
Actin, cytoplasmic 1	Actb	ACTB_RAT	P60711	236	4 (4)	4 (4)
Serum albumin	Alb	ALBU_RAT	P02770	385	8 (7)	8 (7)
Annexin A2	Anxa2	ANXA2_RAT	Q07936	112	2 (2)	2 (2)
Carbonic anhydrase 3	Ca3	CAH3_RAT	P14141	177	4 (4)	4 (4)
Histone H2A type 1-C		H2A1C_RAT	P0C169	122	2 (2)	2 (2)
Histone H3.1		H31_RAT	Q6LED0	81	4 (4)	3 (3)
Histone H4	Hist1h4b	H4_RAT	P62804	52	1 (1)	1 (1)
Hemoglobin subunit alpha-1/2	Hba1	HBA_RAT	P01946	228	2 (2)	2 (2)
Hemoglobin subunit beta-1	Hbb	HBB1_RAT	P02091	56	1 (1)	1 (1)
Lumican	Lum	LUM_RAT	P51886	29	1 (1)	1 (1)
Vimentin	Vim	VIME_RAT	P31000	95	1 (1)	1 (1)

Supplemental Table B 2 - Proteins of visceral adipose tissue extracted from protocol - Urea

Protein name	Gene name	Entry name	Accession number	Mascot score	Matching peptides	Sequence coverage
14-3-3 protein gamma	Ywhag	1433G_RAT	P61983	73	4 (4)	4 (4)
14-3-3 protein epsilon	Ywhae	1433E_RAT	P62260	146	7 (4)	7 (4)
14-3-3 protein theta	Ywhaq	1433T_RAT	P68255	55	4 (2)	4 (2)
14-3-3 protein zeta/delta	Ywhaz	1433Z_RAT	P63102	211	7 (5)	7 (5)
Alpha-1-antiproteinase	Serpina1	A1AT_RAT	P17475	82	1 (1)	1 (1)
Alpha-1-macroglobulin	A1m	A1M_RAT	Q63041	62	9 (2)	4 (2)
1-acylglycerol-3-phosphate O-acyltransferase ABHD5	Abhd5	ABHD5_RAT	Q6QA69	51	4 (1)	3 (1)
Aconitate hydratase, mitochondrial	Aco2	ACON_RAT	Q9ER34	81	8 (4)	7 (3)
Long-chain-fatty-acid--CoA ligase 1	Acsl1	ACSL1_RAT	P18163	225	12 (7)	10 (5)
Long-chain-fatty-acid--CoA ligase 6	Acsl6	ACSL6_RAT	P33124	92	4 (2)	3 (1)
Actin, aortic smooth muscle	Acta2	ACTA_RAT	P62738	1329	36 (34)	21 (21)
Actin, cytoplasmic 2	Actg1	ACTG_RAT	P63259	1641	45 (39)	24 (23)
Alpha-actinin-1	Actn1	ACTN1_RAT	Q9Z1P2	56	16 (4)	14 (4)
Serum albumin	Alb	ALBU_RAT	P02770	1833	55 (44)	25 (19)
Aldehyde dehydrogenase, mitochondrial	Aldh2	ALDH2_RAT	P11884	100	7 (3)	7 (3)
Fructose-bisphosphate aldolase A	Aldoa	ALDOA_RAT	P05065	129	9 (5)	8 (4)
Aldose reductase	Akr1b1	ALDR_RAT	P07943	142	6 (3)	5 (3)
Annexin A1	Anxa1	ANXA2_RAT	Q07936	868	27 (19)	15 (10)
Annexin A2	Anxa2	ANXA3_RAT	P14669	530	17 (15)	15 (14)
Annexin A3	Anxa3	ANXA6_RAT	P48037	122	5 (4)	5 (4)

Annexin A4	Anxa4	ANXA5_RAT	P14668	51	7 (2)	7 (2)
Annexin A5	Anxa5	ANXA1_RAT	P07150	517	13 (13)	13 (13)
Annexin A6	Anxa6	ANXA4_RAT	P55260	332	15 (9)	10 (6)
Membrane primary amine oxidase	Aoc3	AOC3_RAT	O08590	118	11 (5)	8 (3)
Apolipoprotein A-I	Apoa1	APOA1_RAT	P04639	157	7 (5)	7 (5)
Apolipoprotein E	Apoe	APOE_RAT	P02650	39	6 (1)	4 (1)
Actin-related protein 3	Actr3	ARP3_RAT	Q4V7C7	49	4 (1)	4 (1)
ATP synthase subunit alpha, mitochondrial	Atp5a1	ATPA_RAT	P15999	188	9 (4)	5 (3)
ATP synthase subunit beta, mitochondrial	Atp5b	ATPB_RAT	P10719	221	8 (5)	7 (5)
Cadherin-23	Cdh23	CAD23_RAT	P58365	56	15 (3)	9 (1)
Carbonic anhydrase 2	Ca2	CAH2_RAT	P27139	52	6 (1)	2 (1)
Carbonic anhydrase 3	Ca3	CAH3_RAT	P14141	1302	33 (27)	22 (21)
Calreticulin	Calr	CALR_RAT	P18418	158	5 (4)	5 (4)
Calumenin	Calu	CALU_RAT	O35783	37	2 (1)	2 (1)
Calnexin	Canx	CALX_RAT	P35565	85	4 (2)	3 (1)
Macrophage-capping protein	Capg	CAPG_RAT	Q6AYC4	212	6 (4)	6 (4)
F-actin-capping protein subunit beta	Capzb	CAPZB_RAT	Q5XI32	41	3 (1)	3 (1)
Catalase	Cat	CATA_RAT	P04762	291	13 (9)	13 (9)
Carbonyl reductase [NADPH] 1	Cbr1	CBR1_RAT	P47727	59	2 (1)	1 (1)
Carboxylesterase 1D	Ces1d	CES1D_RAT	P16303	71	3 (2)	3 (2)
60 kDa heat shock protein, mitochondrial	Hspd1	CH60_RAT	P63039	131	4 (1)	4 (1)
Citrate synthase, mitochondrial	Cs	CISY_RAT	Q8VHF5	69	9 (2)	8 (2)
Calponin-1	Cnn1	CNN1_RAT	Q08290	42	5 (1)	5 (1)
Collagen alpha-1(I) chain	Col1a1	CO1A1_RAT	P02454	45	8 (2)	5 (2)
Calpain small subunit 1	Capns1	CPNS1_RAT	Q64537	39	1 (1)	1 (1)
High affinity cationic amino acid transporter 1	Slc7a1	CTR1_RAT	P30823	34	4 (1)	2 (1)
Cytochrome c, somatic	Cycs	CYC_RAT	P62898	43	1 (1)	1 (1)
Cystatin-B	Cstb	CYTB_RAT	P01041	39	1 (1)	1 (1)
Desmin	Des	DESM_RAT	P48675	244	11 (7)	7 (5)
Destrin	Dstn	DEST_RAT	Q7M0E3	52	2 (1)	2 (1)
Glutamate dehydrogenase 1, mitochondrial	Glud1	DHE3_RAT	P10860	44	3 (1)	3 (1)
Succinate dehydrogenase [ubiquinone] iron-sulfur subunit, mitochondrial	Sdhb	DHSB_RAT	P21913	36	2 (1)	2 (1)
D-dopachrome decarboxylase	Ddt	DOPD_RAT	P80254	46	1 (1)	1 (1)
Dihydropyrimidinase-related protein 2	Dpysl2	DPYL2_RAT	P47942	53	2 (2)	2 (2)
Trifunctional enzyme subunit alpha, mitochondrial	Hadha	ECHA_RAT	Q64428	108	7 (4)	5 (4)
Elongation factor 1-gamma	Eef1g	EF1G_RAT	Q68FR6	71	4 (3)	3 (3)
EH domain-containing protein 2	Ehd2	EHD2_RAT	Q4V8H8	278	16 (7)	12 (4)
Alpha-enolase	Eno1	ENOA_RAT	P04764	335	10 (7)	7 (4)
Endoplasmin	Hsp90b1	ENPL_RAT	Q66HD0	93	12 (3)	9 (3)
Ectonucleoside triphosphate diphosphohydrolase 2	Entpd2	ENTP2_RAT	O35795	46	1 (1)	1 (1)
Endoplasmic reticulum resident protein 29	Erp29	ERP29_RAT	P52555	171	5 (4)	5 (4)
Fatty acid-binding protein, adipocyte	Fabp4	FABP4_RAT	P70623	322	9 (9)	5 (5)
Fibulin-5	Fbln5	FBLN5_RAT	Q9WVH8	70	2 (2)	2 (2)

Ferritin heavy chain	Fth1	FRIH_RAT	P19132	70	3 (2)	3 (2)
Ferritin light chain 1	Ftl1	FRIL1_RAT	P02793	60	4 (2)	4 (2)
Glyceraldehyde-3-phosphate dehydrogenase	Gapdh	G3P_RAT	P04797	66	6 (2)	3 (1)
Guanine nucleotide-binding protein subunit beta-2-like 1	Gnb2l1	GBLP_RAT	P63245	47	4 (1)	4 (1)
Rho GDP-dissociation inhibitor 1	Arhgdia	GDIR1_RAT	Q5XI73	129	3 (3)	3 (3)
Gelsolin	Gsn	GELS_RAT	Q68FP1	115	9 (3)	5 (1)
Glutamine synthetase	Glul	GLNA_RAT	P09606	65	4 (3)	4 (3)
Guanine nucleotide-binding protein G(s) subunit alpha isoforms Xlas	Gnas	GNAS1_RAT	Q63803	34	4 (1)	4 (1)
Glycerol-3-phosphate dehydrogenase [NAD(+)], cytoplasmic	Gpd1	GPDA_RAT	O35077	92	6 (3)	6 (3)
Glutathione peroxidase 1	Gpx1	GPX1_RAT	P04041	62	3 (2)	3 (2)
78 kDa glucose-regulated protein	Hspa5	GRP78_RAT	P06761	516	19 (13)	17 (13)
Glutathione S-transferase alpha-3	Gsta3	GSTA3_RAT	P04904	60	4 (2)	4 (2)
Glutathione S-transferase P	Gstp1	GSTP1_RAT	P04906	128	5 (3)	5 (3)
Guanine deaminase	Gda	GUAD_RAT	Q9WTT6	267	9 (7)	9 (7)
Histone H2B type 1-A	Hist1h2ba	H2B1A_RAT	Q00729	52	4 (1)	4 (1)
Hemoglobin subunit alpha-1/2	Hba1	HBA_RAT	P01946	402	11 (8)	7 (6)
Hemoglobin subunit beta-2	-	HBB2_RAT	P11517	361	11 (10)	8 (7)
Hemoglobin subunit beta-1	Hbb	HBB1_RAT	P02091	333	10 (9)	8 (7)
Hydroxyacyl-coenzyme A dehydrogenase, mitochondrial	Hadh	HCDH_RAT	Q9WVK7	41	2 (1)	2 (1)
Hemopexin	Hpx	HEMO_RAT	P20059	52	6 (3)	5 (3)
Histidine triad nucleotide-binding protein 1	Hint1	HINT1_RAT	P62959	40	2 (1)	2 (1)
Heat shock cognate 71 kDa protein	Hspa8	HSP7C_RAT	P63018	343	14 (9)	13 (9)
Heat shock protein beta-1	Hspb1	HSPB1_RAT	P42930	128	6 (3)	5 (3)
Isocitrate dehydrogenase [NAD] subunit alpha, mitochondrial	Idh3a	IDH3A_RAT	Q99NA5	33	3 (1)	3 (1)
Ig gamma-2A chain C region	Igg-2a	IGG2A_RAT	P20760	38	1 (1)	1 (1)
Integrin beta-1	Itgb1	ITB1_RAT	P49134	45	4 (1)	4 (1)
Keratin, type I cytoskeletal 10	Krt10	K1C10_RAT	Q6IFW6	100	7 (4)	3 (2)
Keratin, type II cytoskeletal 6A	Krt6a	K2C6A_RAT	Q4FZU2	156	12 (7)	7 (5)
Keratin, type II cytoskeletal 1	Krt1	K2C1_RAT	Q6IMF3	147	12 (5)	5 (3)
Creatine kinase B-type	Ckb	KCRB_RAT	P07335	62	4 (2)	4 (2)
Laminin subunit beta-2	Lamb2	LAMB2_RAT	P15800	38	12 (1)	11 (1)
L-lactate dehydrogenase A chain	Ldha	LDHA_RAT	P04642	93	6 (3)	6 (3)
L-lactate dehydrogenase B chain	Ldhb	LDHB_RAT	P42123	73	5 (1)	5 (1)
Galectin-1	Lgals1	LEG1_RAT	P11762	152	6 (4)	5 (4)
Galectin-3	Lgals3	LEG3_RAT	P08699	243	7 (4)	5 (4)
Prelamin-A/C	Lmna	LMNA_RAT	P48679	218	23 (8)	20 (8)
Lumican	Lum	LUM_RAT	P51886	226	8 (7)	6 (6)
Myristoylated alanine-rich C-kinase substrate	Marcks	MARCS_RAT	P30009	76	2 (1)	2 (1)
Malate dehydrogenase, cytoplasmic	Mdh1	MDHC_RAT	O88989	72	2 (1)	2 (1)
Malate dehydrogenase, mitochondrial	Mdh2	MDHM_RAT	P04636	177	8 (4)	8 (4)
Monoglyceride lipase	Mgll	MGLL_RAT	Q8R431	144	8 (2)	8 (2)

Moesin	Msn	MOES_RAT	O35763	63	7 (2)	5 (2)
Myosin regulatory light chain RLC-A	Rlc-a	MRLCA_RAT	P13832	40	1 (1)	1 (1)
Myosin-10	Myh10	MYH10_RAT	Q9JLT0	85	11 (2)	11 (2)
Myosin-11	Myh11	MYH11_RAT	Q63862	215	17 (8)	16 (8)
Myosin regulatory light polypeptide 9	Myl9	MYL9_RAT	Q64122	55	19 (1)	17 (1)
Myosin light polypeptide 6	Myl6	MYL6_RAT	Q64119	223	5 (4)	4 (3)
Myosin-9	Myh9	MYH9_RAT	Q62812	66	1 (1)	1 (1)
NADH-cytochrome b5 reductase 3	Cyb5r3	NB5R3_RAT	P20070	157	7 (5)	6 (5)
Nucleoside diphosphate kinase A	Nme1	NDKA_RAT	Q05982	32	2 (1)	2 (1)
NADH dehydrogenase [ubiquinone] flavoprotein 2, mitochondrial	Ndufv2	NDUV2_RAT	P19234	36	1 (1)	1 (1)
Nidogen-2	Nid2	NID2_RAT	B5DFC9	85	12 (4)	10 (4)
Protein disulfide-isomerase A3	Pdia3	PDIA3_RAT	P11598	192	9 (4)	8 (4)
Protein disulfide-isomerase	P4hb	PDIA1_RAT	P04785	608	17 (14)	17 (14)
Protein disulfide-isomerase A6	Pdia6	PDIA6_RAT	Q63081	208	6 (4)	4 (2)
Peripherin	Prph	PERI_RAT	P21807	99	9 (5)	7 (3)
Phosphoglycerate mutase 1	Pgam1	PGAM1_RAT	P25113	59	5 (2)	4 (2)
Phosphoglycerate kinase 1	Pgk1	PGK1_RAT	P16617	155	6 (3)	6 (3)
Membrane-associated progesterone receptor component 1	Pgrmc1	PGRC1_RAT	P70580	154	6 (4)	6 (4)
Membrane-associated progesterone receptor component 2	Pgrmc2	PGRC2_RAT	Q5XIU9	75	6 (2)	6 (2)
Prohibitin	Phb	PHB_RAT	P67779	44	3 (1)	3 (1)
Perilipin-1	Plin1	PLIN1_RAT	P43884	99	2 (1)	1 (1)
Peptidyl-prolyl cis-trans isomerase A	Ppia	PPIA_RAT	P10111	53	8 (3)	6 (3)
Protein kinase C delta-binding protein	Prkcdbp	PRDBP_RAT	Q9Z1H9	43	2 (1)	2 (1)
Peroxiredoxin-1	Prdx1	PRDX1_RAT	Q63716	189	6 (5)	6 (5)
Prolargin	Prelp	PRELP_RAT	Q9EQP5	96	5 (3)	5 (3)
Profilin-1	Pfn1	PROF1_RAT	P62963	170	4 (3)	4 (3)
Polymerase I and transcript release factor	Ptrf	PTRF_RAT	P85125	157	7 (6)	4 (3)
Ras-related protein Rab-7a	Rab7a	RAB7A_RAT	P09527	32	3 (1)	2 (1)
Ras-related C3 botulinum toxin substrate 1	Rac1	RAC1_RAT	Q6RUV5	35	5 (1)	4 (1)
Ras-related protein Rab-11B	Rab11b	RB11B_RAT	O35509	106	6 (4)	6 (4)
All-trans-retinol 13,14-reductase	Retsat	RETST_RAT	Q8VHE9	33	1 (1)	1 (1)
Ubiquitin-60S ribosomal protein L40	Uba52	RL40_RAT	P62986	45	4 (3)	3 (2)
Heterogeneous nuclear ribonucleoproteins A2/B1	Hnrnpa2b1	ROA2_RAT	A7VJC2	108	7 (4)	7 (4)
Heterogeneous nuclear ribonucleoprotein A3	Hnrnpa3	ROA3_RAT	Q6URK4	161	4 (1)	4 (1)
40S ribosomal protein SA	Rpsa	RSSA_RAT	P38983	55	4 (3)	3 (2)
Protein S100-A10	S100a10	S10AA_RAT	P05943	111	5 (3)	5 (3)
Serpin H1	Serpinh1	SERPH_RAT	P29457	224	10 (4)	5 (4)
Superoxide dismutase [Cu-Zn]	Sod1	SODC_RAT	P07632	44	2 (2)	2 (2)
Serine protease inhibitor A3K	Serpina3k	SPA3K_RAT	P05545	39	4 (1)	4 (1)
Serine protease inhibitor A3N	Serpina3n	SPA3N_RAT	P09006	66	3 (1)	3 (1)
SPARC	Sparc	SPRC_RAT	P16975	57	1 (1)	1 (1)
Spectrin alpha chain, non-erythrocytic 1	Sptan1	SPTN1_RAT	P16086	294	34 (9)	29 (8)
Gamma-synuclein	Sncg	SYUG_RAT	Q63544	97	5 (3)	5 (3)

Transgelin	Tagln	TAGL_RAT	P31232	90	7 (3)	6 (3)
Tubulin alpha-1B chain	Tuba1b	TBA1B_RAT	Q6P9V9	713	21 (18)	10 (10)
Tubulin beta-2A chain	Tubb2a	TBB2A_RAT	P85108	417	13 (10)	7 (5)
Tubulin beta-4B chain	Tubb4b	TBB4B_RAT	Q6P9T8	441	14 (11)	8 (6)
Tubulin beta-5 chain	Tubb5	TBB5_RAT	P69897	332	13 (10)	8 (6)
3-ketoacyl-CoA thiolase, mitochondrial	Acaa2	THIM_RAT	P13437	36	6 (2)	5 (2)
Thioredoxin	Txn	THIO_RAT	P11232	47	2 (1)	2 (1)
Tubulointerstitial nephritis antigen-like	Tinagl1	TINAL_RAT	Q9EQT5	55	4 (2)	3 (1)
Transmembrane emp24 domain-containing protein 9	Tmed9	TMED9_RAT	Q5I0E7	40	2 (1)	2 (1)
Triosephosphate isomerase	Tpi1	TPIS_RAT	P48500	94	2 (1)	2 (1)
Tropomyosin alpha-1 chain	Tpm1	TPM1_RAT	P04692	266	16 (10)	13 (8)
Tropomyosin beta chain	Tpm2	TPM2_RAT	P58775	265	20 (9)	17 (7)
Tropomyosin alpha-3 chain	Tpm3	TPM3_RAT	Q63610	293	22 (11)	19 (9)
Serotransferrin	Tf	TRFE_RAT	P12346	258	16 (9)	15 (9)
Vesicle-associated membrane protein-associated protein A	Vapa	VAPA_RAT	Q9Z270	55	3 (1)	3 (1)
Voltage-dependent anion-selective channel protein 1	Vdac1	VDAC1_RAT	Q9Z2L0	65	4 (2)	4 (2)
Voltage-dependent anion-selective channel protein 2	Vdac2	VDAC2_RAT	P81155	48	2 (1)	2 (1)
Vimentin	Vim	VIME_RAT	P31000	2191	63 (49)	32 (26)
Vinculin	Vcl	VINC_RAT	P85972	86	14 (4)	13 (4)

Supplemental Table B 3 - Proteins of visceral adipose tissue extracted from protocol – Tris and Urea.

Protein name	Gene name	Entry name	Accession number	Mascot score	Matching peptides	Sequence coverage
14-3-3 protein epsilon	Ywhae	1433E_RAT	P62260	156	12 (8)	8 (6)
14-3-3 protein gamma	Ywhag	1433G_RAT	P61983	36	2 (1)	2 (1)
14-3-3 protein zeta/delta	Ywhaz	1433Z_RAT	P63102	69	2 (2)	2 (2)
40S ribosomal protein SA	Rpsa	RSSA_RAT	P38983	31	2 (1)	2 (1)
78 kDa glucose-regulated protein	Hspa5	GRP78_RAT	P06761	87	8 (1)	8 (1)
Aconitate hydratase, mitochondrial	Aco2	ACON_RAT	Q9ER34	42	5 (2)	4 (1)
Actin, aortic smooth muscle	Acta2	ACTA_RAT	P62738	39	4 (2)	3 (1)
Actin, cytoplasmic 2	Actg1	ACTG_RAT	P63259	591	26 (18)	13 (9)
Aldehyde dehydrogenase, mitochondrial	Aldh2	ALDH2_RAT	P11884	940	34 (27)	16 (14)
Aldose reductase (AR)	Akr1b1	ALDR_RAT	P07943	1398	54 (36)	27 (20)
Alpha-enolase	Eno1	ENOA_RAT	P04764	30	5 (2)	5 (2)
Annexin A1	Anxa1	ANXA1_RAT	P07150	193	6 (6)	6 (6)
Annexin A2	Anxa2	ANXA2_RAT	Q07936	146	5 (3)	4 (3)
Annexin A3	Anxa3	ANXA3_RAT	P14669	406	13 (9)	10 (7)
Annexin A4	Anxa4	ANXA4_RAT	P55260	404	17 (14)	14 (12)
Annexin A5	Anxa5	ANXA5_RAT	P14668	54	4 (3)	4 (3)
Annexin A6	Anxa6	ANXA6_RAT	P48037	32	4 (1)	4 (1)

Apolipoprotein E	Apoe	APOE_RAT	P02650	192	9 (8)	9 (8)
ATP synthase subunit alpha, mitochondrial	Atp5a1	ATPA_RAT	P15999	136	9 (2)	9 (2)
ATP synthase subunit beta, mitochondrial	Atp5b	ATPB_RAT	P10719	37	8 (2)	4 (2)
Cadherin-23	Cdh23	CAD23_RAT	P58365	36	8 (1)	6 (1)
Calnexin	Canx	CALX_RAT	P35565	86	4 (3)	3 (2)
Carbonic anhydrase 2	Ca2	CAH2_RAT	P27139	173	4 (3)	4 (3)
Carbonic anhydrase 3	Ca3	CAH3_RAT	P14141	38	12 (3)	6 (1)
Carbonyl reductase [NADPH] 1	Cbr1	CBR1_RAT	P47727	47	7 (3)	2 (1)
Catalase	Cat	CATA_RAT	P04762	537	26 (19)	13 (9)
Citrate synthase, mitochondrial	Cs	CISY_RAT	Q8VHF5	44	1 (1)	1 (1)
Collagen alpha-1(I) chain	Col1a1	CO1A1_RAT	P02454	197	7 (2)	5 (2)
Creatine kinase B-type	Ckb	KCRB_RAT	P07335	91	11 (4)	9 (3)
Cystatin-B	Cstb	CYTB_RAT	P01041	78	4 (1)	3 (1)
Cystatin-C	Cst3	CYTC_RAT	P14841	34	5 (1)	4 (1)
Cytochrome b5	Cyb5a	CYB5_RAT	P00173	98	9 (3)	7 (2)
Cytochrome c, somatic	Cycs	CYC_RAT	P62898	68	2 (1)	2 (1)
D-dopachrome decarboxylase	Ddt	DOPD_RAT	P80254	46	1 (1)	1 (1)
Decorin	Dcn	PGS2_RAT	Q01129	56	1 (1)	1 (1)
Desmin	Des	DESM_RAT	P48675	38	1 (1)	1 (1)
Destrin	Dstn	DEST_RAT	Q7M0E3	94	7 (3)	6 (3)
EH domain-containing protein 2	Ehd2	EHD2_RAT	Q4V8H8	84	3 (2)	3 (2)
Endoplasmic reticulum resident protein 29	Erp29	ERP29_RAT	P52555	40	1 (1)	1 (1)
Endoplasmin	Hsp90b1	ENPL_RAT	Q66HD0	136	10 (5)	6 (4)
Ezrin	Ezr	EZRI_RAT	P31977	132	8 (4)	7 (4)
Fatty acid-binding protein, adipocyte	Fabp4	FABP4_RAT	P70623	39	8 (1)	7 (1)
Ferritin heavy chain	Fth1	FRIH_RAT	P19132	40	3 (1)	3 (1)
Fibrinogen beta chain	Fgb	FIBB_RAT	P14480	53	7 (1)	6 (1)
Fructose-bisphosphate aldolase A	Aldoa	ALDOA_RAT	P05065	302	11 (8)	4 (4)
Galectin-1	Lgals1	LEG1_RAT	P11762	35	2 (1)	2 (1)
Galectin-3	Lgals3	LEG3_RAT	P08699	29	2 (1)	2 (1)
Gelsolin	Gsn	GELS_RAT	Q68FP1	49	6 (2)	5 (2)
Glial fibrillary acidic protein	Gfap	GFAP_RAT	P47819	32	4 (2)	4 (2)
Glutathione S-transferase alpha-3	Gsta3	GSTA3_RAT	P04904	59	8 (1)	5 (1)
Glutathione S-transferase P	Gstp1	GSTP1_RAT	P04906	60	3 (2)	3 (2)
Glyceraldehyde-3-phosphate dehydrogenase	Gapdh	G3P_RAT	P04797	75	2 (2)	2 (2)
Glycerol-3-phosphate dehydrogenase [NAD(+)], cytoplasmic	Gpd1	GPDA_RAT	O35077	331	15 (9)	14 (9)
Guanine deaminase	Gda	GUAD_RAT	Q9WTT6	52	5 (1)	4 (1)
Heat shock cognate 71 kDa protein	Hspa8	HSP7C_RAT	P63018	31	4 (1)	4 (1)
Heat shock protein beta-1 (HspB1)	Hspb1	HSPB1_RAT	P42930	127	7 (3)	7 (3)
Hemoglobin subunit alpha-1/2	Hba1	HBA_RAT	P01946	122	9 (7)	4 (3)
Hemoglobin subunit beta-1	Hbb	HBB1_RAT	P02091	121	5 (4)	5 (4)
Heterogeneous nuclear ribonucleoproteins A2/B1	Hnrnpa2b1	ROA2_RAT	A7VJC2	68	6 (2)	4 (2)

Histidine triad nucleotide-binding protein 1	Hint1	HINT1_RAT	P62959	76	4 (2)	3 (2)
Histone H2A type 1-C	-	H2A1C_RAT	P0C169	374	11 (9)	7 (7)
Histone H2B type 1	-	H2B1_RAT	Q00715	380	10 (8)	8 (8)
Histone H3.1	-	H31_RAT	Q6LED0	45	2 (1)	2 (1)
Histone H4	Hist1h4b	H4_RAT	P62804	365	12 (9)	12 (9)
Ig gamma-2A chain C region	Igg-2a	IGG2A_RAT	P20760	48	4 (2)	4 (2)
Keratin, type I cytoskeletal 10	Krt10	K1C10_RAT	Q6IFW6	31	1 (1)	1 (1)
Keratin, type I cytoskeletal 19	Krt19	K1C19_RAT	Q63279	157	11 (8)	4 (2)
Keratin, type II cytoskeletal 1	Krt1	K2C1_RAT	Q6IMF3	40	6 (1)	4 (1)
Keratin, type II cytoskeletal 6A	Krt6a	K2C6A_RAT	Q4FZU2	219	14 (9)	5 (4)
Long-chain-fatty-acid--CoA ligase 1	Acsl1	ACSL1_RAT	P18163	280	17 (11)	5 (4)
Long-chain-fatty-acid--CoA ligase 6	Acsl6	ACSL6_RAT	P33124	35	2 (1)	2 (1)
Lumican	Lum	LUM_RAT	P51886	102	5 (3)	3 (3)
Macrophage-capping protein	Capg	CAPG_RAT	Q6AYC4	156	3 (3)	3 (3)
Malate dehydrogenase, cytoplasmic	Mdh1	MDHC_RAT	O88989	111	6 (3)	6 (3)
Malate dehydrogenase, mitochondrial	Mdh2	MDHM_RAT	P04636	83	7 (5)	3 (3)
Membrane primary amine oxidase	Aoc3	AOC3_RAT	O08590	89	4 (2)	4 (2)
Myosin light polypeptide 6	Myl6	MYL6_RAT	Q64119	34	3 (1)	3 (1)
Myosin regulatory light chain RLC-A	Rlc-a	MRLCA_RAT	P13832	96	2 (2)	1 (1)
Myosin regulatory light polypeptide 9	Myl9	MYL9_RAT	Q64122	43	7 (1)	7 (1)
Myosin-11	Myh11	MYH11_RAT	Q63862	179	5 (5)	5 (5)
NADH-cytochrome b5 reductase 3	Cyb5r3	NB5R3_RAT	P20070	89	3 (2)	2 (1)
Nidogen-2	Nid2	NID2_RAT	B5DFC9	79	6 (2)	4 (2)
Nucleoside diphosphate kinase B	Nme2	NDKB_RAT	P19804	40	2 (2)	2 (2)
Peptidyl-prolyl cis-trans isomerase A	Ppia	PPIA_RAT	P10111	69	15 (3)	10 (3)
Peroxiredoxin-1	Prdx1	PRDX1_RAT	Q63716	80	7 (3)	7 (3)
Peroxiredoxin-2	Prdx2	PRDX2_RAT	P35704	62	5 (1)	5 (1)
Phosphoglycerate kinase 1	Pgk1	PGK1_RAT	P16617	101	9 (3)	9 (3)
Polymerase I and transcript release factor	Ptrf	PTRF_RAT	P85125	63	3 (1)	3 (1)
Prelamin-A/C	Lmna	LMNA_RAT	P48679	29	2 (1)	2 (1)
Profilin-1	Pfn1	PROF1_RAT	P62963	137	3 (3)	3 (3)
Protein disulfide-isomerase A3	Pdia3	PDIA3_RAT	P11598	107	4 (3)	4 (3)
Protein disulfide-isomerase A6	Pdia6	PDIA6_RAT	Q63081	33	1 (1)	1 (1)
Protein phosphatase 1 regulatory subunit 7	Ppp1r7	PP1R7_RAT	Q5HZV9	159	3 (3)	3 (3)
Protein S100-A10	S100a10	S10AA_RAT	P05943	106	6 (4)	4 (3)
Ras-related C3 botulinum toxin substrate 1	Rac1	RAC1_RAT	Q6RUV5	29	3 (1)	3 (1)
Rho GDP-dissociation inhibitor 1	Arhgdia	GDIR1_RAT	Q5XI73	45	2 (1)	2 (1)
Serotransferrin	Tf	TRFE_RAT	P12346	62	3 (2)	3 (2)
Serpin H1	Serpinh1	SERPH_RAT	P29457	105	2 (2)	2 (2)
Serum albumin	Alb	ALBU_RAT	P02770	90	4 (1)	3 (1)
SPARC	Sparc	SPRC_RAT	P16975	67	3 (3)	3 (3)
Spectrin alpha chain, non-erythrocytic 1	Sptan1	SPTN1_RAT	P16086	41	2 (1)	2 (1)

Superoxide dismutase [Cu-Zn]	Sod1	SODC_RAT	P07632	100	20 (3)	18 (3)
Thioredoxin	Txn	THIO_RAT	P11232	142	6 (6)	3 (3)
Transgelin	Tagln	TAGL_RAT	P31232	355	15 (10)	9 (5)
Triosephosphate isomerase	Tpi1	TPIS_RAT	P48500	106	7 (4)	6 (4)
Tropomyosin alpha-3 chain	Tpm3	TPM3_RAT	Q63610	198	8 (6)	6 (5)
Tropomyosin alpha-4 chain	Tpm4	TPM4_RAT	P09495	87	5 (4)	5 (4)
Tropomyosin beta chain	Tpm2	TPM2_RAT	P58775	76	2 (2)	2 (2)
Tubulin alpha-1B chain	Tuba1b	TBA1B_RAT	Q6P9V9	52	2 (1)	1 (1)
Tubulin beta-2A chain	Tubb2a	TBB2A_RAT	P85108	182	15 (7)	10 (5)
Tubulin beta-4B chain	Tubb4b	TBB4B_RAT	Q6P9T8	179	14 (7)	10 (5)
Tubulin beta-5 chain	Tubb5	TBB5_RAT	P69897	227	16 (9)	15 (9)
Ubiquitin-conjugating enzyme E2 N	Ube2n	UBE2N_RAT	Q9EQX9	59	2 (1)	2 (1)
Vimentin	Vim	VIME_RAT	P31000	715	31 (25)	20 (17)

Supplemental Table B 4 - Proteins of epicardial adipose tissue extracted from protocol - Tris

Protein name	Gene name	Entry name	Accession number	Mascot score	Matching peptides	Sequence coverage
Alpha-1-macroglobulin	A1m	A1M_RAT	Q63041	59	5 (4)	5 (4)
Aconitate hydratase, mitochondrial	Aco2	ACON_RAT	Q9ER34	38	1 (1)	1 (1)
Actin, aortic smooth muscle	Acta2	ACTA_RAT	P62738	160	5 (5)	5 (5)
Actin, cytoplasmic 1	Actb	ACTB_RAT	P60711	263	7 (7)	7 (7)
Serum albumin	Alb	ALBU_RAT	P02770	627	24 (21)	18 (15)
Annexin A2	Anxa2	ANXA2_RAT	Q07936	184	6 (5)	6 (5)
Casein kinase II subunit alpha	Csnk2a1	CSK21_RAT	P19139	16	9 (1)	2 (1)
Fibrinogen alpha chain	Fga	FIBA_RAT	P06399	351	17 (10)	11 (7)
Fibrinogen beta chain	Fgb	FIBB_RAT	P14480	348	13 (10)	10 (8)
Fibrinogen gamma chain	Fgg	FIBG_RAT	P02680	133	13 (9)	10 (7)
Fibronectin	Fn1	FINC_RAT	P04937	42	7 (1)	6 (1)
Histone H2A type 1-C	-	H2A1C_RAT	P0C169	175	2 (2)	2 (2)
Histone H3.1	-	H31_RAT	Q6LED0	77	6 (2)	3 (2)
Hemoglobin subunit alpha-1/2	Hba1	HBA_RAT	P01946	588	7 (6)	5 (4)
Hemoglobin subunit beta-2	-	HBB2_RAT	P11517	748	10 (10)	8 (8)
Hemoglobin subunit beta-1	Hbb	HBB1_RAT	P02091	376	7 (7)	6 (6)
Lumican	Lum	LUM_RAT	P51886	28	2 (1)	2 (1)
Murinoglobulin-1	Mug1	MUG1_RAT	Q03626	33	6 (3)	6 (3)
Decorin	Dcn	PGS2_RAT	Q01129	51	2 (1)	2 (1)
Plectin	Plec	PLEC_RAT	P30427	27	11 (1)	11 (1)
Prolargin	Prelp	PRELP_RAT	Q9EQP5	34	1 (1)	1 (1)
Serpin H1	Serpinh1	SERPH_RAT	P29457	77	2 (1)	2 (1)
Serine protease inhibitor A3N	Serpina3n	SPA3N_RAT	P09006	65	2 (1)	2 (1)
Tubulin alpha-1A chain	Tuba1a	TBA1A_RAT	P68370	61	2 (1)	2 (1)
Serotransferrin	Tf	TRFE_RAT	P12346	183	6 (5)	5 (4)
Vimentin	Vim	VIME_RAT	P31000	42	2 (1)	2 (1)

Supplemental Table B 5 - Proteins of epicardial adipose tissue extracted from protocol - Urea

Protein name	Gene name	Entry name	Accession number	Mascot score	Matching peptides	Sequence coverage
14-3-3 protein gamma	Ywhag	1433G_RAT	P61983	32	3 (2)	2 (2)
Alpha-1-acid glycoprotein	Orm1	A1AG_RAT	P02764	31	2 (1)	2 (1)
Alpha-1-antiproteinase	Serpina1	A1AT_RAT	P17475	39	1 (1)	1 (1)
Alpha-1-inhibitor 3	A1i3	A1I3_RAT	P14046	182	8 (6)	8 (6)
Alpha-1-macroglobulin	A1m	A1M_RAT	Q63041	194	9 (4)	9 (4)
Aconitate hydratase, mitochondrial	Aco2	ACON_RAT	Q9ER34	329	19 (10)	15 (10)
Actin, cytoplasmic 1	Actb	ACTB_RAT	P60711	50	5 (1)	4 (1)
Actin, alpha cardiac muscle 1	Actc1	ACTC_RAT	P68035	570	26 (17)	12 (9)
Alpha-actinin-1	Actn1	ACTN1_RAT	Q9Z1P2	337	17 (12)	9 (7)
Serum albumin	Alb	ALBU_RAT	P02770	51	9 (1)	8 (1)
Aldehyde dehydrogenase, mitochondrial	Aldh2	ALDH2_RAT	P11884	2287	58 (48)	26 (22)
Fructose-bisphosphate aldolase A	Aldoa	ALDOA_RAT	P05065	35	4 (2)	4 (2)
Annexin A2	Anxa2	ANXA2_RAT	Q07936	55	4 (2)	3 (2)
Annexin A3	Anxa3	ANXA3_RAT	P14669	229	8 (5)	8 (5)
Annexin A6	Anxa6	ANXA6_RAT	P48037	73	7 (3)	4 (2)
Annexin A5	Anxa5	ANXA5_RAT	P14668	211	11 (5)	11 (5)
Annexin A1	Anxa1	ANXA1_RAT	P07150	185	8 (7)	8 (7)
Membrane primary amine oxidase	Aoc3	AOC3_RAT	O08590	54	5 (1)	5 (1)
Apolipoprotein A-I	Apoa1	APOA1_RAT	P04639	31	5 (1)	2 (1)
Beta-2-glycoprotein 1	Apoh	APOH_RAT	P26644	321	15 (10)	15 (10)
Apolipoprotein E	Apoe	APOE_RAT	P02650	156	8 (5)	7 (5)
ATP synthase subunit alpha, mitochondrial	Atp5a1	ATPA_RAT	P15999	61	4 (3)	4 (3)
ATP synthase subunit beta, mitochondrial	Atp5b	ATPB_RAT	P10719	62	2 (1)	2 (1)
Cadherin-23	Cdh23	CAD23_RAT	P58365	253	11 (5)	10 (5)
Carbonic anhydrase 2	Ca2	CAH2_RAT	P27139	36	10 (3)	6 (1)
Carbonic anhydrase 3	Ca3	CAH3_RAT	P14141	38	6 (2)	3 (2)
Catalase	Cat	CATA_RAT	P04762	241	9 (7)	8 (7)
Carbonyl reductase [NADPH] 1	Cbr1	CBR1_RAT	P47727	124	8 (5)	8 (5)
Ceruloplasmin	Cp	CERU_RAT	P13635	47	1 (1)	1 (1)
60 kDa heat shock protein, mitochondrial	Hspd1	CH60_RAT	P63039	96	6 (3)	6 (3)
Citrate synthase, mitochondrial	Cs	CISY_RAT	Q8VHF5	41	4 (1)	4 (1)
Collagen alpha-1(I) chain	Col1a1	CO1A1_RAT	P02454	48	6 (2)	6 (2)
C-reactive protein	Crp	CRP_RAT	P48199	182	6 (3)	6 (3)
Alpha-enolase	Eno1	ENOA_RAT	P04764	36	4 (1)	3 (1)
Beta-enolase	Eno3	ENOB_RAT	P15429	45	5 (2)	5 (2)
Endoplasmin	Hsp90b1	ENPL_RAT	Q66HD0	77	4 (2)	4 (2)
Fatty acid-binding protein, adipocyte	Fabp4	FABP4_RAT	P70623	31	2 (2)	2 (2)
Alpha-2-HS-glycoprotein	Ahsg	FETUA_RAT	P24090	50	2 (2)	1 (1)
Fibrinogen alpha chain	Fga	FIBA_RAT	P06399	126	5 (3)	5 (3)
Fibrinogen beta chain	Fgb	FIBB_RAT	P14480	378	18 (15)	10 (9)
Fibrinogen gamma chain	Fgg	FIBG_RAT	P02680	463	20 (15)	15 (12)
Fibronectin (FN)	Fn1	FINC_RAT	P04937	166	10 (6)	6 (5)

Gelsolin	Gsn	GELS_RAT	Q68FP1	184	22 (8)	19 (8)
Glycerol-3-phosphate dehydrogenase [NAD(+)], cytoplasmic	Gpd1	GPDA_RAT	O35077	78	6 (2)	3 (1)
Glutathione peroxidase 3	Gpx3	GPX3_RAT	P23764	44	2 (1)	2 (1)
78 kDa glucose-regulated protein	Hspa5	GRP78_RAT	P06761	39	2 (1)	2 (1)
Glutathione S-transferase alpha-3	Gsta3	GSTA3_RAT	P04904	118	4 (2)	4 (2)
Glutathione S-transferase P	Gstp1	GSTP1_RAT	P04906	34	3 (1)	3 (1)
Guanine deaminase	Gda	GUAD_RAT	Q9WTT6	36	3 (2)	3 (2)
Histone H2A type 1-C	-	H2A1C_RAT	P0C169	100	1 (1)	1 (1)
Hemoglobin subunit alpha-1/2	Hba1	HBA_RAT	P01946	528	22 (16)	6 (6)
Hemoglobin subunit beta-2	-	HBB2_RAT	P11517	1157	32 (23)	10 (10)
Hemoglobin subunit beta-1	Hbb	HBB1_RAT	P02091	874	27 (18)	10 (9)
Hemopexin	Hpx	HEMO_RAT	P20059	118	5 (3)	5 (3)
Heat shock cognate 71 kDa protein	Hspa8	HSP7C_RAT	P63018	247	5 (4)	5 (4)
Heat shock protein beta-1	Hspb1	HSPB1_RAT	P42930	35	4 (1)	3 (1)
Ig gamma-2A chain C region	Igg-2a	IGG2A_RAT	P20760	78	3 (1)	3 (1)
Keratin, type I cytoskeletal 10	Krt10	K1C10_RAT	Q6IFW6	58	5 (2)	3 (1)
Keratin, type II cytoskeletal 1b	Krt77	K2C1B_RAT	Q6IG01	103	6 (4)	3 (2)
Keratin, type II cytoskeletal 6A	Krt6a	K2C6A_RAT	Q4FZU2	33	8 (2)	4 (2)
Creatine kinase M-type	Ckm	KCRM_RAT	P00564	146	11 (5)	9 (5)
T-kininogen 1	Map1	KNT1_RAT	P01048	83	4 (3)	4 (3)
Galectin-1	Lgals1	LEG1_RAT	P11762	46	1 (1)	1 (1)
Galectin-3	Lgals3	LEG3_RAT	P08699	74	3 (3)	3 (3)
Prelamin-A/C	Lmna	LMNA_RAT	P48679	118	14 (5)	12 (5)
Lumican	Lum	LUM_RAT	P51886	358	16 (12)	9 (9)
Mast cell protease 1	Mcpt1	MCPT1_RAT	P09650	47	2 (2)	1 (1)
Myosin regulatory light chain RLC-A	Rlc-a	MRLCA_RAT	P13832	41	1 (1)	1 (1)
Murinoglobulin-1	Mug1	MUG1_RAT	Q03626	153	8 (4)	8 (4)
Myosin light polypeptide 6	Myl6	MYL6_RAT	Q64119	71	5 (2)	5 (2)
Myelin protein P0	Mpz	MYP0_RAT	P06907	380	13 (10)	6 (4)
NADH-cytochrome b5 reductase 3	Cyb5r3	NB5R3_RAT	P20070	106	4 (3)	4 (3)
Neurofilament light polypeptide	Nefl	NFL_RAT	P19527	54	9 (3)	7 (3)
Nidogen-2	Nid2	NID2_RAT	B5DFC9	58	14 (4)	11 (4)
Protein disulfide-isomerase A3	Pdia3	PDIA3_RAT	P11598	43	2 (1)	2 (1)
Protein disulfide-isomerase	P4hb	PDIA1_RAT	P04785	52	5 (2)	5 (2)
Phosphoglycerate kinase 1	Pgk1	PGK1_RAT	P16617	39	4 (1)	4 (1)
Plasminogen	Plg	PLMN_RAT	Q01177	35	3 (1)	3 (1)
Serum paraoxonase/arylesterase 1	Pon1	PON1_RAT	P55159	71	2 (1)	2 (1)
Peptidyl-prolyl cis-trans isomerase A	Ppia	PPIA_RAT	P10111	34	3 (1)	3 (1)
Periaxin	Prx	PRAX_RAT	Q63425	70	15 (4)	12 (4)
Prolargin	Prelp	PRELP_RAT	Q9EQP5	134	10 (7)	10 (7)
Polymerase I and transcript release factor	Ptrf	PTRF_RAT	P85125	42	5 (2)	4 (2)
Ras-related C3 botulinum toxin substrate 1	Rac1	RAC1_RAT	Q6RUV5	34	6 (1)	3 (1)
Serpin H1	Serpinh1	SERPH_RAT	P29457	38	5 (2)	3 (2)
Serine protease inhibitor A3K	Serpina3k	SPA3K_RAT	P05545	126	7 (2)	7 (2)
Serine protease inhibitor A3N	Serpina3n	SPA3N_RAT	P09006	100	8 (2)	7 (2)

Spectrin alpha chain, non-erythrocytic 1	Sptan1	SPTN1_RAT	P16086	190	27 (7)	23 (7)
Tubulin alpha-1B chain	Tuba1b	TBA1B_RAT	Q6P9V9	160	11 (4)	8 (4)
Tubulin beta-3 chain	Tubb3	TBB3_RAT	Q4QRB4	176	7 (3)	7 (3)
Tubulin beta-4B chain	Tubb4b	TBB4B_RAT	Q6P9T8	170	10 (5)	10 (5)
Tropomyosin beta chain	Tpm2	TPM2_RAT	P58775	88	7 (4)	4 (3)
Tropomyosin alpha-3 chain	Tpm3	TPM3_RAT	Q63610	137	11 (5)	9 (5)
Tropomyosin alpha-4 chain (Tropomyosin-4) (TM-4)	Tpm4	TPM4_RAT	P09495	148	9 (4)	7 (4)
Serotransferrin	Tf	TRFE_RAT	P12346	643	25 (18)	19 (16)
Voltage-dependent anion-selective channel protein 1	Vdac1	VDAC1_RAT	Q9Z2L0	33	3 (1)	3 (1)
Vimentin	Vim	VIME_RAT	P31000	540	23 (17)	13 (11)
Vitamin D-binding protein	Gc	VTDB_RAT	P04276	58	6 (2)	5 (2)

Supplemental Table B 6 - Proteins of epicardial adipose tissue extracted from protocol – Tris and Urea

Protein name	Gene name	Entry name	Accession number	Mascot score	Matching peptides	Sequence coverage
14-3-3 protein gamma	Ywhag	1433G_RAT	P61983	37	1 (1)	1 (1)
14-3-3 protein epsilon	Ywhae	1433E_RAT	P62260	30	2 (1)	2 (1)
Alpha-1-antiproteinase	Serpina1	A1AT_RAT	P17475	39	1 (1)	1 (1)
Alpha-1-inhibitor 3	A1i3	A1I3_RAT	P14046	70	3 (3)	3 (3)
Alpha-1-macroglobulin	A1m	A1M_RAT	Q63041	167	11 (4)	10 (4)
Aconitate hydratase, mitochondrial	Aco2	ACON_RAT	Q9ER34	514	27 (17)	19 (16)
Long-chain-fatty-acid--CoA ligase 6	Acsl6	ACSL6_RAT	P33124	84	6 (1)	5 (1)
Actin, cytoplasmic 1 (Beta-actin)	Actb	ACTB_RAT	P60711	34	4 (1)	4 (1)
Actin, alpha cardiac muscle 1	Actc1	ACTC_RAT	P68035	552	24 (17)	18 (13)
Serum albumin	Alb	ALBU_RAT	P02770	381	16 (12)	11 (9)
Aldehyde dehydrogenase, mitochondrial	Aldh2	ALDH2_RAT	P11884	1804	54 (43)	25 (21)
Fructose-bisphosphate aldolase A	Aldoa	ALDOA_RAT	P05065	45	2 (2)	2 (2)
Aldose reductase	Akr1b1	ALDR_RAT	P07943	48	3 (2)	3 (2)
Ankyrin repeat domain-containing protein 54	Ankrd54	ANR54_RAT	Q566C8	33	2 (1)	2 (1)
Annexin A2	Anxa2	ANXA2_RAT	Q07936	27	4 (1)	1 (1)
Annexin A5	Anxa5	ANXA5_RAT	P14668	280	11 (8)	7 (6)
Annexin A1	Anxa1	ANXA1_RAT	P07150	377	15 (10)	11 (8)
Membrane primary amine oxidase	Aoc3	AOC3_RAT	O08590	190	7 (7)	7 (7)
Apolipoprotein A-I	Apoa1	APOA1_RAT	P04639	62	6 (3)	3 (2)
Apolipoprotein A-IV	Apoa4	APOA4_RAT	P02651	143	9 (6)	7 (6)
Beta-2-glycoprotein 1	Apoh	APOH_RAT	P26644	32	4 (2)	4 (2)
Apolipoprotein E	Apoe	APOE_RAT	P02650	111	8 (5)	7 (5)
ATP synthase subunit beta, mitochondrial	Atp5b	ATPB_RAT	P10719	33	3 (1)	2 (1)
Protein bassoon	Bsn	BSN_RAT	O88778	236	12 (5)	9 (5)
Cadherin-23	Cdh23	CAD23_RAT	P58365	28	7 (1)	7 (1)

Carbonic anhydrase 2	Ca2	CAH2_RAT	P27139	47	11 (1)	7 (1)
Carbonic anhydrase 3	Ca3	CAH3_RAT	P14141	49	4 (1)	3 (1)
Catalase	Cat	CATA_RAT	P04762	159	8 (5)	8 (5)
Mast cell carboxypeptidase A	Cpa3	CBPA3_RAT	P21961	60	5 (3)	5 (3)
Carbonyl reductase [NADPH] 1	Cbr1	CBR1_RAT	P47727	244	12 (10)	7 (5)
Cadherin EGF LAG seven-pass G-type receptor 3	Celsr3	CELR3_RAT	O88278	46	1 (1)	1 (1)
Ceruloplasmin	Cp	CERU_RAT	P13635	28	14 (1)	13 (1)
Citrate synthase, mitochondrial	Cs	CISY_RAT	Q8VHF5	66	6 (4)	5 (4)
C-reactive protein	Crp	CRP_RAT	P48199	63	4 (1)	4 (1)
Alpha-enolase	Eno1	ENOA_RAT	P04764	41	3 (1)	2 (1)
Fatty acid-binding protein, adipocyte	Fabp4	FABP4_RAT	P70623	112	4 (3)	3 (3)
Fibrinogen alpha chain	Fga	FIBA_RAT	P06399	65	3 (1)	2 (1)
Fibrinogen beta chain	Fgb	FIBB_RAT	P14480	1348	43 (34)	15 (13)
Fibrinogen gamma chain	Fgg	FIBG_RAT	P02680	735	24 (20)	15 (13)
Fibronectin	Fn1	FINC_RAT	P04937	320	21 (19)	11 (10)
Gelsolin	Gsn	GELS_RAT	Q68FP1	102	20 (5)	16 (5)
Glycerol-3-phosphate dehydrogenase [NAD(+)], cytoplasmic	Gpd1	GPDA_RAT	O35077	25	4 (1)	4 (1)
78 kDa glucose-regulated protein	Hspa5	GRP78_RAT	P06761	32	1 (1)	1 (1)
Guanine deaminase	Gda	GUAD_RAT	Q9WTT6	56	5 (2)	5 (2)
Histone H2A type 1-C		H2A1C_RAT	P0C169	72	3 (2)	3 (2)
Histone H2B type 1		H2B1_RAT	Q00715	67	2 (2)	1 (1)
Hemoglobin subunit alpha-1/2	Hba1	HBA_RAT	P01946	1099	19 (17)	7 (6)
Hemoglobin subunit beta-2		HBB2_RAT	P11517	1459	31 (30)	8 (8)
Hemoglobin subunit beta-1	Hbb	HBB1_RAT	P02091	1315	27 (25)	9 (8)
Hemopexin	Hpx	HEMO_RAT	P20059	69	5 (2)	5 (2)
Haptoglobin	Hp	HPT_RAT	P06866	26	5 (1)	4 (1)
Heat shock-related 70 kDa protein 2	Hspa2	HSP72_RAT	P14659	52	7 (1)	7 (1)
Ig gamma-2A chain C region	Igg-2a	IGG2A_RAT	P20760	49	3 (1)	3 (1)
Keratin, type I cytoskeletal 10	Krt10	K1C10_RAT	Q6IFW6	96	12 (6)	5 (2)
Keratin, type I cytoskeletal 17	Krt17	K1C17_RAT	Q6IFU8	37	5 (2)	3 (1)
Keratin, type II cytoskeletal 6A	Krt6a	K2C6A_RAT	Q4FZU2	324	14 (10)	5 (3)
Keratin, type II cytoskeletal 1	Krt1	K2C1_RAT	Q6IMF3	193	11 (10)	5 (4)
Creatine kinase M-type	Ckm	KCRM_RAT	P00564	68	4 (2)	3 (2)
KH domain-containing, RNA-binding, signal transduction-associated protein 2	Khdrbs2	KHDR2_RAT	Q920F3	25	4 (1)	3 (1)
T-kininogen 1	Map1	KNT1_RAT	P01048	30	4 (1)	4 (1)
Galectin-1	Lgals1	LEG1_RAT	P11762	44	1 (1)	1 (1)
Galectin-3	Lgals3	LEG3_RAT	P08699	69	3 (2)	3 (2)
Prelamin-A/C	Lmna	LMNA_RAT	P48679	27	10 (1)	9 (1)
Latrophilin-2	Lphn2	LPHN2_RAT	O88923	27	3 (1)	3 (1)
Lumican	Lum	LUM_RAT	P51886	55	5 (5)	3 (3)
Myelin basic protein	Mbp	MBP_RAT	P02688	60	4 (2)	4 (2)
Monoglyceride lipase	Mgll	MGLL_RAT	Q8R431	28	2 (1)	2 (1)

Multidrug resistance-associated protein 6	Abcc6	MRP6_RAT	O88269	27	5 (1)	2 (1)
Murinoglobulin-1	Mug1	MUG1_RAT	Q03626	185	12 (5)	11 (5)
Myosin light polypeptide 6	Myl6	MYL6_RAT	Q64119	62	1 (1)	1 (1)
Myelin protein P0	Mpz P0	MYP0_RAT	P06907	285	10 (6)	5 (3)
NADH-cytochrome b5 reductase 3	Cyb5r3	NB5R3_RAT	P20070	54	3 (1)	3 (1)
Nucleoside diphosphate kinase A	Nme1	NDKA_RAT	Q05982	26	1 (1)	1 (1)
Neurofilament light polypeptide	Nefl	NFL_RAT	P19527	35	6 (3)	6 (3)
Phosphoglycerate kinase 1	Pgk1	PGK1_RAT	P16617	56	3 (1)	3 (1)
Decorin	Dcn	PGS2_RAT	Q01129	114	5 (3)	4 (2)
Serum paraoxonase/arylesterase 1	Pon1	PON1_RAT	P55159	100	1 (1)	1 (1)
Peptidyl-prolyl cis-trans isomerase A	Ppia	PPIA_RAT	P10111	26	1 (1)	1 (1)
Ryanodine receptor 2	Ryr2	RYR2_RAT	B0LPN4	35	28 (10)	10 (1)
Serpin H1	Serpinh1	SERPH_RAT	P29457	100	5 (1)	4 (1)
Serine protease inhibitor A3K	Serpina3k	SPA3K_RAT	P05545	65	3 (2)	3 (2)
Serine protease inhibitor A3N	Serpina3n	SPA3N_RAT	P09006	31	2 (2)	2 (2)
Spectrin alpha chain, non-erythrocytic 1	Sptan1	SPTN1_RAT	P16086	35	23 (1)	14 (1)
Synaptonemal complex protein 3	Sycp3	SYCP3_RAT	Q63520	27	4 (1)	4 (1)
Synaptotagmin-like protein 5	Sytl5	SYTL5_RAT	Q812E4	28	7 (1)	4 (1)
Tubulin alpha-1A chain	Tuba1a	TBA1A_RAT	P68370	128	9 (5)	4 (2)
3-ketoacyl-CoA thiolase, mitochondrial	Acaa2	THIM_RAT	P13437	51	4 (2)	4 (2)
Tropomyosin alpha-1 chain	Tpm1	TPM1_RAT	P04692	43	9 (2)	6 (2)
Tropomyosin alpha-4 chain	Tpm4	TPM4_RAT	P09495	62	9 (2)	7 (2)
Serotransferrin	Tf	TRFE_RAT	P12346	517	19 (15)	17 (13)
Vimentin	Vim	VIME_RAT	P31000	500	20 (15)	16 (14)
Vitamin D-binding protein	Gc	VTDB_RAT	P04276	37	2 (1)	2 (1)

Appendix C – Identified proteins of visceral and epicardial adipose tissue

Supplemental Table C 1 - Proteins of visceral adipose tissue identified in lean ZSF1

Entry	Entry name	Protein Name	Gene name	MW (kDa)
Q6QA69	ABHD5_RAT	1-acylglycerol-3-phosphate O-acyltransferase ABHD5	Abhd5	39079
P60711	ACTB_RAT	Actin, cytoplasmic 1	Actb	41710
P85970	ARPC2_RAT	Actin-related protein 2/3 complex subunit 2	Arpc2	34370
Q5XI32	CAPZB_RAT	F-actin-capping protein subunit beta	Capzb	30609
P41350	CAV1_RAT	Caveolin-1	Cav1	20539
P10252	CD48_RAT	CD48 antigen	Cd48	27662
P26772	CH10_RAT	10 kDa heat shock protein, mitochondrial	Hspe1	10895
P45592	COF1_RAT	Cofilin-1	Cfl1	18521
Q91ZN1	COR1A_RAT	Coronin-1A	Coro1a	51033
P63255	CRIP1_RAT	Cysteine-rich protein 1	Crip1	8544
P10860	DHE3_RAT	Glutamate dehydrogenase 1, mitochondrial	Glud1	61377
Q4KLP0	DHTK1_RAT	Probable 2-oxoglutarate dehydrogenase E1 component DHKTD1, mitochondrial	Dhtkd1	102576
P31977	EZRI_RAT	Ezrin	Ezr	69348
P63245	GBLP_RAT	Guanine nucleotide-binding protein subunit beta-2-like 1	Gnb2l1	35055
P48721	GRP75_RAT	Stress-70 protein, mitochondria	Hspa9	73812
P0C169	H2A1C_RAT	Histone H2A type 1-C	type-1c	14097
P62804	H4_RAT	Histone H4	Hist1h4b	11360
P82995	HS90A_RAT	Heat shock protein HSP 90-alpha	Hsp90aa1	84762
P35704	PRDX2_RAT	Peroxiredoxin-2	Prdx2	21770
Q9Z0V6	PRDX3_RAT	Thioredoxin-dependent peroxide reductase, mitochondrial	Prdx3	28277
Q63797	PSME1_RAT	Proteasome activator complex subunit 1	Psme1	28559
Q63798	PSME2_RAT	Proteasome activator complex subunit 2	Psme2	26840
P09527	RAB7A_RAT	Ras-related protein Rab-7a	Rab7a	23489
P62494	RB11A_RAT	Ras-related protein Rab-11A	Rab11a	24378
P19945	RLA0_RAT	60S acidic ribosomal protein P0	Rplp0 Arbp	34194
P19944	RLA1_RAT	60S acidic ribosomal protein P1	Rplp1	11491
P38983	RSSA_RAT	40S ribosomal protein SA	Rpsa	32803
P05964	S10A6_RAT	Protein S100-A6	S100a6	10028
P05943	S10AA_RAT	Protein S100-A10	S100a10	11068
P10960	SAP_RAT	Sulfated glycoprotein 1	Psap	61084
P29457	SERPH_RAT	Serpin H1	Serpinh1	46488
P16086	SPTN1_RAT	Spectrin alpha chain, non-erythrocytic 1	Sptan1	284462
P63029	TCTP_RAT	Translationally-controlled tumor protein	Tpt1	19450
P17764	THIL_RAT	Acetyl-CoA acetyltransferase, mitochondrial	Acat1	44666
P50137	TKT_RAT	Transketolase	Tkt	67601

Supplemental Table C 2 - Proteins of visceral adipose tissue identified in obese ZSF1

Entry	Entry name	Protein Name	Gene name	MW (kDa)
P63259	ACTG_RAT	Actin, cytoplasmic 2	Actg1	41766
Q9Z1P2	ACTN1_RAT	Alpha-actinin-1	Actn1	102896
P36972	APT_RAT	Adenine phosphoribosyltransferase	Aprt	19533
P58365	CAD23_RAT	Cadherin-23	Cdh23	365230
P16303	CES1D_RAT	Carboxylesterase 1D	Ces1d	62108
P61023	CHP1_RAT	Calcineurin B homologous protein 1	Chp1	22418
Q9Z0W7	CLIC4_RAT	Chloride intracellular channel protein 4	Clic4	28615
P08649	CO4_RAT	Complement C4	C4	192042
B0BNA5	COTL1_RAT	Coactosin-like protein	Cotl1	15922
Q64537	CPNS1_RAT	Calpain small subunit 1	Capns1	28552
P48675	DESM_RAT	Desmin	Des	53424
Q64428	ECHA_RAT	Trifunctional enzyme subunit alpha, mitochondrial	Hadha	82613
Q9Z1X1	ESYT1_RAT	Extended synaptotagmin-1	Esyt1	121084
P13803	ETFA_RAT	Electron transfer flavoprotein subunit alpha, mitochondrial	Etfa	34929
Q9WVH8	FBLN5_RAT	Fibulin-5	Fbln5	50127
P24090	FETUA_RAT	Alpha-2-HS-glycoprotein	Ahsg	37958
Q9QX79	FETUB_RAT	Fetuin-B	Fetub	41506
P47819	GFAP_RAT	Glial fibrillary acidic protein	Gfap	49927
O35077	GPDA_RAT	Glycerol-3-phosphate dehydrogenase [NAD(+)], cytoplasmic	Gpd1	37428
Q99NA5	IDH3A_RAT	Isocitrate dehydrogenase [NAD] subunit alpha, mitochondrial	Idh3a	39588
Q3T1J1	IF5A1_RAT	Eukaryotic translation initiation factor 5A-1	Eif5a	16821
Q63862	MYH11_RAT	Myosin-11	Myh11	152398
Q62812	MYH9_RAT	Myosin-9	Myh9	226197
O35264	PA1B2_RAT	Platelet-activating factor acetylhydrolase IB subunit beta	Pafah1b2	25565
P47853	PGS1_RAT	Biglycan	Bgn	41680
O35244	PRDX6_RAT	Peroxiredoxin-6	Prdx6	24803
Q8VHE9	RETST_RAT	All-trans-retinol 13,14-reductase	Retsat	67487
P09006	SPA3N_RAT	Serine protease inhibitor A3N	Serpina3n	46622
Q505J8	SYFA_RAT	Phenylalanine--tRNA ligase alpha subunit	Farsa	57684
Q5XFX0	TAGL2_RAT	Transgelin-2	Tagln2	22379
P85108	TBB2A_RAT	Tubulin beta-2A chain	Tubb2a	49875
P69897	TBB5_RAT	Tubulin beta-5 chain	Tubb5	49639
Q9EQT5	TINAL_RAT	Tubulointerstitial nephritis antigen-like	Tinagl1	52786
Q7M767	UB2V2_RAT	Ubiquitin-conjugating enzyme E2 variant 2		16342

Supplemental Table C 3 - Visceral adipose tissue common proteins between obese and lean ZSF1 model

Entry	Entry Name	Protein name	Gene name	emPAI ratio	MW (kDa)
P19804	NDKB_RAT	Nucleoside diphosphate kinase B	Nme2	2.89	17272
P02466	CO1A2_RAT	Collagen alpha-2(I) chain	Col1a2	2.67	129486
P12346	TRFE_RAT	Serotransferrin (Transferrin)	Tf	2.53	76346
P14668	ANXA5_RAT	Annexin A5	Anxa5	2.02	35722
P02793	FRIL1_RAT	Ferritin light chain 1	Ftl1	1.51	20736
P08699	LEG3_RAT	Galectin-3	Lgals3	1.38	27184
P02454	CO1A1_RAT	Collagen alpha-1(I) chain	Col1a1	1.33	137869
P42930	HSPB1_RAT	Heat shock protein beta-1	Hspb1	1.30	22879
P09495	TPM4_RAT	Tropomyosin alpha-4 chain	Tpm4	1.23	28492
Q4V8H8	EHD2_RAT	EH domain-containing protein 2	Ehd2	1.18	61199
P17475	A1AT_RAT	Alpha-1-antiproteinase	Serpina1	1.14	46107
P11598	PDIA3_RAT	Protein disulfide-isomerase A3	Pdia3	1.11	56588
P55260	ANXA4_RAT	Annexin A4	Anxa4	1.08	35826
Q63716	PRDX1_RAT	Peroxiredoxin-1	Prdx1	1.06	22095
P35565	CALX_RAT	Calnexin	Canx	1.00	67213
P07150	ANXA1_RAT	Annexin A1	Anxa1	0.95	38805
P02091	HBB1_RAT	Hemoglobin subunit beta-1	Hbb	0.77	15969
P02767	TTHY_RAT	Transthyretin	Ttr	0.76	15710
P07632	SODC_RAT	Superoxide dismutase	Sod1	0.73	15902
P61983	1433G_RAT	14-3-3 protein gamma	Ywhag	0.66	28285
P70623	FABP4_RAT	Fatty acid-binding protein, adipocyte	Fabp4	0.57	14699
P63039	CH60_RAT	60 kDa heat shock protein, mitochondrial	Hspd1	0.57	60917
P04692	TPM1_RAT	Tropomyosin alpha-1 chain	Tpm1	0.56	32661
Q9WTT6	GUAD_RAT	Guanine deaminase	Gda	0.53	50984
P11762	LEG1_RAT	Galectin-1	Lgals1	0.49	14847
P52555	ERP29_RAT	Endoplasmic reticulum resident protein 29	Erp29	0.46	28557
Q07936	ANXA2_RAT	Annexin A2	Anxa2	0.45	38654
P58775	TPM2_RAT	Tropomyosin beta chain	Tpm2	0.43	32817
P25113	PGAM1_RAT	Phosphoglycerate mutase 1	Pgam1	0.43	28814
P02770	ALBU_RAT	Serum albumin	Alb	0.42	68686
P31000	VIME_RAT	Vimentin	Vim	0.41	53700
P85973	PNPH_RAT	Purine nucleoside phosphorylase	Pnp	0.38	32281
P62836	RAP1A_RAT	Ras-related protein Rap-1A	Rap1a	0.37	20974
P05065	ALDOA_RAT	Fructose-bisphosphate aldolase A	Aldoa	0.35	39327
P62738	ACTA_RAT	Actin, aortic smooth muscle	Acta2	0.34	41982
P04639	APOA1_RAT	Apolipoprotein A-I	Apoa1	0.29	30043
P63018	HSP7C_RAT	Heat shock cognate 71 kDa protein	Hspa8	0.29	70827
Q6IMF3	K2C1_RAT	Keratin, type II cytoskeletal 1	Krt1	0.20	64791
P62982	RS27A_RAT	Ubiquitin-40S ribosomal protein S27a	Rps27a	0.20	17939
P14141	CAH3_RAT	Carbonic anhydrase 3	Ca3	0.19	29413
P68370	TBA1A_RAT	Tubulin alpha-1A chain	Tuba1a	0.16	50104

Q6P9V9	TBA1B_RAT	Tubulin alpha-1B chain	Tuba1b	0.15	50120
Q6P9T8	TBB4B_RAT	Tubulin beta-4B chain	Tubb4b	0.12	49769
P19132	FRIH_RAT	Ferritin heavy chain	Fth1	0.05	21113
P24368	PPIB_RAT	Peptidyl-prolyl cis-trans isomerase B	Ppib	0.02	23788
P04631	S100B_RAT	Protein S100-B	S100b	0.01	10737
P01946	HBA_RAT	Hemoglobin subunit alpha-1/2	Hba1	0.01	15319
P35213	1433B_RAT	14-3-3 protein beta/alpha	Ywhab	0.00	28037
P68255	1433T_RAT	14-3-3 protein theta	Ywhaq	0.00	27761
P18163	ACSL1_RAT	Long-chain-fatty-acid--CoA ligase 1	Acsl1	0.00	78128
P33124	ACSL6_RAT	Long-chain-fatty-acid--CoA ligase 6	Acsl6	0.00	78130
P07943	ALDR_RAT	Aldose reductase (AR)	Akr1b1	0.00	35774
P48037	ANXA6_RAT	Annexin A6	Anxa6	0.00	75706
P35434	ATPD_RAT	ATP synthase subunit delta, mitochondrial	Atp5d	0.00	17584
Q62736	CALD1_RAT	Non-muscle caldesmon	Cald1	0.00	60548
P62161	CALM_RAT	Calmodulin	Calm1	0.00	16827
P18418	CALR_RAT	Calreticulin	Calr	0.00	47966
P47727	CBR1_RAT	Carbonyl reductase	Cbr1	0.00	30559
P27274	CD59_RAT	CD59 glycoprotein	Cd59	0.00	13781
P00173	CYB5_RAT	Cytochrome b5	Cyb5a	0.00	15346
P62898	CYC_RAT	Cytochrome c, somatic	Cycs	0.00	11598
Q7M0E3	DEST_RAT	Destrin	Dstn	0.00	18522
P14604	ECHM_RAT	Enoyl-CoA hydratase, mitochondrial	Echs1	0.00	31496
Q66HD0	ENPL_RAT	Endoplasmin	Hsp90b1	0.00	92713
Q5XI73	GDIR1_RAT	Rho GDP-dissociation inhibitor 1	Arhgdia	0.00	23393
Q68FP1	GELS_RAT	Gelsolin	Gsn	0.00	86014
P04041	GPX1_RAT	Glutathione peroxidase 1	Gpx1	0.00	22292
P04904	GSTA3_RAT	Glutathione S-transferase alpha-3	Gsta3	0.00	25303
P04906	GSTP1_RAT	Glutathione S-transferase P	Gstp1	0.00	23424
P11517	HBB2_RAT	Hemoglobin subunit beta-2		0.00	15972
P20059	HEMO_RAT	Hemopexin	Hpx	0.00	51318
Q10758	K2C8_RAT	Keratin, type II cytoskeletal 8	Krt8	0.00	53985
P04642	LDHA_RAT	L-lactate dehydrogenase A chain	Ldha	0.00	36427
P48679	LMNA_RAT	Prelamin-A/C	Lmna	0.00	74279
P51886	LUM_RAT	Lumican	Lum	0.00	38255
O88989	MDHC_RAT	Malate dehydrogenase, cytoplasmic	Mdh1	0.00	36460
P04636	MDHM_RAT	Malate dehydrogenase, mitochondrial	Mdh2	0.00	35661
Q8R431	MGLL_RAT	Monoglyceride lipase	Mgll	0.00	33478
P08011	MGST1_RAT	Microsomal glutathione S-transferase 1	Mgst1	0.00	17460
Q64119	MYL6_RAT	Myosin light polypeptide 6	Myl6	0.00	16964
Q64122	MYL9_RAT	Myosin regulatory light polypeptide 9	Myl9	0.00	19708
P19234	NDUV2_RAT	NADH dehydrogenase [ubiquinone] flavoprotein 2, mitochondrial	Ndufv2	0.00	27361
Q63081	PDIA6_RAT	Protein disulfide-isomerase A6	Pdia6	0.00	48143
P70580	PGRC1_RAT	Membrane-associated progesterone receptor component 1	Pgrmc1	0.00	21585
P10111	PPIA_RAT	Peptidyl-prolyl cis-trans isomerase A	Ppia	0.00	17863
Q9EQP5	PRELP_RAT	Prolargin	Prelp	0.00	43152

P85125	PTRF_RAT	Polymerase I and transcript release factor	Ptrf	0.00	43882
Q6RUV5	RAC1_RAT	Ras-related C3 botulinum toxin substrate 1	Rac1	0.00	21436
B0LPN4	RYR2_RAT	Ryanodine receptor 2	Ryr2	0.00	562594
Q63544	SYUG_RAT	Gamma-synuclein	Sncg	0.00	12969
P31232	TAGL_RAT	Transgelin	Tagln	0.00	22588
P48500	TPIS_RAT	Triosephosphate isomerase	Tpi1	0.00	26832
P85972	VINC_RAT	Vinculin	Vcl	0.00	116542
P20070	NB5R3_RAT	NADH-cytochrome b5 reductase 3	Cyb5r3	-0.02	34153
P04785	PDIA1_RAT	Protein disulfide-isomerase	P4hb	-0.04	56916
P15999	ATPA_RAT	ATP synthase subunit alpha, mitochondrial	Atp5a1	-0.17	59717
Q6IFW6	K1C10_RAT	Keratin, type I cytoskeletal 10	Krt10	-0.21	56470
P10719	ATPB_RAT	ATP synthase subunit beta, mitochondrial	Atp5b	-0.23	56318
P62630	EF1A1_RAT	Elongation factor 1-alpha 1	Eef1a1	-0.26	50082
Q63610	TPM3_RAT	Tropomyosin alpha-3 chain	Tpm3	-0.26	28989
Q4FZU2	K2C6A_RAT	Keratin, type II cytoskeletal 6A	Krt6a	-0.26	59213
P63102	1433Z_RAT	14-3-3 protein zeta/delta	Ywhaz	-0.26	27754
O35783	CALU_RAT	Calumenin	Calu	-0.27	36973
A7VJC2	ROA2_RAT	Heterogeneous nuclear ribonucleoproteins A2/B1	Hnrnpa2b1	-0.31	37455
P62963	PROF1_RAT	Profilin-1	Pfn1	-0.33	14948
P40307	PSB2_RAT	Proteasome subunit beta type-2	Psmb2	-0.36	22898
P20760	IGG2A_RAT	Ig gamma-2A chain C region	Igg-2a	-0.37	35163
P16617	PGK1_RAT	Phosphoglycerate kinase 1	Pgk1	-0.38	44510
P02650	APOE_RAT	Apolipoprotein E	Apoe	-0.39	35731
P13832	MRLCA_RAT	Myosin regulatory light chain RLC-A	Rlc-a	-0.40	19883
P06761	GRP78_RAT	78 kDa glucose-regulated protein	Hspa5	-0.48	72302
P04762	CATA_RAT	Catalase	Cat	-0.48	59719
P07335	KCRB_RAT	Creatine kinase B-type	Ckb	-0.50	42698
P05545	SPA3K_RAT	Serine protease inhibitor A3K	Serpina3k	-0.50	46532
O08590	AOC3_RAT	Membrane primary amine oxidase	Aoc3	-0.53	84928
P11884	ALDH2_RAT	Aldehyde dehydrogenase, mitochondrial	Aldh2	-0.53	56453
P62260	1433E_RAT	14-3-3 protein epsilon	Ywhae	-0.53	29155
P27139	CAH2_RAT	Carbonic anhydrase 2	Ca2	-0.53	29096
Q4V7C7	ARP3_RAT	Actin-related protein 3	Actr3	-0.53	47327
Q8CFN2	CDC42_RAT	Cell division control protein 42 homolog	Cdc42	-0.56	21245
P04797	G3P_RAT	Glyceraldehyde-3-phosphate dehydrogenase	Gapdh	-0.68	35805
Q8VHF5	CISY_RAT	Citrate synthase, mitochondrial	Cs	-0.68	51833
P43884	PLIN1_RAT	Perilipin-1	Plin1	-0.70	55579
Q9ER34	ACON_RAT	Aconitate hydratase, mitochondrial	Aco2	-0.71	85380
Q9EQX9	UBE2N_RAT	Ubiquitin-conjugating enzyme E2 N	Ube2n	-0.76	17113
P04764	ENOA_RAT	Alpha-enolase	Eno1	-0.77	47098

Supplemental Table C 4 - Proteins of epicardial adipose tissue identified in lean ZSF1

Entry	Entry name	Protein name	Gene name	MW (kDa)
P11951	CX6C2_RAT	Cytochrome c oxidase subunit 6C-2	Cox6c2	8449
P35171	CX7A2_RAT	Cytochrome c oxidase subunit 7A2, mitochondrial	Cox7a2	9347
Q7TQ16	QCR8_RAT	Cytochrome b-c1 complex subunit 8	Uqcrq	9843
P80254	DOPD_RAT	D-dopachrome decarboxylase	Ddt	13125
P47967	LEG5_RAT	Galectin-5	Lgals5	16186
P10888	COX41_RAT	Cytochrome c oxidase subunit 4 isoform 1, mitochondrial	Cox4i1	19502
B2RZ37	REEP5_RAT	Receptor expression-enhancing protein 5	Reep5	21417
P35704	PRDX2_RAT	Peroxiredoxin-2	Prdx2	21770
P29117	PPIF_RAT	Peptidyl-prolyl cis-trans isomerase F, mitochondrial	Ppif	21796
P31232	TAGL_RAT	Transgelin	Tagln	22588
P29410	KAD2_RAT	Adenylate kinase 2, mitochondrial	Ak2	26363
P19234	NDUV2_RAT	NADH dehydrogenase [ubiquinone] flavoprotein 2, mitochondrial	Ndufv2	27361
P09650	MCPT1_RAT	Mast cell protease 1	Mcpt1	28599
P20788	UCRI_RAT	Cytochrome b-c1 complex subunit Rieske, mitochondrial	Uqcrfs1	29427
Q497B0	NIT2_RAT	Omega-amidase NIT2	Nit2	30682
P23965	ECI1_RAT	Enoyl-CoA delta isomerase 1, mitochondrial	Eci1	32234
Q09073	ADT2_RAT	ADP/ATP translocase 2	Slc25a5	32880
P97521	MCAT_RAT	Mitochondrial carnitine/acylcarnitine carrier protein	Slc25a20	33132
P13086	SUCA_RAT	Succinyl-CoA ligase [ADP/GDP-forming] subunit alpha, mitochondrial	Suclg1	36125
Q62651	ECH1_RAT	Delta(3,5)-Delta(2,4)-dienoyl-CoA isomerase, mitochondrial	Ech1	36148
P04642	LDHA_RAT	L-lactate dehydrogenase A chain	Ldha	36427
O88989	MDHC_RAT	Malate dehydrogenase, cytoplasmic	Mdh1	36460
Q6QA69	ABHD5_RAT	1-acylglycerol-3-phosphate O-acyltransferase ABHD5	Abhd5	39079
Q924T8	CLTR1_RAT	Cysteinyl leukotriene receptor 1	Cysltr1	39117
Q561S0	NDUAA_RAT	NADH dehydrogenase [ubiquinone] 1 alpha subcomplex subunit 10, mitochondrial	Ndufa10	40468
P62738	ACTA_RAT	Actin, aortic smooth muscle	Acta2	41982
P09606	GLNA_RAT	Glutamine synthetase	Glul	42240
Q68FX0	IDH3B_RAT	Isocitrate dehydrogenase [NAD] subunit beta, mitochondrial	Idh3B	42327
Q5BK63	NDUA9_RAT	NADH dehydrogenase [ubiquinone] 1 alpha subcomplex subunit 9, mitochondrial	Ndufa9	42532
Q9EQP5	PRELP_RAT	Prolargin	Prelp	43152
P26284	ODPA_RAT	Pyruvate dehydrogenase E1 component subunit alpha, somatic form, mitochondrial	Pdha1	43199
P15651	ACADS_RAT	Short-chain specific acyl-CoA dehydrogenase, mitochondrial	Acads	44737
P12007	IVD_RAT	Isovaleryl-CoA dehydrogenase, mitochondrial	Ivd	46406
P08503	ACADM_RAT	Medium-chain specific acyl-CoA dehydrogenase, mitochondrial	Acadm	46526
Q01205	ODO2_RAT	Dihydrolipoyllysine-residue succinyltransferase component of 2-oxoglutarate dehydrogenase complex, mitochondrial	Dlst	48894
P68370	TBA1A_RAT	Tubulin alpha-1A chain	Tuba1a	50104

P56574	IDHP_RAT	Isocitrate dehydrogenase [NADP], mitochondrial	Idh2	50935
Q60587	ECHB_RAT	Trifunctional enzyme subunit beta, mitochondrial	Hadhb	51382
Q68FY0	QCR1_RAT	Cytochrome b-c1 complex subunit 1, mitochondrial	Uqcrc1	52815
Q6P6R2	DLDH_RAT	Dihydrolipoyl dehydrogenase, mitochondrial	Dld	54004
P43884	PLIN1_RAT	Perilipin-1	Plin1	55579
P11884	ALDH2_RAT	Aldehyde dehydrogenase, mitochondrial	Aldh2	56453
Q6IFW6	K1C10_RAT	Keratin, type I cytoskeletal 10	Krt10	56470
Q02253	MMSA_RAT	Methylmalonate-semialdehyde dehydrogenase [acylating], mitochondrial	Aldh6a1	57771
P07633	PCCB_RAT	Propionyl-CoA carboxylase beta chain, mitochondrial	Pccb	58589
Q4FZU2	K2C6A_RAT	Keratin, type II cytoskeletal 6A	Krt6a	59213
Q4V8H8	EHD2_RAT	EH domain-containing protein 2	Ehd2	61199
P10860	DHE3_RAT	Glutamate dehydrogenase 1, mitochondrial	Glud1	61377
P08461	ODP2_RAT	Dihydrolipoyllysine-residue acetyltransferase component of pyruvate dehydrogenase complex, mitochondrial	Dlat	67123
P50137	TKT_RAT	Transketolase	Tkt	67601
Q920L2	DHSA_RAT	Succinate dehydrogenase [ubiquinone] flavoprotein subunit, mitochondrial	Sdha	71570
P18886	CPT2_RAT	Carnitine O-palmitoyltransferase 2, mitochondrial	Cpt2	74063
P18163	ACSL1_RAT	Long-chain-fatty-acid--CoA ligase 1	Acsl1	78128
Q66HF1	NDUS1_RAT	NADH-ubiquinone oxidoreductase 75 kDa subunit, mitochondrial	Ndufs1	79362
P35571	GPDM_RAT	Glycerol-3-phosphate dehydrogenase, mitochondrial	Gpd2	80921
P02466	CO1A2_RAT	Collagen alpha-2(I) chain	Col1a2	129486
P52873	PYC_RAT	Pyruvate carboxylase, mitochondrial	Pc	129695
Q9WUJ3	MYOME_RAT	Myomegalin	Pde4dip	261881
B0LPN4	RYR2_RAT	Ryanodine receptor 2	Ryr2	562594

Supplemental Table C 5 - Proteins of epicardial adipose tissue identified in obese ZSF1

Entry	Entry name	Protein name	Gene name	MW (kDa)
P61959	SUMO2_RAT	Small ubiquitin-related modifier 2	Sumo2	10864
P06759	APOC3_RAT	Apolipoprotein C-III	Apoc3	11110
P20767	LAC2_RAT	Ig lambda-2 chain C region		11311
P62804	H4_RAT	Histone H4	Hist1h4b	11360
P19944	RLA1_RAT	60S acidic ribosomal protein P1	Rplp1	11491
Q5I0H3	SUMO1_RAT	Small ubiquitin-related modifier 1	Sumo1	11550
P07151	B2MG_RAT	Beta-2-microglobulin	B2m	13711
Q00715	H2B1_RAT	Histone H2B type 1		13982
P55797	APOC4_RAT	Apolipoprotein C-IV	Apoc4	14522
P62963	PROF1_RAT	Profilin-1	Pfn1	14948
P84245	H33_RAT	Histone H3.3	H3f3b	15319
Q80T18	GMFG_RAT	Glia maturation factor gamma	Gmfg	16769
Q3T1J1	IF5A1_RAT	Eukaryotic translation initiation factor 5A-1	Eif5a	16821
P13668	STMN1_RAT	Stathmin	Stmn1	17278

P41498	PPAC_RAT	Low molecular weight phosphotyrosine protein phosphatase	Acp1	18140
P01830	THY1_RAT	Thy-1 membrane glycoprotein	Thy1	18161
P45592	COF1_RAT	Cofilin-1	Cfl1	18521
Q7M0E3	DEST_RAT	Destrin	Dstn	18522
P31044	PEBP1_RAT	Phosphatidylethanolamine-binding protein 1	Pebp1	20788
P19132	FRIH_RAT	Ferritin heavy chain	Fth1	21113
Q8CFN2	CDC42_RAT	Cell division control protein 42 homolog	Cdc42	21245
Q6RUV5	RAC1_RAT	Ras-related C3 botulinum toxin substrate 1	Rac1	21436
P14630	APOM_RAT	Apolipoprotein M	Apom	21499
Q63716	PRDX1_RAT	Peroxiredoxin-1	Prdx1	22095
Q5XI73	GDIR1_RAT	Rho GDP-dissociation inhibitor 1	Arhgdia	23393
P24368	PPIB_RAT	Peptidyl-prolyl cis-trans isomerase B	Ppib	23788
P52925	HMGB2_RAT	High mobility group protein B2	Hmgb2	24144
P00502	GSTA1_RAT	Glutathione S-transferase alpha-1	Gsta1	25591
P48500	TPIS_RAT	Triosephosphate isomerase	Tpi1	26832
Q6MG61	CLIC1_RAT	Chloride intracellular channel protein 1	Clic1	26964
P63102	1433Z_RAT	14-3-3 protein zeta/delta	Ywhaz	27754
P68255	1433T_RAT	14-3-3 protein theta	Ywhaq	27761
P35213	1433B_RAT	14-3-3 protein beta/alpha	Ywhab	28037
P52555	ERP29_RAT	Endoplasmic reticulum resident protein 29	Erp29	28557
Q63610	TPM3_RAT	Tropomyosin alpha-3 chain	Tpm3	28989
P30009	MARCS_RAT	Myristoylated alanine-rich C-kinase substrate	Marcks	29777
P67779	PHB_RAT	Prohibitin	Phb	29802
P85973	PNPH_RAT	Purine nucleoside phosphorylase (PNP)	Pnp	32281
P38983	RSSA_RAT	40S ribosomal protein SA	Rpsa	32803
P26644	APOH_RAT	Beta-2-glycoprotein 1	Apoh	33175
P04256	ROA1_RAT	Heterogeneous nuclear ribonucleoprotein A1	Hnrnpa1	34191
P19945	RLA0_RAT	60S acidic ribosomal protein P0	Rplp0	34194
P07943	ALDR_RAT	Aldose reductase	Akr1b1	35774
P04797	G3P_RAT	Glyceraldehyde-3-phosphate dehydrogenase (GAPDH)	Gapdh	35805
P55260	ANXA4_RAT	Annexin A4	Anxa4	35826
P55159	PON1_RAT	Serum paraoxonase/arylesterase 1	Pon1	39333
P04897	GNAI2_RAT	Guanine nucleotide-binding protein G(i) subunit alpha-2	Gnai2	40473
Q9QX79	FETUB_RAT	Fetuin-B	Fetub	41506
P70473	AMACR_RAT	Alpha-methylacyl-CoA racemase	Amacr	41801
P68035	ACTC_RAT	Actin, alpha cardiac muscle 1	Actc1	41992
Q4V898	RBMX_RAT	RNA-binding motif protein, X chromosome	Rbmx	42232
P02651	APOA4_RAT	Apolipoprotein A-IV	Apoa4	44429
P31211	CBG_RAT	Corticosteroid-binding globulin	Serpina6	44642
Q794E4	HNRPF_RAT	Heterogeneous nuclear ribonucleoprotein F	Hnrnpf	45701
Q4V7C7	ARP3_RAT	Actin-related protein 3	Actr3	47327

O35254	GORS1_RAT	Golgi reassembly-stacking protein 1	Gorasp1	47643
Q5BJY9	K1C18_RAT	Keratin, type I cytoskeletal 18	Krt18	47732
P01048	KNT1_RAT	T-kininogen 1	Map1	47745
Q63081	PDIA6_RAT	Protein disulfide-isomerase A6	Pdia6	48143
P69897	TBB5_RAT	Tubulin beta-5 chain	Tubb5	49639
P62630	EF1A1_RAT	Elongation factor 1-alpha 1	Eef1a1	50082
Q6P9V9	TBA1B_RAT	Tubulin alpha-1B chain	Tuba1b	50120
Q4QRB4	TBB3_RAT	Tubulin beta-3 chain	Tubb3	50386
P50399	GDIB_RAT	Rab GDP dissociation inhibitor beta	Gdi2	50505
P02680	FIBG_RAT	Fibrinogen gamma chain	Fgg	50600
Q6IG12	K2C7_RAT	Keratin, type II cytoskeletal 7	Krt7	50678
P61980	HNRPK_RAT	Heterogeneous nuclear ribonucleoprotein K	Hnrnpk	50944
Q91ZN1	COR1A_RAT	Coronin-1A	Coro1a	51033
Q6IFV1	K1C14_RAT	Keratin, type I cytoskeletal 14	Krt14	52651
Q10758	K2C8_RAT	Keratin, type II cytoskeletal 8	Krt8	53985
P00689	AMYP_RAT	Pancreatic alpha-amylase	Amy2	57141
P28480	TCPA_RAT	T-complex protein 1 subunit alpha	Tcp1	60322
Q9EQ25	S38A4_RAT	Sodium-coupled neutral amino acid transporter 4	Slc38a4	60573
Q6P6Q2	K2C5_RAT	Keratin, type II cytoskeletal 5	Krt5	61788
Q3KR86	IMMT_RAT	MICOS complex subunit Mic60	Immt	67135
Q32PX7	FUBP1_RAT	Far upstream element-binding protein 1	Fubp1	67155
P35565	CALX_RAT	Calnexin	Canx	67213
O35763	MOES_RAT	Moesin	Msn	67697
P08934	KNG1_RAT	Kininogen-1	Kng1	70889
P06761	GRP78_RAT	78 kDa glucose-regulated protein	Hspa5	72302
Q62826	HNRPM_RAT	Heterogeneous nuclear ribonucleoprotein M	Hnrnpm	73733
P34058	HS90B_RAT	Heat shock protein HSP 90-beta	Hsp90ab1	83229
P82995	HS90A_RAT	Heat shock protein HSP 90-alpha	Hsp90aa1	84762
P06399	FIBA_RAT	Fibrinogen alpha chain	Fga	86632
O08629	TIF1B_RAT	Transcription intermediary factor 1-beta	Trim28	88900
Q01177	PLMN_RAT	Plasminogen	Plg	90477
Q66HD0	ENPL_RAT	Endoplasmin	Hsp90b1	92713
P05197	EF2_RAT	Elongation factor 2	Eef2	95223
Q63416	ITIH3_RAT	Inter-alpha-trypsin inhibitor heavy chain H3	Itih3	99036
Q9QXQ0	ACTN4_RAT	Alpha-actinin-4	Actn4	104849
Q5U300	UBA1_RAT	Ubiquitin-like modifier-activating enzyme 1	Uba1	117713
Q1JU68	EIF3A_RAT	Eukaryotic translation initiation factor 3 subunit A	Eif3a	163097
P14046	A1I3_RAT	Alpha-1-inhibitor 3	A1i3	163670
Q03626	MUG1_RAT	Murinoglobulin-1	Mug1	165221
P01026	CO3_RAT	Complement C3	C3	186342
Q62812	MYH9_RAT	Myosin-9	Myh9	226197
P04937	FINC_RAT	Fibronectin	Fn1	272341
P58365	CAD23_RAT	Cadherin-23	Cdh23	365230
P30427	PLEC_RAT	Plectin	Plec	533214

Supplemental Table C 6 - Proteins of epicardial adipose tissue common between obese and lean ZSF1 model. Values above zero correspond to values of up-regulated proteins in obese ZSF1; Values below zero correspond to values down-regulated proteins in obese ZSF1.

Entry	Entry Name	Protein name	Gene name	emPAI ratio	MW (kDa)
P14480	FIBB_RAT	Fibrinogen beta chain	Fgb	4.98	54201
A7VJC2	ROA2_RAT	Heterogeneous nuclear ribonucleoproteins A2/B1	Hnrnpa2b1	3.26	37455
Q63041	A1M_RAT	Alpha-1-macroglobulin	A1m	2.32	167019
P17475	A1AT_RAT	Alpha-1-antiproteinase	Serpina1	2.24	46107
P20059	HEMO_RAT	Hemopexin	Hpx	2.20	51318
P02770	ALBU_RAT	Serum albumin	Alb	2.12	68686
P04639	APOA1_RAT	Apolipoprotein A-I	Apoa1	2.09	30043
P12346	TRFE_RAT	Serotransferrin	Tf	2.08	76346
P48037	ANXA6_RAT	Annexin A6	Anxa6	1.89	75706
P02793	FRIL1_RAT	Ferritin light chain 1	Ftl1	1.78	20736
P05545	SPA3K_RAT	Serine protease inhibitor A3K	Serpina3k	1.75	46532
P11598	PDIA3_RAT	Protein disulfide-isomerase A3	Pdia3	1.66	56588
P0C169	H2A1C_RAT	Histone H2A type 1-C		1.43	14097
P26772	CH10_RAT	10 kDa heat shock protein, mitochondrial	Hspe1	1.35	10895
P14141	CAH3_RAT	Carbonic anhydrase 3	Car3	1.22	29413
P51886	LUM_RAT	Lumican	Lum	1.19	38255
P04762	CATA_RAT	Catalase	Cat	1.17	59719
P60711	ACTB_RAT	Actin, cytoplasmic 1	Actb	1.14	41710
Q8R431	MGLL_RAT	Monoglyceride lipase	Mgll	1.04	33478
P62982	RS27A_RAT	Ubiquitin-40S ribosomal protein S27a	Rps27a	0.93	17939
Q6P9T8	TBB4B_RAT	Tubulin beta-4B chain	Tubb4b	0.89	49769
P02454	CO1A1_RAT	Collagen alpha-1(I) chain	Col1a1	0.81	137869
P02650	APOE_RAT	Apolipoprotein E	Apoe	0.69	35731
P23764	GPX3_RAT	Glutathione peroxidase 3	Gpx3	0.67	25409
Q6URK4	ROA3_RAT	Heterogeneous nuclear ribonucleoprotein A3	Hnrnpa3	0.66	39628
P29457	SERPH_RAT	Serpin H1	Serpinh1	0.63	46488
Q07936	ANXA2_RAT	Annexin A2	Anxa2	0.50	38654
P63018	HSP7C_RAT	Heat shock cognate 71 kDa protein	Hspa8	0.48	70827
P42930	HSPB1_RAT	Heat shock protein beta-1	Hspb1	0.47	22879
P10719	ATPB_RAT	ATP synthase subunit beta, mitochondrial	Atp5b	0.45	56318
P09006	SPA3N_RAT	Serine protease inhibitor A3N	Serpina3n	0.44	46622
P14668	ANXA5_RAT	Annexin A5	Anxa5	0.43	35722
P18418	CALR_RAT	Calreticulin	Calr	0.42	47966
P13635	CERU_RAT	Ceruloplasmin	Cp	0.39	120764
P85125	PTRF_RAT	Polymerase I and transcript release factor	Ptrf	0.33	43882
P16617	PGK1_RAT	Phosphoglycerate kinase 1	Pgk1	0.31	44510
P04764	ENOA_RAT	Alpha-enolase	Eno1	0.27	47098
P07632	SODC_RAT	Superoxide dismutase [Cu-Zn]	Sod1	0.13	15902
O35077	GPDA_RAT	Glycerol-3-phosphate dehydrogenase [NAD(+)], cytoplasmic	Gpd1	0.13	37428
P58775	TPM2_RAT	Tropomyosin beta chain	Tpm2	0.08	32817
P10818	CX6A1_RAT	Cytochrome c oxidase subunit 6A1, mitochondrial	Cox6a1	0.00	12293
P12075	COX5B_RAT	Cytochrome c oxidase subunit 5B, mitochondrial	Cox5b	0.00	13906

P70623	FABP4_RAT	Fatty acid-binding protein, adipocyte	Fabp4	0.00	14699
P11762	LEG1_RAT	Galectin-1	Lgals1	0.00	14847
P62161	CALM_RAT	Calmodulin	Calm1	0.00	16827
Q64119	MYL6_RAT	Myosin light polypeptide 6	Myl6	0.00	16964
P19804	NDKB_RAT	Nucleoside diphosphate kinase B	Nme2	0.00	17272
Q64122	MYL9_RAT	Myosin regulatory light polypeptide 9	Myl9	0.00	19708
P13832	MRLCA_RAT	Myosin regulatory light chain RLC-A	Rlc-a	0.00	19883
P04906	GSTP1_RAT	Glutathione S-transferase P	Gstp1	0.00	23424
P61983	1433G_RAT	14-3-3 protein gamma	Ywhag	0.00	28285
P20760	IGG2A_RAT	Ig gamma-2A chain C region	Igg-2a	0.00	35163
Q64591	DECR_RAT	2,4-dienoyl-CoA reductase, mitochondrial	Decr1	0.00	36110
P07150	ANXA1_RAT	Annexin A1	Anxa1	0.00	38805
P16036	MPCP_RAT	Phosphate carrier protein, mitochondrial	Slc25a3	0.00	39419
P85834	EFTU_RAT	Elongation factor Tu, mitochondrial	Tufm	0.00	49491
P31000	VIME_RAT	Vimentin	Vim	0.00	53700
P15999	ATPA_RAT	ATP synthase subunit alpha, mitochondrial	Atp5a1	0.00	59717
Q6UPE1	ETFD_RAT	Electron transfer flavoprotein-ubiquinone oxidoreductase, mitochondrial	Etfdh	0.00	68155
Q5BJQ0	ADCK3_RAT	Chaperone activity of bc1 complex-like, mitochondrial	Adck3	0.00	72180
Q68FP1	GELS_RAT	Gelsolin	Gsn	0.00	86014
P08649	CO4_RAT	Complement C4	C4	0.00	192042
P16086	SPTN1_RAT	Spectrin alpha chain, non-erythrocytic 1	Sptan1	-0.22	284462
Q68FU3	ETFB_RAT	Electron transfer flavoprotein subunit beta	Etfb	-0.31	27670
P05065	ALDOA_RAT	Fructose-bisphosphate aldolase A	Aldoa	-0.37	39327
P48721	GRP75_RAT	Stress-70 protein, mitochondrial	Hspa9	-0.45	73812
P01946	HBA_RAT	Hemoglobin subunit alpha-1/2	Hba1	-0.50	15319
O08590	AOC3_RAT	Membrane primary amine oxidase	Aoc3	-0.55	84928
P24090	FETUA_RAT	Alpha-2-HS-glycoprotein	Ahsg	-0.62	37958
O55171	ACOT2_RAT	Acyl-coenzyme A thioesterase 2, mitochondrial	Acot2	-0.68	49670
P10111	PPIA_RAT	Peptidyl-prolyl cis-trans isomerase A	Ppia	-0.72	17863
P21913	DHSB_RAT	Succinate dehydrogenase [ubiquinone] iron-sulfur subunit, mitochondrial	Sdhb	-0.73	31809
Q6IG01	K2C1B_RAT	Keratin, type II cytoskeletal 1b	Krt77	-0.78	57220
P17764	THIL_RAT	Acetyl-CoA acetyltransferase, mitochondrial	Acat1	-0.80	44666
P05943	S10AA_RAT	Protein S100-A10	S100a10	-0.82	11068
P02091	HBB1_RAT	Hemoglobin subunit beta-1	Hbb	-0.88	15969
P13437	THIM_RAT	3-ketoacyl-CoA thiolase, mitochondrial	Acaa2	-0.89	41844
Q99NA5	IDH3A_RAT	Isocitrate dehydrogenase [NAD] subunit alpha, mitochondrial	Idh3a	-0.93	39588
P04276	VTDB_RAT	Vitamin D-binding protein	Gc	-1.00	53509
P14604	ECHM_RAT	Enoyl-CoA hydratase, mitochondrial	Echs1	-1.08	31496
Q68FT1	COQ9_RAT	Ubiquinone biosynthesis protein COQ9, mitochondrial	Coq9	-1.09	35123
P04636	MDHM_RAT	Malate dehydrogenase, mitochondrial	Mdh2	-1.11	35661
B0BNN3	CAH1_RAT	Carbonic anhydrase 1	Ca1	-1.15	28282
P14408	FUMH_RAT	Fumarate hydratase, mitochondrial	Fh	-1.15	54429
Q9R063	PRDX5_RAT	Peroxiredoxin-5, mitochondrial	Prdx5	-1.17	22165
Q9WVK7	HCDH_RAT	Hydroxyacyl-coenzyme A dehydrogenase, mitochondrial	Hadh	-1.20	34426

P02767	TTHY_RAT	Transthyretin	Ttr	-1.25	15710
Q8VHF5	CISY_RAT	Citrate synthase, mitochondrial	Cs	-1.28	51833
P11517	HBB2_RAT	Hemoglobin subunit beta-2		-1.34	15972
Q64428	ECHA_RAT	Trifunctional enzyme subunit alpha, mitochondrial	Hadha	-1.38	82613
P32551	QCR2_RAT	Cytochrome b-c1 complex subunit 2, mitochondrial	Uqcrc2	-1.50	48366
P27139	CAH2_RAT	Carbonic anhydrase 2	Ca2	-1.64	29096
P00173	CYB5_RAT	Cytochrome b5	Cyb5a	-1.71	15346
P15650	ACADL_RAT	Long-chain specific acyl-CoA dehydrogenase, mitochondrial	Acadl	-1.71	47842
P63039	CH60_RAT	60 kDa heat shock protein, mitochondrial	Hspd1	-1.84	60917
P04633	UCP1_RAT	Mitochondrial brown fat uncoupling protein 1	Ucp1	-1.91	33190
P11240	COX5A_RAT	Cytochrome c oxidase subunit 5A, mitochondrial	Cox5a	-2.04	16119
P45953	ACADV_RAT	Very long-chain specific acyl-CoA dehydrogenase, mitochondrial	Acadvl	-2.19	70705
P62898	CYC_RAT	Cytochrome c, somatic	Cycs	-2.25	11598
P13803	ETFA_RAT	Electron transfer flavoprotein subunit alpha, mitochondrial	Etfa	-2.30	34929
Q9ER34	ACON_RAT	Aconitate hydratase, mitochondrial	Aco2	-2.38	85380
Q5XI78	ODO1_RAT	2-oxoglutarate dehydrogenase, mitochondrial	Ogdh	-2.82	116221

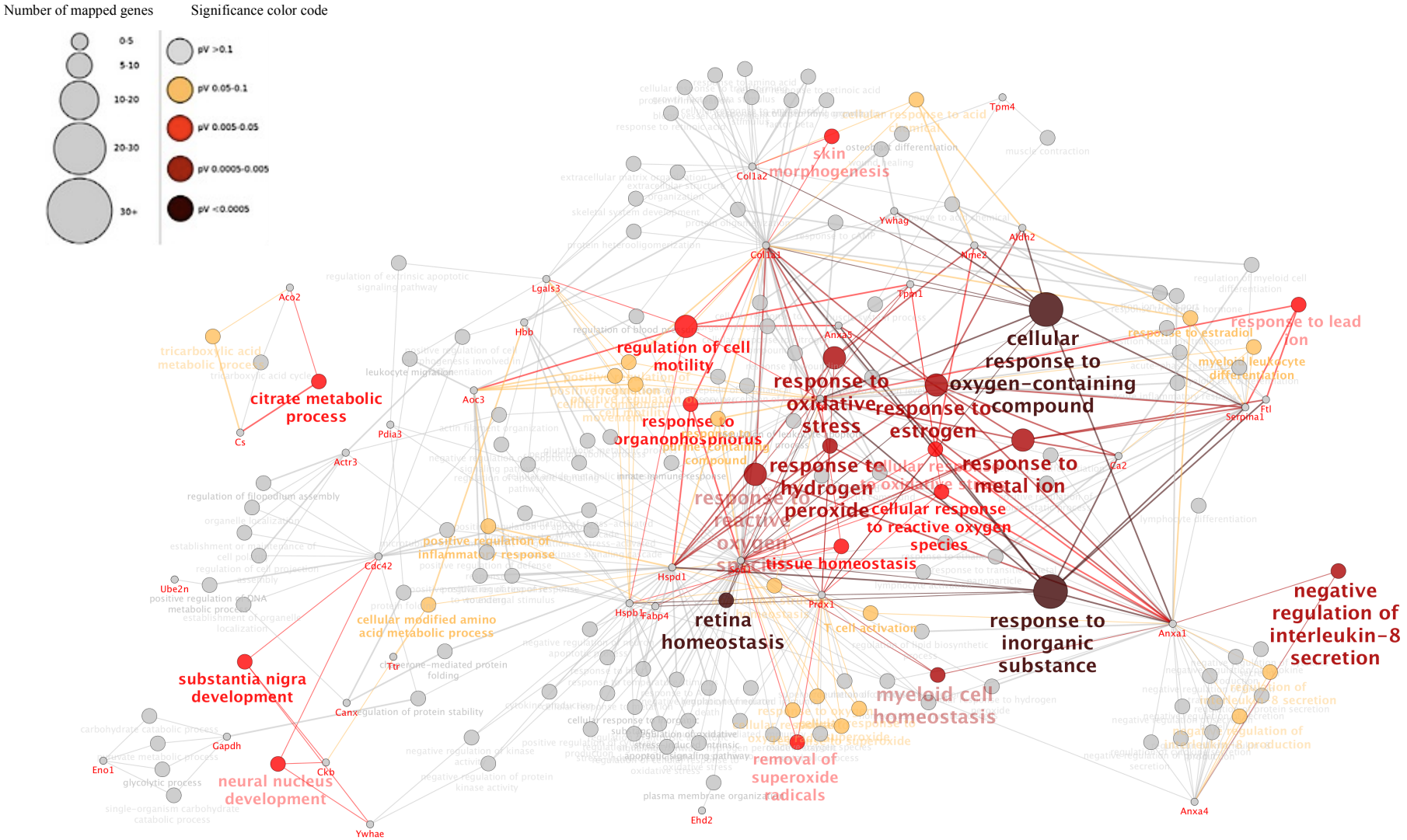

Supplemental Figure C 1 - ClueGo and CluePedia significance analysis of protein-protein interaction considering common proteins present in visceral adipose tissue of obese and lean ZSF1 rat (based on emPAI values).

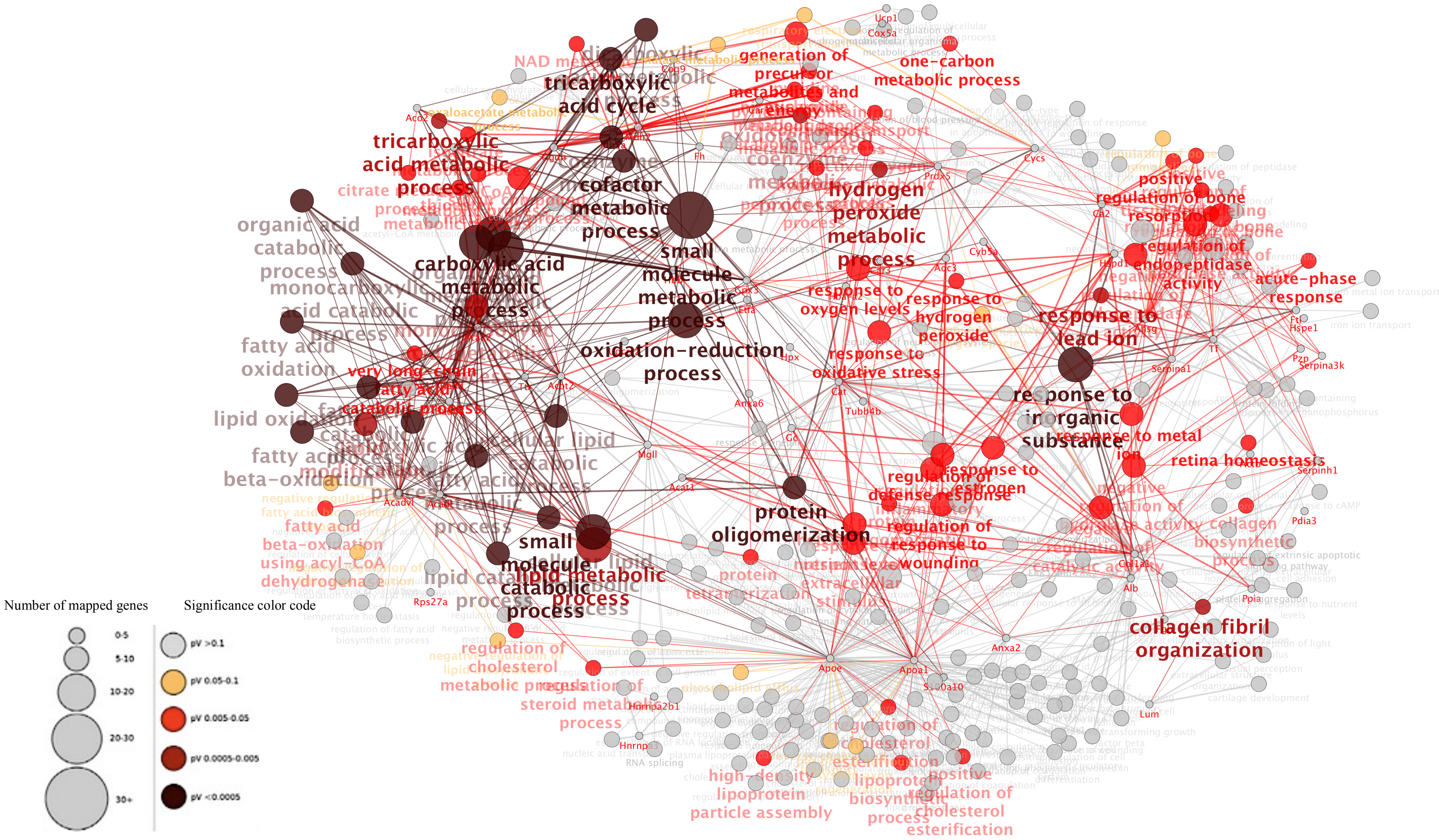

Supplemental Figure C 2 - ClueGo and CluePedia significance analysis of protein-protein interaction considering common proteins present in epicardial adipose tissue of obese and lean ZSF1 rat (based on emPAI values).

Appendix D – Characterization and comparison of epicardial and visceral adipose tissue proteome

Supplemental Table D 1 - Proteins of common between epicardial and visceral adipose tissue in lean ZSF1 model. Values above zero correspond to values of up-regulated proteins in epicardial adipose tissue in lean ZSF1; Values below zero correspond to values up-regulated in visceral adipose tissue in lean ZSF1

Entry	Entry name	Protein name	Gene name	emPAI Ratio
Q9ER34	ACON_RAT	Aconitate hydratase, mitochondrial	Aco2	11.53
P63039	CH60_RAT	60 kDa heat shock protein, mitochondrial	Hspd1	7.71
P02091	HBB1_RAT	Hemoglobin subunit beta-1	Hbb	5.56
P11517	HBB2_RAT	Hemoglobin subunit beta-2		5.51
P04636	MDHM_RAT	Malate dehydrogenase, mitochondrial	Mdh2	4.89
P62898	CYC_RAT	Cytochrome c, somatic	Cycs	4.50
P17764	THIL_RAT	Acetyl-CoA acetyltransferase, mitochondrial	Acat1	4.50
Q8VHF5	CISY_RAT	Citrate synthase, mitochondrial	Cs	3.00
P19234	NDUV2_RAT	NADH dehydrogenase [ubiquinone] flavoprotein 2, mitochondrial	Ndufv2	2.59
P48721	GRP75_RAT	Stress-70 protein, mitochondrial	Hspa9	2.33
P12346	TRFE_RAT	Serotransferrin	Tf	1.95
P19804	NDKB_RAT	Nucleoside diphosphate kinase B	Nme2	1.64
P14604	ECHM_RAT	Enoyl-CoA hydratase, mitochondrial	Echs1	1.40
P05065	ALDOA_RAT	Fructose-bisphosphate aldolase A	Aldoa	1.00
P01946	HBA_RAT	Hemoglobin subunit alpha-1/2	Hba1	0.88
P16086	SPTN1_RAT	Spectrin alpha chain, non-erythrocytic 1	Sptan1	0.75
P50137	TKT_RAT	Transketolase	Tkt	0.71
P27139	CAH2_RAT	Carbonic anhydrase 2	Ca2	0.65
P18163	ACSL1_RAT	Long-chain-fatty-acid--CoA ligase 1	Acsl1	0.48
P02466	CO1A2_RAT	Collagen alpha-2(I) chain	Col1a2	0.33
P02454	CO1A1_RAT	Collagen alpha-1(I) chain	Col1a1	0.33
P70623	FABP4_RAT	Fatty acid-binding protein, adipocyte	Fabp4	0.20
Q68FP1	GELS_RAT	Gelsolin	Gsn	0.20
P62161	CALM_RAT	Calmodulin	Calm1	0.19
P05943	S10AA_RAT	Protein S100-A10	S100a10	0.18
P02767	TTHY_RAT	Transthyretin	Ttr	0.17
P07632	SODC_RAT	Superoxide dismutase [Cu-Zn]	Sod1	0.17
P85125	PTRF_RAT	Polymerase I and transcript release factor	Ptrf	0.16
P26772	CH10_RAT	10 kDa heat shock protein, mitochondrial	Hspe1	0.15
P35704	PRDX2_RAT	Peroxiredoxin-2	Prdx2	0.14
P42930	HSPB1_RAT	Heat shock protein beta-1	Hspb1	0.14
P11884	ALDH2_RAT	Aldehyde dehydrogenase, mitochondrial	Aldh2	0.09
P31000	VIME_RAT	Vimentin	Vim	0.07
B0LPN4	RYR2_RAT	Ryanodine receptor 2	Ryr2	0.00
P00173	CYB5_RAT	Cytochrome b5	Cyb5a	-0.06

P16617	PGK1_RAT	Phosphoglycerate kinase 1	Pgk1	-0.07
O08590	AOC3_RAT	Membrane primary amine oxidase	Aoc3	-0.08
P61983	1433G_RAT	14-3-3 protein gamma	Ywhag	-0.14
P10111	PPIA_RAT	Peptidyl-prolyl cis-trans isomerase A	Ppia	-0.16
P17475	A1AT_RAT	Alpha-1-antiproteinase	Serpina1	-0.18
P63018	HSP7C_RAT	Heat shock cognate 71 kDa protein	Hspa8	-0.18
P04764	ENOA_RAT	Alpha-enolase	Eno1	-0.18
P02770	ALBU_RAT	Serum albumin	Alb	-0.20
P29457	SERPH_RAT	Serpin H1	Serpinh1	-0.27
P20760	IGG2A_RAT	Ig gamma-2A chain C region	Igg-2a	-0.27
Q4V8H8	EHD2_RAT	EH domain-containing protein 2	Ehd2	-0.27
P10860	DHE3_RAT	Glutamate dehydrogenase 1, mitochondrial	Glud1	-0.27
P62738	ACTA_RAT	Actin, aortic smooth muscle	Acta2	-0.28
P02650	APOE_RAT	Apolipoprotein E	Apoe	-0.30
Q6QA69	ABHD5_RAT	1-acylglycerol-3-phosphate O-acyltransferase ABHD5	Abhd5	-0.30
P04906	GSTP1_RAT	Glutathione S-transferase P	Gstp1	-0.30
Q6P9T8	TBB4B_RAT	Tubulin beta-4B chain	Tubb4b	-0.31
Q4FZU2	K2C6A_RAT	Keratin, type II cytoskeletal 6A	Krt6a	-0.32
P68370	TBA1A_RAT	Tubulin alpha-1A chain	Tuba1a	-0.34
P60711	ACTB_RAT	Actin, cytoplasmic 1	Actb	-0.35
P18418	CALR_RAT	Calreticulin	Calr	-0.35
P04639	APOA1_RAT	Apolipoprotein A-I	Apoa1	-0.36
P10719	ATPB_RAT	ATP synthase subunit beta, mitochondrial	Atp5b	-0.36
P20059	HEMO_RAT	Hemopexin	Hpx	-0.44
Q8R431	MGLL_RAT	Monoglyceride lipase	Mgll	-0.45
P05545	SPA3K_RAT	Serine protease inhibitor A3K	Serpina3k	-0.45
Q9EQP5	PRELP_RAT	Prolargin	Prelp	-0.45
P11598	PDIA3_RAT	Protein disulfide-isomerase A3	Pdia3	-0.47
P14668	ANXA5_RAT	Annexin A5	Anxa5	-0.48
Q64122	MYL9_RAT	Myosin regulatory light polypeptide 9	Myl9	-0.48
P04642	LDHA_RAT	L-lactate dehydrogenase A chain	Ldha	-0.48
O88989	MDHC_RAT	Malate dehydrogenase, cytoplasmic	Mdh1	-0.48
P02793	FRIL1_RAT	Ferritin light chain 1	Ftl1	-0.49
Q64119	MYL6_RAT	Myosin light polypeptide 6	Myl6	-0.52
P62982	RS27A_RAT	Ubiquitin-40S ribosomal protein S27a	Rps27a	-0.54
P04762	CATA_RAT	Catalase	Cat	-0.58
Q6IFW6	K1C10_RAT	Keratin, type I cytoskeletal 10	Krt10	-0.58
Q07936	ANXA2_RAT	Annexin A2	Anxa2	-0.61
P51886	LUM_RAT	Lumican	Lum	-0.62
P15999	ATPA_RAT	ATP synthase subunit alpha, mitochondrial	Atp5a1	-0.67
P43884	PLIN1_RAT	Perilipin-1	Plin1	-0.67
P58775	TPM2_RAT	Tropomyosin beta chain	Tpm2	-0.68
P13832	MRLCA_RAT	Myosin regulatory light chain RLC-A	Rlc-a	-0.70

P48037	ANXA6_RAT	Annexin A6	Anxa6	-0.73
P0C169	H2A1C_RAT	Histone H2A type 1-C	0	-0.74
A7VJC2	ROA2_RAT	Heterogeneous nuclear ribonucleoproteins A2/B1	Hnrnpa2b1	-0.76
P31232	TAGL_RAT	Transgelin	Tagln	-0.79
P11762	LEG1_RAT	Galectin-1	Lgals1	-0.82
P07150	ANXA1_RAT	Annexin A1	Anxa1	-0.82
P14141	CAH3_RAT	Carbonic anhydrase 3	Car3	-0.84

Supplemental Table D 2 - Proteins of common between epicardial and visceral adipose tissue in obese ZSF1 model. Values above zero correspond to values of up-regulated proteins in epicardial adipose tissue in obese ZSF1; Values below zero correspond to values up-regulated in visceral adipose tissue in obese ZSF1

Entry	Entry name	Protein name	Gene name	emPAI Ratio
Q9ER34	ACON_RAT	Aconitate hydratase, mitochondrial	Aco2	7.20
Q8VHF5	CISY_RAT	Citrate synthase, mitochondrial	Cs	4.11
P04764	ENOA_RAT	Alpha-enolase	Eno1	3.35
P05545	SPA3K_RAT	Serine protease inhibitor A3K	Serpina3k	2.70
Q99NA5	IDH3A_RAT	Isocitrate dehydrogenase [NAD] subunit alpha, mitochondrial	Idh3a	2.67
P12346	TRFE_RAT	Serotransferrin	Tf	2.52
A7VJC2	ROA2_RAT	Heterogeneous nuclear ribonucleoproteins A2/B1	Hnrnpa2b1	2.28
Q62812	MYH9_RAT	Myosin-9	Myh9	2.25
P69897	TBB5_RAT	Tubulin beta-5 chain	Tubb5	2.13
P04636	MDHM_RAT	Malate dehydrogenase, mitochondrial	Mdh2	1.72
P04797	G3P_RAT	Glyceraldehyde-3-phosphate dehydrogenase (GAPDH)	Gapdh	1.58
P11517	HBB2_RAT	Hemoglobin subunit beta-2		1.57
P20059	HEMO_RAT	Hemopexin	Hpx	1.56
P02770	ALBU_RAT	Serum albumin	Alb	1.46
P09006	SPA3N_RAT	Serine protease inhibitor A3N	Serpina3n	1.30
P04639	APOA1_RAT	Apolipoprotein A-I	Apoa1	1.10
Q64428	ECHA_RAT	Trifunctional enzyme subunit alpha, mitochondrial	Hadha	1.06
P02091	HBB1_RAT	Hemoglobin subunit beta-1	Hbb	1.01
P16617	PGK1_RAT	Phosphoglycerate kinase 1	Pgk1	0.86
P04762	CATA_RAT	Catalase	Cat	0.85
P02650	APOE_RAT	Apolipoprotein E	Apoe	0.85
P17475	A1AT_RAT	Alpha-1-antiproteinase	Serpina1	0.82
P07943	ALDR_RAT	Aldose reductase	Akr1b1	0.77
Q6P9V9	TBA1B_RAT	Tubulin alpha-1B chain	Tuba1b	0.67
P63039	CH60_RAT	60 kDa heat shock protein, mitochondrial	Hspd1	0.55
Q4V7C7	ARP3_RAT	Actin-related protein 3	Actr3	0.53
P85125	PTRF_RAT	Polymerase I and transcript release factor	Ptrf	0.45
P06761	GRP78_RAT	78 kDa glucose-regulated protein	Hspa5	0.37
O08590	AOC3_RAT	Membrane primary amine oxidase	Aoc3	0.32
P01946	HBA_RAT	Hemoglobin subunit alpha-1/2	Hba1	0.32
Q68FP1	GELS_RAT	Gelsolin	Gsn	0.20

P48500	TPIS_RAT	Triosephosphate isomerase	Tpi1	0.20
P62161	CALM_RAT	Calmodulin	Calm1	0.19
P24090	FETUA_RAT	Alpha-2-HS-glycoprotein	Ahsg	0.17
P62898	CYC_RAT	Cytochrome c, somatic	Cycs	0.16
P20760	IGG2A_RAT	Ig gamma-2A chain C region	Igg-2a	0.15
P13803	ETFA_RAT	Electron transfer flavoprotein subunit alpha, mitochondrial	Etfa	0.15
P05065	ALDOA_RAT	Fructose-bisphosphate aldolase A	Aldoa	0.15
P10719	ATPB_RAT	ATP synthase subunit beta, mitochondrial	Atp5b	0.14
Q3T1J1	IF5A1_RAT	Eukaryotic translation initiation factor 5A-1	Eif5a	0.14
Q8R431	MGLL_RAT	Monoglyceride lipase	Mgll	0.14
Q8CFN2	CDC42_RAT	Cell division control protein 42 homolog	Cdc42	0.14
Q6RUV5	RAC1_RAT	Ras-related C3 botulinum toxin substrate 1	Rac1	0.14
Q6P9T8	TBB4B_RAT	Tubulin beta-4B chain	Tubb4b	0.14
P14604	ECHM_RAT	Enoyl-CoA hydratase, mitochondrial	Echs1	0.13
P19132	FRIH_RAT	Ferritin heavy chain	Fth1	0.13
P27139	CAH2_RAT	Carbonic anhydrase 2	Ca2	0.13
Q9QX79	FETUB_RAT	Fetuin-B	Fetub	0.09
Q66HD0	ENPL_RAT	Endoplasmin	Hsp90b1	0.00
P58365	CAD23_RAT	Cadherin-23	Cdh23	0.00
P48037	ANXA6_RAT	Annexin A6	Anxa6	0.00
P02454	CO1A1_RAT	Collagen alpha-1(I) chain	Col1a1	0.00
Q5XI73	GDIR1_RAT	Rho GDP-dissociation inhibitor 1	Arhgdia	-0.07
O35077	GPDA_RAT	Glycerol-3-phosphate dehydrogenase [NAD(+)], cytoplasmic	Gpd1	-0.11
P63018	HSP7C_RAT	Heat shock cognate 71 kDa protein	Hspa8	-0.11
P51886	LUM_RAT	Lumican	Lum	-0.13
P18418	CALR_RAT	Calreticulin	Calr	-0.14
P35565	CALX_RAT	Calnexin	Canx	-0.14
Q63081	PDIA6_RAT	Protein disulfide-isomerase A6	Pdia6	-0.18
P11598	PDIA3_RAT	Protein disulfide-isomerase A3	Pdia3	-0.20
P70623	FABP4_RAT	Fatty acid-binding protein, adipocyte	Fabp4	-0.24
P31000	VIME_RAT	Vimentin	Vim	-0.24
P07632	SODC_RAT	Superoxide dismutase [Cu-Zn]	Sod1	-0.26
P62982	RS27A_RAT	Ubiquitin-40S ribosomal protein S27a	Rps27a	-0.27
P62630	EF1A1_RAT	Elongation factor 1-alpha 1	Eef1a1	-0.29
P02793	FRIL1_RAT	Ferritin light chain 1	Ftl1	-0.30
P04906	GSTP1_RAT	Glutathione S-transferase P	Gstp1	-0.30
P42930	HSPB1_RAT	Heat shock protein beta-1	Hspb1	-0.32
P19804	NDKB_RAT	Nucleoside diphosphate kinase B	Nme2	-0.32
P63102	1433Z_RAT	14-3-3 protein zeta/delta	Ywhaz	-0.35
Q10758	K2C8_RAT	Keratin, type II cytoskeletal 8	Krt8	-0.38
P08649	CO4_RAT	Complement C4	C4	-0.40
P35213	1433B_RAT	14-3-3 protein beta/alpha	Ywhab	-0.47
P55260	ANXA4_RAT	Annexin A4	Anxa4	-0.48

Q64122	MYL9_RAT	Myosin regulatory light polypeptide 9	Myl9	-0.48
Q7M0E3	DEST_RAT	Destrin	Dstn	-0.48
P61983	1433G_RAT	14-3-3 protein gamma	Ywhag	-0.48
P85973	PNPH_RAT	Purine nucleoside phosphorylase (PNP)	Pnp	-0.48
P10111	PPIA_RAT	Peptidyl-prolyl cis-trans isomerase A	Ppia	-0.49
P24368	PPIB_RAT	Peptidyl-prolyl cis-trans isomerase B	Ppib	-0.50
P13832	MRLCA_RAT	Myosin regulatory light chain RLC-A	Rlc-a	-0.50
Q64119	MYL6_RAT	Myosin light polypeptide 6	Myl6	-0.52
P15999	ATPA_RAT	ATP synthase subunit alpha, mitochondrial	Atp5a1	-0.60
Q07936	ANXA2_RAT	Annexin A2	Anxa2	-0.62
P52555	ERP29_RAT	Endoplasmic reticulum resident protein 29	Erp29	-0.65
Q63716	PRDX1_RAT	Peroxiredoxin-1	Prdx1	-0.66
P68255	1433T_RAT	14-3-3 protein theta	Ywhaq	-0.68
P14141	CAH3_RAT	Carbonic anhydrase 3	Car3	-0.68
P00173	CYB5_RAT	Cytochrome b5	Cyb5a	-0.71
Q63610	TPM3_RAT	Tropomyosin alpha-3 chain	Tpm3	-0.71
P02767	TTHY_RAT	Transthyretin	Ttr	-0.72
P58775	TPM2_RAT	Tropomyosin beta chain	Tpm2	-0.76
P14668	ANXA5_RAT	Annexin A5	Anxa5	-0.77
P62963	PROF1_RAT	Profilin-1	Pfn1	-0.82
P11762	LEG1_RAT	Galectin-1	Lgals1	-0.88
P07150	ANXA1_RAT	Annexin A1	Anxa1	-0.91

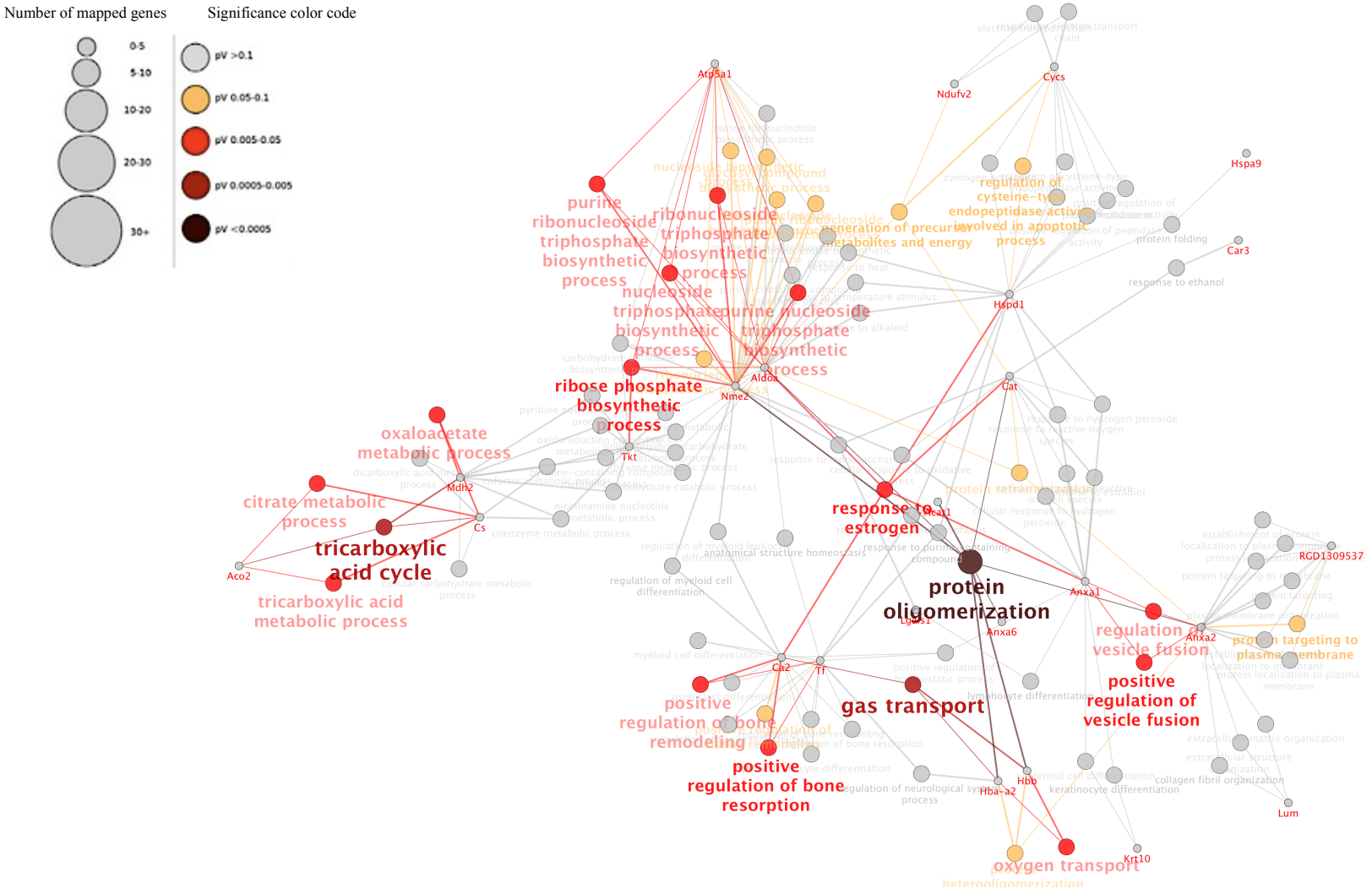

Supplemental Figure D 1 - ClueGo and CluePedia significance analysis of protein-protein interaction considering proteins present in epicardial and visceral adipose tissue of lean ZSF1 rat (based on emPAI values).

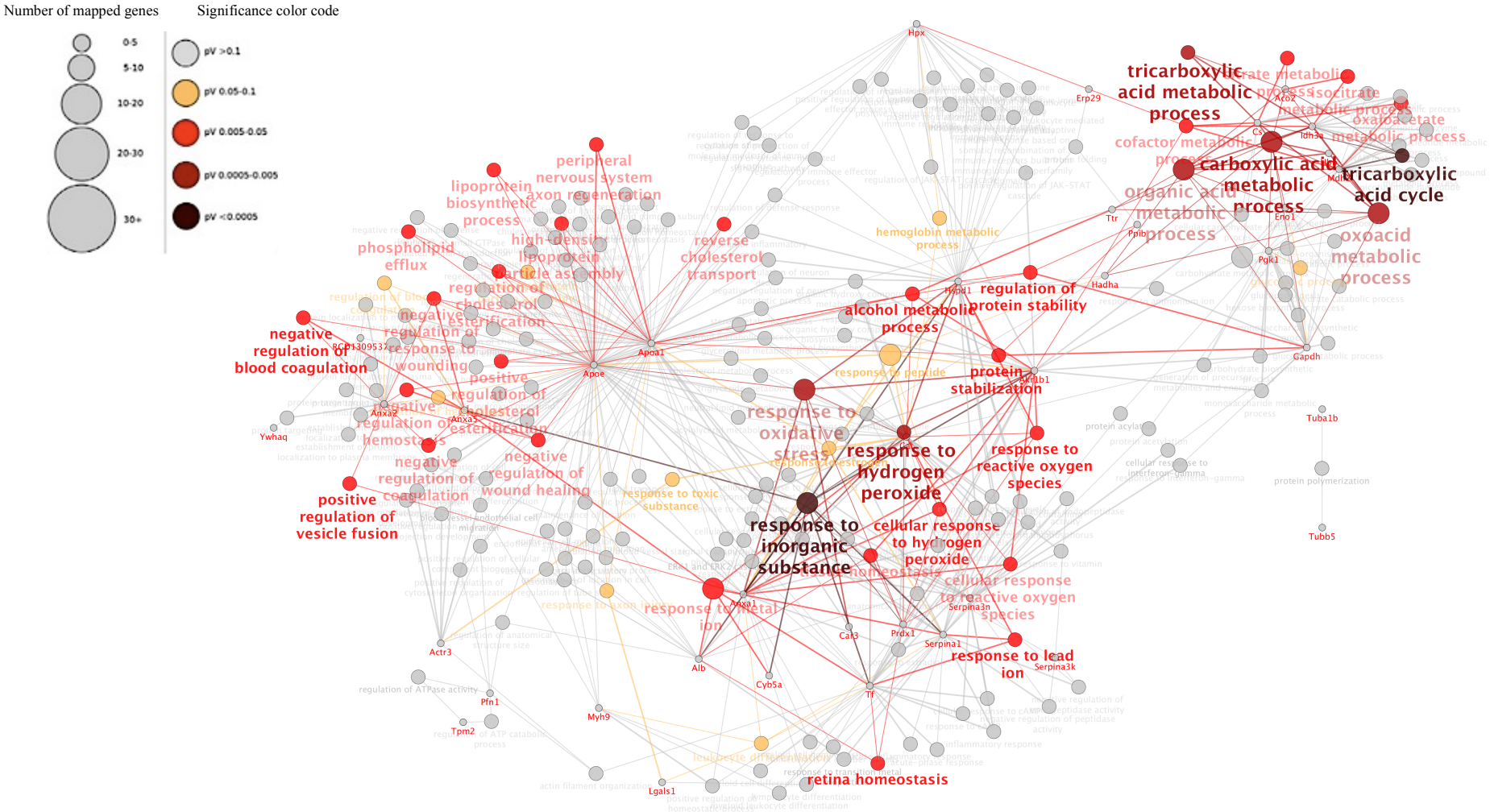

Supplemental Figure D 2 - ClueGo and CluePedia significance analysis of protein-protein interaction considering proteins present in epicardial and visceral adipose tissue of obese ZSF1 rat (based on emPAI values).